

T-3155

RESIDENCE TIME DISTRIBUTIONS IN
PACKED BED REACTOR FLOWS DOMINATED
BY FREE CONVECTION

ARTHUR LAKES LIBRARY
COLORADO SCHOOL of MINES
BY: GOLDEN, COLORADO 80401

K. Y. GALLAGHER

ProQuest Number: 10782768

All rights reserved

INFORMATION TO ALL USERS

The quality of this reproduction is dependent upon the quality of the copy submitted.

In the unlikely event that the author did not send a complete manuscript and there are missing pages, these will be noted. Also, if material had to be removed, a note will indicate the deletion.



ProQuest 10782768

Published by ProQuest LLC (2018). Copyright of the Dissertation is held by the Author.

All rights reserved.

This work is protected against unauthorized copying under Title 17, United States Code
Microform Edition © ProQuest LLC.

ProQuest LLC.
789 East Eisenhower Parkway
P.O. Box 1346
Ann Arbor, MI 48106 – 1346

A thesis submitted to the Faculty and the Board of Trustees of the Colorado School of Mines in partial fulfillment of the requirements for the degree of Master of Science (Chemical and Petroleum-Refining Engineering).

Golden, Colorado

Date 11/20/85

Signed: Karin Y. Gallagher
Karin Y. Gallagher

Approved: Michael C. Jones
Michael C. Jones
Thesis Advisor

Approved: Sami Selim
Sami Selim
Thesis Advisor

Golden, Colorado

Date 11/20/85

Arthur J. Kidnay
Arthur J. Kidnay
Chemical and Petroleum
Refining Engineering
Department Head

ABSTRACT

This thesis presents a numerical study of the Residence Time Distributions (RTDs) resulting from a pulse input to a packed bed reactor where the flow is dominated by free convection. A two-dimensional solution is obtained for porous media confined between vertical side walls and heated from below. Net vertical flow is imposed.

The approach was to solve the governing time-dependent partial differential equations for flow to produce velocity profiles at steady state. Using the steady state profiles a second time dependent calculation was performed to obtain tracer responses to a pulse input. Resulting RTDs for the onset of free convection were correlated with flow patterns, the Rayleigh number (Ra) - a measure of stability, and a parameter $RePr$, the product of a Reynolds number and a Prandtl number - characteristic of through-flow strength. The achievement of steady state was clearly indicated by plots of the natural logarithm of the root mean square average vorticity against time. The RTDs for steady convecting flow were intermediate to the perfectly mixed vessel and plug flow models and characterized by multiple peaks. The peaks were determined to result from recirculation of tracer in the rotating convection cells.

The pulse response was a function of Ra , $RePr$, and vessel height. It was independent of the number of convecting cells, and the vessel width. A mixing time characteristic of the RTD increased with increasing $RePr$ and decreased with increasing Ra and height.

In summation, RTD methods are decisive in detecting free convection and capable of qualitatively characterizing the flow.

TABLE OF CONTENTS

	PAGE
ABSTRACT	iii
TABLE OF CONTENTS	v
LIST OF FIGURES	ix
LIST OF TABLES	xv
ACKNOWLEDGEMENTS	xvi
1. INTRODUCTION	1
1.1 Objective	1
1.2 Approach	2
1.3 Previous Work: Convecting Flow	4
1.4 Previous Work: Residence Time Distribution	5
1.4.1 Theory	5
1.4.2 Experimental	9
2. THE GOVERNING EQUATIONS	12
2.1 Flow Calculations	12
2.1.1 Governing System of Equations	12
2.1.2 Initial Conditions	14
2.1.3 Boundary Conditions	16
2.1.4 Dimensionless Form of the Equations	17
2.2 Tracer Calculations	21
2.2.1 Governing Equation, Initial and Boundary Conditions	21
2.2.2 Dimensionless Form of the Equations	21

	PAGE
3. NUMERICAL SOLUTION	23
3.1 Introduction	23
3.2 System of Grid Points	25
3.3 Finite Difference Form of the Governing Equations	28
3.3.1 Stream Function Equation	28
3.3.2 Vorticity Transport Equation	29
3.3.3 Thermal Energy Equation	29
3.3.4 Stream Function Definition	30
3.3.5 Species Equation for Tracer	30
3.4 Finite Difference Form of the Initial Conditions	32
3.4.1 Velocity	32
3.4.2 Stream Function	32
3.4.3 Temperature	32
3.4.4 Vorticity	33
3.4.5 Tracer Concentration	33
3.5 Finite Difference Form of the Boundary Conditions	35
3.5.1 Velocity	35
3.5.2 Stream Function	36
3.5.3 Temperature	36
3.5.4 Vorticity	36

	PAGE
3.5.5 Tracer Concentration	36
3.6 Execution	37
3.6.1 Overview	37
3.6.2 Flow Calculations	38
3.6.3 Tracer Concentration Calculation	40
4. THE PERFECTLY MIXED VESSEL AND PLUG FLOW	45
5. PRESENTATION OF RESULTS	47
5.1 Increase in Vorticity with Time	47
5.2 Stream Function and Temperature Contours	52
5.3 Tracer RTDs and Contours	75
5.4 Verification of RTD Results	103
5.4.1 Plug Flow	103
5.4.2 Convecting Flows	108
6. DISCUSSION OF RESULTS	113
6.1 Detection of Free Convection and the Steady State	113
6.2 The Critical Rayleigh Number	113
6.3 Stream Function and Temperature Contours	115
6.4 Analysis of the RTD's and Tracer Contours	117
6.5 Validity of the Tracer Response Calculations	122
6.5.1 Conservation of the Tracer Species	122
6.5.2 Plug Flow	122

	PAGE
6.5.3 Convecting Flows	126
6.5.4 Summary	127
6.6 Examples: Application to Oil Shale Retorts	127
7. CONCLUSIONS	131
NOMENCLATURE	133
REFERENCES	137
APPENDIX A: TYPICAL PARAMETERS	141
APPENDIX B: COMPUTER PROGRAM	151

LIST OF FIGURES

FIGURE	PAGE
1.1 Stability Limits as a Function of $RePr$	6
1.2 Response to an Impulse Function	8
1.3 Experimental Plug Flow Response, Flow = 819 cc/min, $RePr = 1.6$, $Ra = 0$	10
1.4 Experimental Convecting Flow Response, Flow = 783 cc/min, $RePr = 1.53$, $Ra = 246$	11
2.1 Two-Dimensional Model	15
3.1 Two-Dimensional System of Grid Points	26
3.2 Rectangular Pulse	34
3.3 Flow Diagram for Flow Calculations	39
3.4 Rectangular Pulse in Dimensionless Variables	44
5.1 Increase in Vorticity, $RePr=0$, $M/N=20/20$	48
5.2 Increase in Vorticity, $RePr=1$, $M/N=20/20$	49
5.3 Increase in Vorticity, $RePr=4$, $M/N=20/20$	50
5.4 Increase in Vorticity, $RePr=10$, $M/N=20/20$	51
5.5 Initial Temperature Contour, $RePr=0$, $M/N=20/20$	54
5.6 Stream Function Contour, $RePr=0$, $Ra=200$, $M/N=20/20$	55
5.7 Temperature Contour, $RePr=0$, $Ra=200$, $M/N=20/20$	56
5.8 Stream Function Contour, $RePr=4$, $Ra=100$, $M/N=20/20$	57

FIGURE	PAGE
5.9 Temperature Contour, $RePr=4$, $Ra=100$, $M/N=20/20$	58
5.10 Stream Function Contour, $RePr=4$, $Ra=200$, $M/N=20/20$	59
5.11 Temperature Contour, $RePr=4$, $Ra=200$, $M/N=20/20$	60
5.12 Stream Function Contour, $RePr=4$, $Ra=600$, $M/N=20/20$	61
5.13 Temperature Contour, $RePr=4$, $Ra=600$, $M/N=20/20$	62
5.14 Stream Function Contour, $RePr=4$, $Ra=1000$, $M/N=20/20$	63
5.15 Temperature Contour, $RePr=4$, $Ra=1000$, $M/N=20/20$	64
5.16 Stream Function Contour, $RePr=4$, $Ra=200$, $M/N=30/20$	65
5.17 Temperature Contour, $RePr=4$, $Ra=200$, $M/N=30/20$	66
5.18 Stream Function Contour, $RePr=4$, $Ra=200$, $M/N=60/20$	67
5.19 Temperature Contour, $RePr=4$, $Ra=200$, $M/N=60/20$	68
5.20 Stream Function Contour, $RePr=4$, $Ra=200$, $M/N=20/30$	69
5.21 Temperature Contour, $RePr=4$, $Ra=200$, $M/N=20/30$	70
5.22 Stream Function Contour, $RePr=4$, $Ra=200$, $M/N=20/60$	71
5.23 Temperature Contour, $RePr=4$, $Ra=200$, $M/N=20/60$	72
5.24 Stream Function Contour, $RePr=4$, $Ra=600$,	

FIGURE	PAGE
M/N=20/60	73
5.25 Temperature Contour, $ReP=4$, $Ra=600$, $M/N=20/60$	74
5.26 Residence Time Distribution, $RePr=1$, $Ra=200$, M/N=20/20, $\Delta\tau = .0001$	76
5.27 Residence Time Distribution, $RePr=1$, $Ra=600$, M/N=20/20, $\Delta\tau = .0001$	77
5.28 Residence Time Distribution, $RePr=4$, $Ra=100$, M/N=20/20, $\Delta\tau = .0001$	78
5.29 Residence Time Distribution, $RePr=4$, $Ra=200$, M/N=20/20, $\Delta\tau = .0001$	79
5.30 Residence Time Distribution, $RePr=4$, $Ra=600$, M/N=20/20, $\Delta\tau = .0001$	80
5.31 Residence Time Distribution, $RePr=4$, $Ra=1000$, M/N=20/20, $\Delta\tau = .0001$	81
5.32 Residence Time Distribution, $RePr=10$, $Ra=200$, M/N=20/20, $\Delta\tau = .0001$	82
5.33 Residence Time Distribution, $RePr=10$, $Ra=400$, M/N=20/20, $\Delta\tau = .0001$	83
5.34 Residence Time Distribution, $RePr=10$, $Ra=600$, M/N=20/20, $\Delta\tau = .0001$	84
5.35 Residence Time Distribution, $RePr=10$, $Ra=1000$, M/N=20/20, $\Delta\tau = .0001$	85
5.36 Tracer Concentration Contour, $\tau^* = .057$, $RePr=4$,	

FIGURE	PAGE
Ra=200, M/N=20/20	86
5.37 Tracer Concentration Contour, $\tau^* = .114$, RePr=4, Ra=200, M/N=20/20	87
5.38 Tracer Concentration Contour, $\tau^* = .171$, RePr=4, Ra=200, M/N=20/20	88
5.39 Tracer Concentration Contour, $\tau^* = .229$, RePr=4, Ra=200, M/N=20/20	89
5.40 Tracer Concentration Contour, $\tau^* = .286$, RePr=4, Ra=200, M/N=20/20	90
5.41 Tracer Concentration Contour, $\tau^* = .343$, RePr=4, Ra=200, M/N=20/20	91
5.42 Tracer Concentration Contour, $\tau^* = .400$, RePr=4, Ra=200, M/N=20/20	92
5.43 Tracer Concentration Contour, $\tau^* = .457$, RePr=4, Ra=200, M/N=20/20	93
5.44 Tracer Concentration Contour, $\tau^* = .514$, RePr=4, Ra=200, M/N=20/20	94
5.45 Tracer Concentration Contour, $\tau^* = .571$, RePr=4, Ra=200, M/N=20/20	95
5.46 Tracer Concentration Contour, $\tau^* = .629$, RePr=4, Ra=200, M/N=20/20	96
5.47 Tracer Concentration Contour, $\tau^* = .686$, RePr=4, Ra=200, M/N=20/20	97

FIGURE	PAGE
5.48 Residence Time Distributions, $RePr=4$, $Ra=200$, $M/N=60/20$, $\Delta\tau = .0001$	98
5.49 Residence Time Distributions, $RePr=4$, $Ra=200$, $M/N=30/20$, $\Delta\tau = .0001$	99
5.50 Residence Time Distributions, $RePr=4$, $Ra=200$, $M/N=20/30$, $\Delta\tau = .0001$	100
5.51 Residence Time Distributions, $RePr=4$, $Ra=200$, $M/N=20/60$, $\Delta\tau = .0002$	101
5.52 Residence Time Distribution, $RePr=4$, $Ra=600$, $M/N=20/60$, $\Delta\tau = .0002$	102
5.53 Theoretical Residence Time Distributions, Plug Flow and Perfectly Mixed Vessel	104
5.54 Residence Time Distributions, Plug Flow, Explicit Upwind Differencing, $M/N=20/20$	105
5.55 Residence Time Distribution, Plug Flow, Explicit Upwind Differencing, $M/N=40/40$	106
5.56 Residence Time Distributions, Alternating Direction Implicit, $M/N=20/20$	107
5.57 Residence Time Distribution, $RePr=4$, $Ra=1000$, $M/N=20/20$, $\Delta\tau = .00005$	109
5.58 Residence Time Distribution, $RePr=4$, $Ra=1000$, $M/N=40/40$, $\Delta\tau = .0002$	110
5.59 ADI Residence Time Distribution, $RePr=4$, $Ra=200$,	

FIGURE	PAGE
M/N=20/20, $\Delta\tau = .0001$	111
5.60 ADI Residence Time Distribution, $RePr=4$, $Ra=1000$, M/N=30/30, $\Delta\tau = .0001$	112
6.1 Comparison of Cases Studied with Linear Theory	114
6.2 Critical Rayleigh Number Determination for No-Flow	116
6.3 Mixing Time vs. Rayleigh Number	120
6.4 Mixing Time vs. $RePr$	121
6.5 Mixing Time vs. Aspect Ratio (Width/Height)	124

LIST OF TABLES

TABLE	PAGE
5.1 Number of Convection Cells, $M/N = 20/20$	53
6.1 Mixing Times for Various $RePr$ and Ra , $M/N = 20/20$	119
6.2 Mixing Times for Various Aspect Ratios	123
6.3 Area Under the RTD Curve.	125
A.1 Oil Shale Parameters, 1.5 x 0.3m Retort	143
A.2 Oil Shale Parameters, 6.0 x 0.9m Retort	144
A.3 Calculation of Lewis Number	150
B.1 CPU Times for Flow Executions	153
B.2 CPU Times for Tracer Executions	154

ACKNOWLEDGEMENTS

I wish to thank Dr. M. C. Jones for his valuable guidance and suggestions throughout the course of this work. Also Drs. S. Selim, A. J. Kidnay, and R. M. Baldwin for their participation on the thesis defense committee.

Finally, I wish to thank Rockwell International for its financial support.

1. INTRODUCTION

1.1 Objective

The study of free convection in porous media has applications in many areas of chemical engineering. In geothermal reservoirs and pebble bed nuclear reactors free convection is the driving force behind the essential transport of heat. Conversely, the presence of free convection in oil shale retorts and coal and biomass gasifiers could reduce the overall conversion rate. Insight on the flow processes occurring in porous media can be readily obtained by the numerical solution of partial differential equations. This was the general intent of this thesis. In addition, it was desired to choose a numerical approach that could be applied at some future date to extensive experimental work.

Past experimental studies have been largely limited to measurement of the rate of heat transfer or they rely on temperature probes situated in the flow field - which necessarily cause local disturbances - for information on the internal state of the medium. Such heat transfer methods are slow, imprecise, and generally difficult. It is proposed that measurement of the Residence Time Distribution (RTD) can be used as a non-intrusive means of obtaining

information on the internal flow field, and in particular, that it can be applied to detecting free convection. This method has been widely used in mixing studies. Papers of note are as follows. Holmes, Voncken and Decker [1] quantified mixing times in turbine-stirred baffled vessels by measuring the circulation time for a pulse of tracer. Khang and Levenspiel [2] used RTD methods to characterize batch mixing with a decay rate constant. This constant was then used to define a mixing-rate number. Results similar to Khang and Levenspiel were obtained by Sasakura et al. [3].

Measurement of the RTD has not been widely used in the study of free convection. Its application to packed bed reactor flows requires the existence of a net through-flow stream. Such a stream may be a pre-existing condition - as with oil shale retorts - or it may be induced by the introduction of a small amount of through-flow.

The specific intent of this thesis was to conduct a numerical study to correlate the onset of free convection in porous media with flow patterns, numerical parameters characterizing stability and through-flow strength, and the impulse response to a hypothetical tracer input.

1.2 Approach

Free convection is produced when a density gradient

results in buoyant instability. Refer to Chandrasekhar [4] for a thorough discussion of this subject. The density gradient may be induced by a concentration gradient or a thermal gradient. Only thermal gradients were considered here. The model used consisted of a bed of porous media heated from below in a gravitational field. Walls were assumed adiabatic. Presupposing the possible existence of asymmetrical flow patterns, symmetry about the centerline was not used. Both no-flow and net vertical flow cases were studied. The region investigated was restricted to flows sufficiently small that forced convection could not mask the effects of free convection. The cases of interest were above the critical point for the onset of convection.

The approach was to solve the governing time-dependent differential equations for two-dimensional flow under conditions of free convection to produce a velocity profile at steady state. Using the steady state profile a second time-dependent calculation was performed for the solution of a species equation for tracer, which gave the tracer response to a pulse input. The governing equations for the flow were solved with Successive Overrelaxation (SOR) and Alternating Direction Implicit (ADI) methods. The tracer response calculation used an explicit form of upwind differencing after the ADI method was found to be

inadequate. RTDs were generated by graphing the change in exit age distribution against time. As this RTD has no physical meaning for no-flow cases, RTDs were generated for net through-flow cases only.

Refer to Carnahan, Luther and Wilkes [5] and Smith [6] for a general discussion of finite difference methods. Specific application to computational fluid mechanics is covered in Roache [7] and in Chow [8]. Relevant papers include Wilkes and Churchill [9] and Samuels and Churchill [10] who applied ADI techniques to free convection.

1.3 Previous Work: Convecting Flow

The onset of free convection in an initially stagnant layer of fluid by heating the fluid from below in a gravitational field was first observed by Bénard in 1900. In 1916 Lord Rayleigh made the first theoretical analysis. He identified a non-dimensional parameter, the Rayleigh number (Ra), characteristic of stability/instability. It is defined in the literature as the ratio of buoyant to viscous forces. Pellew and Southwell [11] extended the theory of convective currents to explain cell patterns. Lapwood [12] made a theoretical analysis applying criteria for the onset of convection to porous media. Katto and Masuoka [13] refined the theory for porous media, defining an effective

thermal diffusivity that incorporated the thermal conductivity of the bed and the specific heat and density of the fluid.

Of particular interest here is the work of Homsy and Sherwood [14] on the effect of net vertical flow of fluids in porous media. They used linear theory to establish an upper bound on the critical Rayleigh number above which free convection must exist. The critical Rayleigh number in their work is a function of a dimensionless through-flow strength quantified by the product of the Reynolds number and an adjusted Prandtl number, $RePr$. The Prandtl number used is based on a thermal diffusivity adjusted for the thermal conductivity of the bed. The lower limit on the critical Rayleigh number, below which stability is assured, is given by energy theory. Figure 1.1 presents these theoretical results and illustrates that the critical Rayleigh number increases with increasing $RePr$.

1.4 Previous Work: Residence Time Distribution

1.4.1 Theory

Tracer response theory commonly uses an impulse function for the tracer input. Theoretical results are well known for two limiting cases: plug flow, and the perfectly

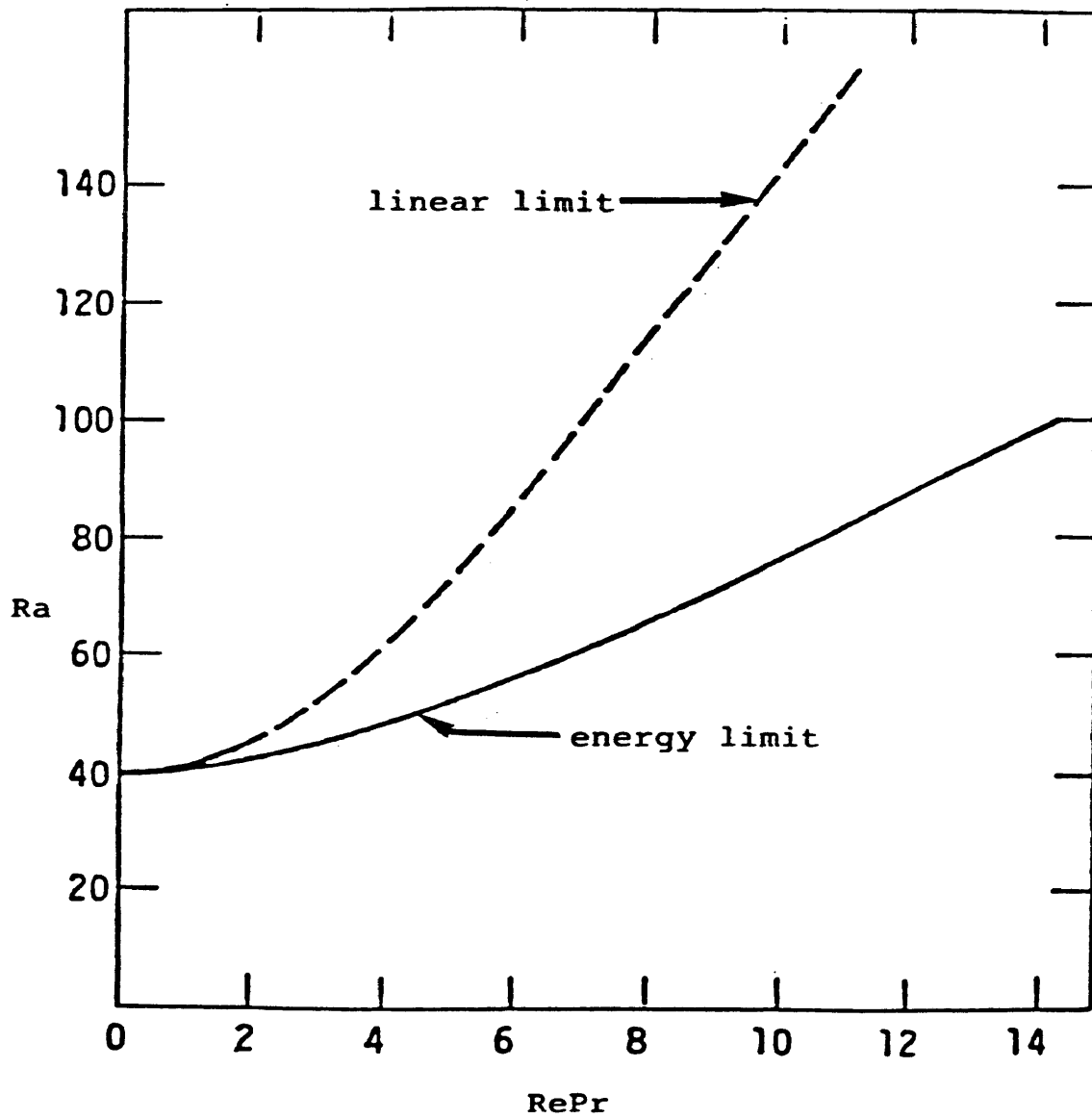


Figure 1.1
Stability Limits as a Function of RePr

mixed vessel. There are many forms, other than these two, that the RTD can take depending on the degree of mixing.

For plug flow, the one-dimensional species equation for tracer concentration, C_A is

$$\frac{\partial C_A}{\partial t} = D \frac{\partial^2 C_A}{\partial y^2} - v \frac{\partial C_A}{\partial y} \quad (1.4-1)$$

with boundary conditions

$$C_A = A \cdot \delta(t) \quad \text{at the entrance} \quad (1.4-2)$$

$$\frac{\partial C_A}{\partial y} = 0 \quad \text{at the exit}$$

Where A is the area under the concentration - time curve, t is time, D is the mass dispersion coefficient, y is the length, and v is velocity. Following the solution presented by Friedley [15], the impulse response, $G(y,t)$, as the overall bed length approaches infinity is given by

$$G(y,t) = \frac{A}{2\sqrt{\pi}} \left(\frac{y^2}{t^3 D} \right)^{1/2} \exp \left[-\frac{v^2}{4tD} \left(t - \frac{y}{v} \right)^2 \right] \quad (1.4-3)$$

This function is plotted in Fig. 1.2. If measured at the outlet the impulse response is the RTD.

The impulse response of a perfectly mixed vessel is given by

$$C_A = A \frac{v}{y} \exp \left(-t \frac{v}{y} \right) \quad (1.4-4)$$

where the term (v/y) is the inverse of the residence time.

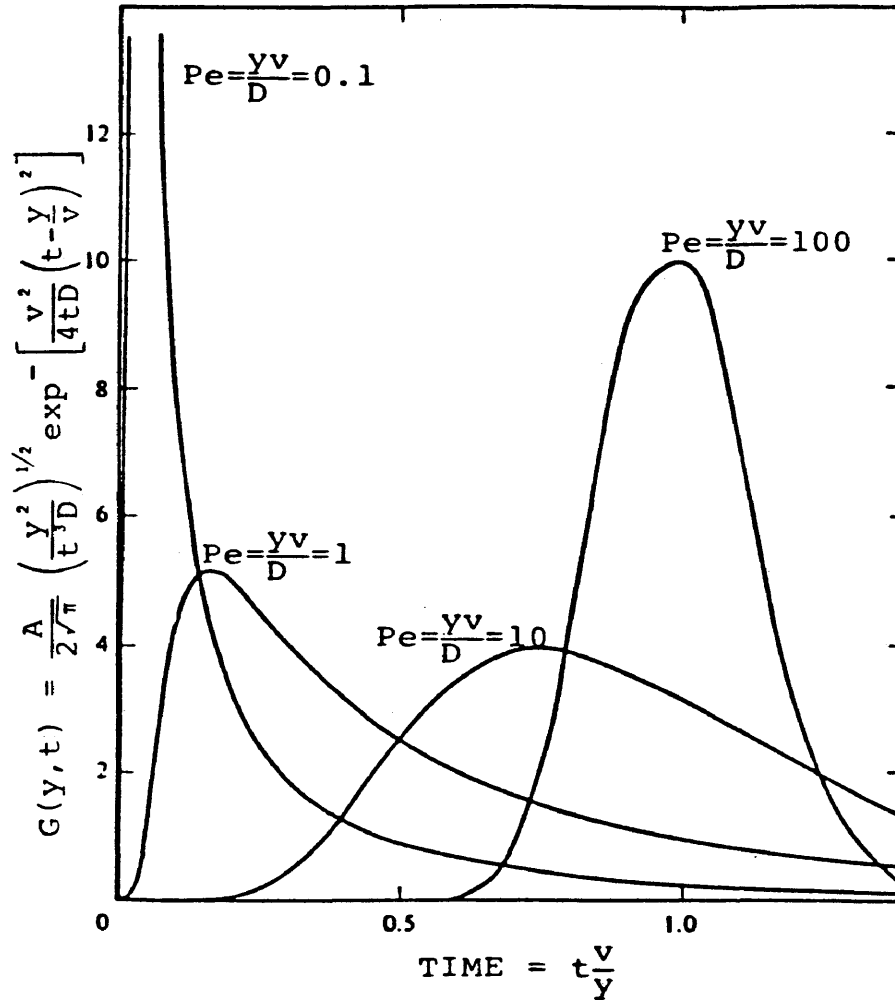


Figure 1.2
Response to an Impulse Function

1.4.2 Experimental

Experimental measurement of the RTD was used by Feuerherm [16] to detect free convection. He used a cylindrical vessel of porous media heated from below with a net vertical downward flow. The saturating fluid was carbon dioxide. Helium was used as the tracer gas since it can readily be detected in carbon dioxide using the thermal conductivity difference. Graphs of the RTD based on average exit age are presented in Figures 1.3 and 1.4 for plug flow and free convection. The average concentration at the exit was determined from the cup mixing average of five points, each at different radii. Since the tracer was distributed across the bed at the inlet these results should approximate the one-dimensional plug flow results of Freidley.

Feuerherm's work was preliminary. He was not able to verify the cause of multiple peaks or to correlate the resulting RTDs with flow patterns or numerical parameters.

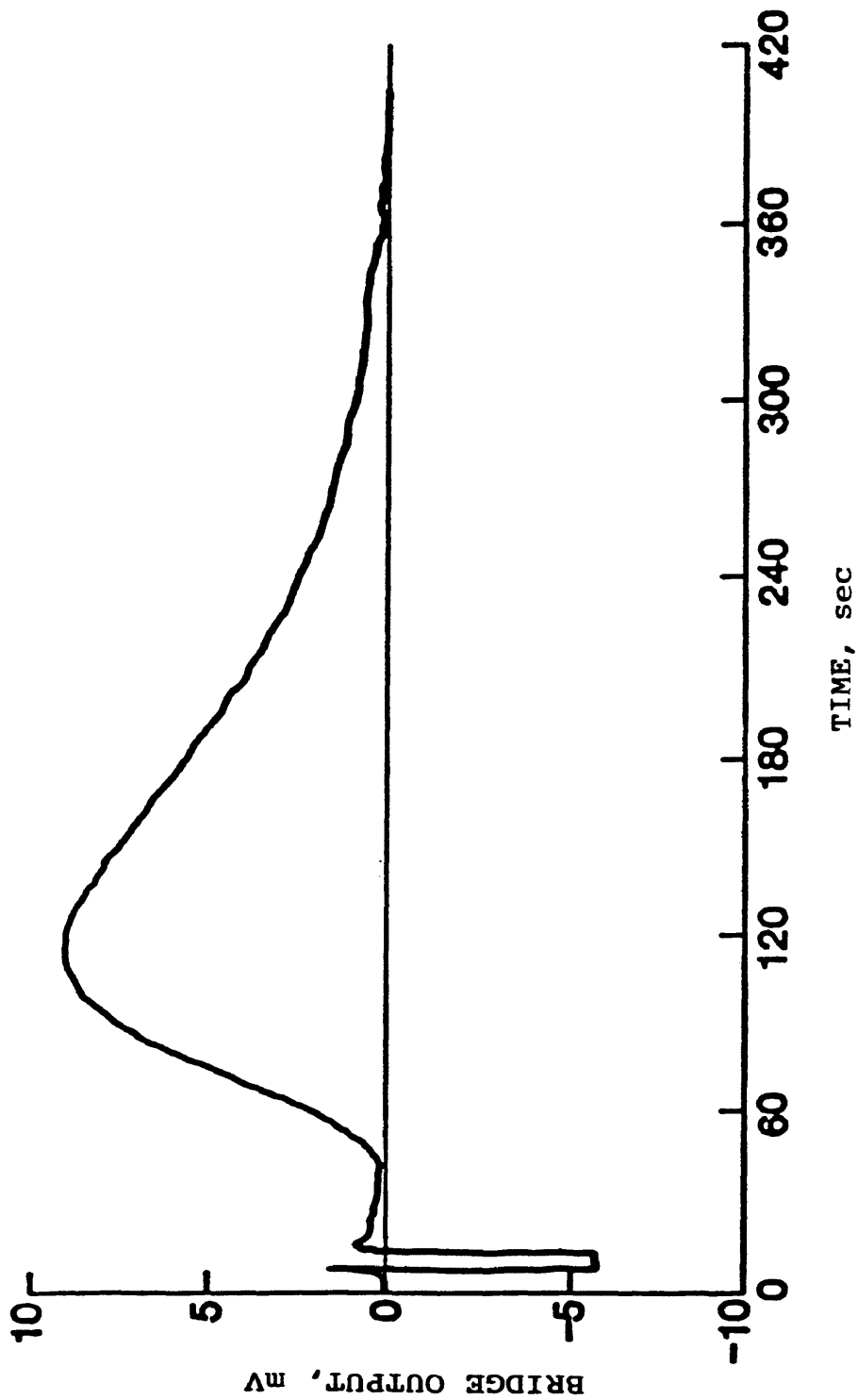


Figure 1.3
Experimental Plug Flow Response
Flow = 819 cc/min, RePr = 1.6, Ra = 0

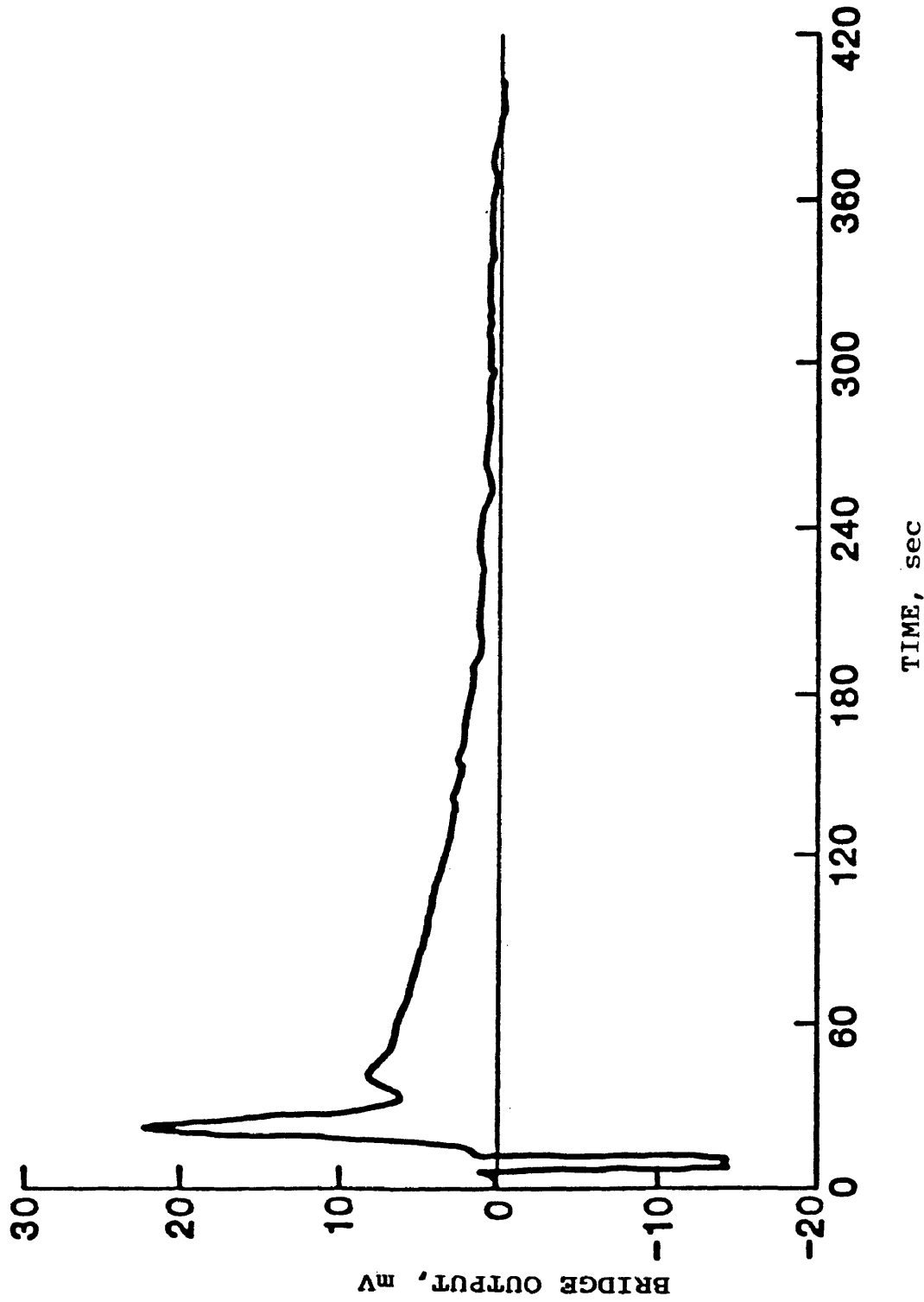


Figure 1.4
Experimental Convecting Flow Response
Flow = 783 cc/min, RePr = 1.53, Ra = 246

2. THE GOVERNING EQUATIONS

2.1 Flow Calculations

2.1.1 Governing System of Equations

Following common practice for studies of convective instability the physical properties of the system, excepting the density, are assumed constant. Applying the Boussinesq approximation [4,8], that for small variations in temperature density can be considered constant everywhere except in the buoyant force term, the governing system of equations for the flow calculations is:

Equation of State

$$\rho = \rho_0 [1 - \beta(T - T_0)] \quad (2.1-1)$$

Continuity Equation

$$\nabla \cdot \vec{v} = 0 \quad (2.1-2)$$

Darcy's Law

$$0 = -\nabla P - \frac{\nu \rho}{K} \vec{v} - \rho g \hat{j} \quad (2.1-3)$$

Thermal Energy Equation

$$\frac{\partial T}{\partial t} + \frac{(\rho C_p)_f}{(\rho C_p)_b} [\vec{v} \cdot \nabla T] = \left(\frac{k}{\rho C_p} \right)_b \nabla^2 T \quad (2.1-4)$$

where β is the coefficient of volume expansion, T is the temperature, ρ is the density with subscript '0' denoting the density at temperature T_0 , \vec{v} is the superficial

velocity, P is the pressure, ν is the kinematic viscosity, K is the bed permeability, g is gravity, \hat{j} is a unit vector in the vertical dimension, t is the time, C_p is the specific heat, and k is the thermal conductivity. Subscripts 'f' and 'b' indicate fluid and bed properties, respectively.

The problem was attacked using a vorticity-stream function approach [7,8]. Vorticity is defined as

$$\vec{\xi} = \nabla \times \vec{v} \quad (2.1-5)$$

The stream function is given by

$$v_x = \frac{\partial \psi}{\partial y}, \quad v_y = -\frac{\partial \psi}{\partial x} \quad (2.1-6)$$

where x denotes the horizontal dimension, y the vertical dimension. Taking the curl of Darcy's Law and applying the above definitions, the system of equations in two-dimensional rectangular coordinates reduces to:

Stream Function Equation

$$\vec{\xi} = -\left[\frac{\partial^2}{\partial x^2} + \frac{\partial^2}{\partial y^2}\right] \psi \quad (2.1-7)$$

Vorticity Transport Equation

$$\vec{\xi} = \frac{\beta g K}{\nu} \frac{\partial T}{\partial x} \quad (2.1-8)$$

Thermal Energy Equation

$$\begin{aligned} \frac{\partial T}{\partial t} + \frac{(\rho C_p)_f}{(\rho C_p)_b} \left[v_x \frac{\partial T}{\partial x} + v_y \frac{\partial T}{\partial y} \right] \\ = \left(\frac{k}{\rho C_p} \right)_b \left[\frac{\partial^2}{\partial x^2} + \frac{\partial^2}{\partial y^2} \right] T \end{aligned} \quad (2.1-9)$$

These equations are now applied to a porous medium confined between vertical side walls and heated from below. Net vertical flow is imposed. See Figure 2.1

2.1.2 Initial Conditions

An initial velocity field is assumed such that there is no horizontal component of velocity and the vertical component is constant

$$v_x = 0, \quad v_y = v_0 \quad (2.1-10)$$

This velocity field requires an initial stream function profile that is linear with respect to x and constant with respect to y

$$\psi = -v_0 x + \frac{v_0 \text{width}}{2} \quad (2.1-11)$$

The initial temperature profile is based on a system at steady state in the absence of free convection: Temperature is constant with respect to x and varies with respect to y as a function of the superficial velocity.

$$T = f(y, v_0) \quad (2.1-12)$$

Since the horizontal temperature gradient is zero and vorticity is proportional to this gradient, the initial vorticity must also be zero.

$$\vec{\xi} = 0 \quad (2.1-13)$$

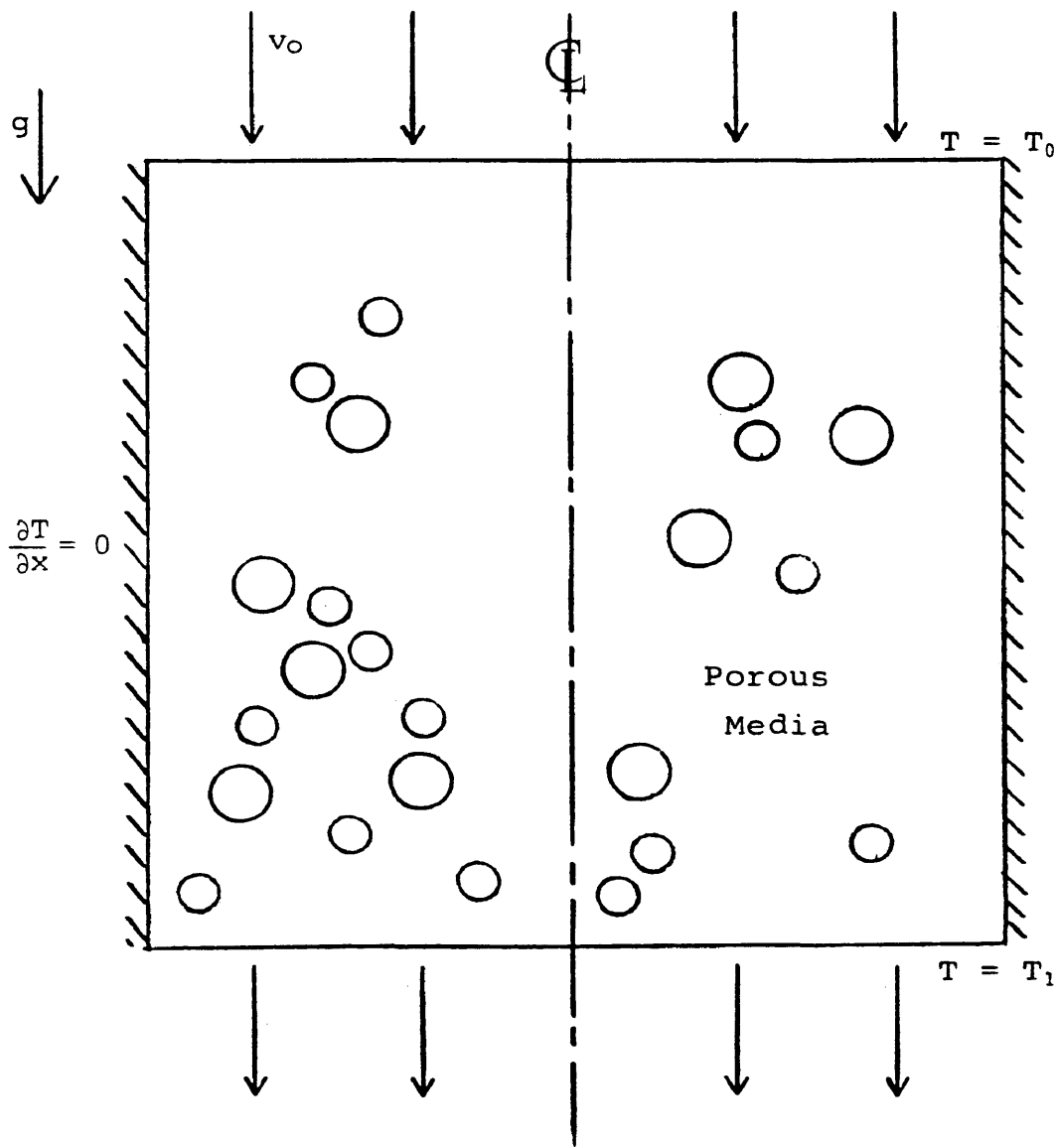


Figure 2.1
Two-Dimensional Model

2.1.3 Boundary Conditions

Boundary conditions for the system are developed in full at this point. Determination of which ones are mathematically required was made after development of the finite difference equations. The temperature and vorticity boundary conditions will be dealt with first. The temperatures at the top (entrance) and bottom (exit) are held at their initial values. This requires vorticity to retain its initial value of zero at the top and bottom. Adiabatic walls are assumed. The requirement for no heat flux through the walls may be written in terms of the horizontal temperature gradient.

$$\left. \frac{\partial T}{\partial x} \right|_{\text{wall}} = 0 \quad (2.1-14)$$

Again, in the absence of a horizontal temperature gradient vorticity is zero

$$\left. \zeta \right|_{\text{wall}} = 0 \quad (2.1-15)$$

Velocity at the top and bottom is held at the initial condition. At the walls the x-component of velocity must vanish

$$\left. v_x \right|_{\text{wall}} = 0 \quad (2.1-16)$$

additionally,

$$\left. \frac{\partial v_x}{\partial y} \right|_{\text{wall}} = 0 \quad (2.1-17)$$

Since

$$\left. \frac{\partial \psi}{\partial y} \right|_{\text{wall}} = 0 \quad (2.1-15)$$

has been established, and from equation (2.1-5)

$$\left. \frac{\partial \psi}{\partial x} \right|_{\text{wall}} = \left. \frac{\partial v_y}{\partial x} \right|_{\text{wall}} - \left. \frac{\partial v_x}{\partial y} \right|_{\text{wall}} \quad (2.1-18)$$

$$\left. \frac{\partial v_y}{\partial x} \right|_{\text{wall}} = 0 \quad (2.1-19)$$

must also be true.

Since velocity at the entrance and exit is held constant, the stream function at these points retains its initial values. Along the walls equation (2.1-16) may be rewritten as

$$v_x \Big|_{\text{wall}} = \frac{\partial \psi}{\partial Y} \Big|_{\text{wall}} = 0 \quad (2.1-20)$$

defining a streamline. The initial condition is used in order to be compatible with inlet and exit stream functions.

2.1.4 Dimensionless Form of the Equations

For the normalizing system to be most effective it must be based on a time interval characteristic of the process. For this flow problem the controlling parameter is the effective thermal diffusivity,

$$\alpha' = \frac{k_b}{(\rho C_p)_f} \quad (2.1-21)$$

and the appropriate time constant was based on thermal

diffusion

$$\tau = t \frac{\alpha'}{H^2} \quad (2.1-22)$$

where H is a reference length. With the addition of a reference temperature difference $(T_1 - T_0)$ where T_1 and T_0 are the temperatures of the bottom and top, respectively, a system of dimensionless variables is defined:

Length

$$X = \frac{x}{H}, \quad Y = \frac{y}{H} \quad (2.1-23)$$

Velocity

$$U = v_x \frac{H}{\alpha'}, \quad V = v_y \frac{H}{\alpha'} \quad (2.1-24)$$

Stream function

$$\Psi = \frac{\psi}{\alpha'} \quad (2.1-25)$$

Vorticity

$$\vec{\omega} = \vec{\omega}' \frac{H^2}{\alpha'} \quad (2.1-26)$$

Temperature difference

$$\Theta = \left(\frac{T - T_0}{T_1 - T_0} \right) \quad (2.1-27)$$

the resulting dimensionless system of equations is:

Stream Function Equation

$$\vec{\omega} = \left[\frac{\partial^2}{\partial Y^2} + \frac{\partial^2}{\partial X^2} \right] \Psi \quad (2.1-28)$$

Vorticity Transport Equation

$$\vec{\omega} = Ra \frac{\partial \theta}{\partial X} \quad (2.1-29)$$

Thermal Energy Equation

$$\frac{\partial \theta}{\gamma \partial \tau} = - \left[\frac{\partial (U\theta)}{\partial X} + \frac{\partial (V\theta)}{\partial Y} \right] + \left[\frac{\partial^2}{\partial X^2} + \frac{\partial^2}{\partial Y^2} \right] \theta \quad (2.1-30)$$

where the stream function in dimensionless terms is defined by

$$U = \frac{\partial \Psi}{\partial Y} , \quad V = - \frac{\partial \Psi}{\partial X} \quad (2.1-31)$$

and the dimensionless constants are the Rayleigh number

$$Ra = \frac{\beta g H (T_1 - T_0) K}{\alpha \nu} \quad (2.1-32)$$

and the ratio of specific heats

$$\gamma = \frac{(\rho C_p)_f}{(\rho C_p)_b} \quad (2.1-33)$$

The thermal energy equation is presented in conservative form by use of the equation of continuity.

The initial conditions in dimensionless form are as follows:

Velocity

$$U = 0 , \quad V = V_0 \quad (2.1-34)$$

Stream Function

$$\Psi = -V_0 X + \frac{V_0}{2} \left(\begin{array}{c} \text{dimensionless} \\ \text{width} \end{array} \right) \quad (2.1-35)$$

Temperature

$$\theta = f(y, V_0) \quad (2.1-36)$$

additionally,

$$\theta \Big|_{\text{top}} = 0 , \quad \theta \Big|_{\text{bottom}} = 1 \quad (2.1-37)$$

Vorticity

$$\vec{\omega} = 0 \quad (2.1-38)$$

The boundary conditions are:

Velocity

At the side walls,

$$U \Big|_{\text{wall}} = 0 , \quad \frac{\partial V}{\partial X} \Big|_{\text{wall}} = 0 \quad (2.1-39)$$

Components of velocity retain their initial values at the entrance and exit.

Stream Function

The stream function retains its initial value at the entrance, exit, and walls.

Temperature

At the side walls,

$$\frac{\partial \theta}{\partial X} \Big|_{\text{wall}} = 0 \quad (2.1-40)$$

Temperature is held constant at its initial value at top and bottom.

Vorticity

Vorticity retains its initial value at the entrance, exit, and side walls.

2.2 Tracer Calculations

2.2.1 Governing Equation, Initial and Boundary Conditions

The species equation for tracer response is given by

$$\epsilon \frac{\partial C_A}{\partial t} + (\vec{v} \cdot \nabla C_A) = D \nabla^2 C_A \quad (2.2-1)$$

where ϵ is the bed porosity, C_A is the concentration of tracer, and D is the dispersion coefficient. In two-dimensional rectangular coordinates the conservative form of the equation is

$$\epsilon \frac{\partial C_A}{\partial t} + \left[\frac{\partial(C_A v_x)}{\partial x} + \frac{\partial(C_A v_y)}{\partial y} \right] = D \left[\frac{\partial^2 C_A}{\partial x^2} + \frac{\partial^2 C_A}{\partial y^2} \right] \quad (2.2-2)$$

Tracer is introduced at the top as a rectangular pulse with concentration C_{initial} . The duration of the pulse is small in comparison with the residence time of the vessel in order to approximate a delta function. The boundary condition at the side walls is derived from the physical constraint of no mass flux through the walls

$$\left. \frac{C_A}{x} \right|_{\text{wall}} = 0 \quad (2.2-3)$$

The exit concentration, following Danckwerts' [17] analysis, will be specified by

$$\left. \frac{C_A}{y} \right|_{\text{exit}} = 0 \quad (2.2-4)$$

2.2.2 Dimensionless Form of the Equation

The normalizing system developed for the flow problem is carried over to the tracer equation with the addition of a dimensionless concentration E ,

$$E = \frac{C_A}{C_{A0}} \quad (2.2-5)$$

where C_{A0} is a reference concentration. The resulting dimensionless equation is

$$\epsilon \frac{\partial E}{\partial \tau} = - \frac{\partial (UE)}{\partial X} - \frac{\partial (VE)}{\partial Y} + \frac{1}{Le} \left[\frac{\partial^2}{\partial X^2} + \frac{\partial^2}{\partial Y^2} \right] E \quad (2.2-6)$$

where the Lewis number is not the standard ratio of thermal to mass diffusivity but is defined as the ratio of the effective thermal diffusivity to the mass dispersion coefficient.

$$Le = \frac{\alpha'}{D} \quad (2.2-7)$$

Concentration of tracer in the impulse is given by E_{initial} . Boundary conditions at the side walls and exit are

$$\left. \frac{\partial E}{\partial X} \right|_{\text{wall}} = 0 \quad (2.2-8)$$

$$\left. \frac{\partial E}{\partial Y} \right|_{\text{exit}} = 0 \quad (2.2-9)$$

3. NUMERICAL SOLUTION

3.1 Introduction

The system of partial differential equations, initial and boundary conditions governing the flow and tracer response calculations has been established. The problem at hand is to obtain finite difference approximations to the partial differential equations.

In general, central differences were used for spatial derivatives, and forward differences for time derivatives. The stream function, thermal energy and species equations require additional consideration.

The stream function equation

$$\omega = \left[\frac{\partial^2}{\partial X^2} + \frac{\partial^2}{\partial Y^2} \right] \psi \quad (2.1-28)$$

is Poisson's equation, a special case of the more general elliptic equation. Following common practice it was solved by Successive Overrelaxation (SOR).

The thermal energy equation

$$\frac{\partial \theta}{\gamma \partial \tau} = - \left[\frac{\partial(U\theta)}{\partial X} + \frac{\partial(V\theta)}{\partial Y} \right] + \left[\frac{\partial^2}{\partial X^2} + \frac{\partial^2}{\partial Y^2} \right] \theta \quad (2.1-30)$$

and the species equation for tracer

$$\epsilon \frac{\partial E}{\partial \tau} = - \frac{\partial(UE)}{\partial X} - \frac{\partial(VE)}{\partial Y} + \frac{1}{Le} \left[\frac{\partial^2}{\partial X^2} + \frac{\partial^2}{\partial Y^2} \right] E \quad (2.2-6)$$

are mixed parabolic-hyperbolic equations. They have been

formulated as conservative equations (the first derivative is taken on the product of velocity and temperature/concentration) to ensure conservation of thermal energy/tracer in the finite difference calculations [7]. The thermal energy equation requires current values of both velocity and temperature; it is non-linear. The species equation for tracer, because it uses velocities at steady state, is linear.

There are many approaches to the numerical solution of these mixed parabolic-hyperbolic equations. Two finite difference methods were considered here: Alternating Direction Implicit (ADI) and upwind-differencing.

Implicit methods have the advantage of being unconditionally stable when applied to a single equation. As a consequence larger time steps can be used than with explicit methods. ADI was initially chosen because of the success Churchill [9,10] had in applying it to free convection. ADI techniques resolve the partial differential equation into two finite difference equations: the first implicit in the x-direction only, the second implicit only in the y-direction. These finite difference equations are applied successively, the execution of each occurring over one-half the time step. The ADI method was successfully applied to the thermal energy equation. Application to the

species equation for tracer, however, resulted in excessive and unrealistic overshoot and oscillations. At this point it was decided to investigate upwind differencing of the velocity components, a technique known to damp such oscillations, for the species equation.

The salient feature of upwind differencing is that a perturbation is convected only in the direction of fluid motion. To its detriment, it works by introducing an artificial viscosity analogous to a diffusive viscous force whose effect is to introduce artificial damping and diffusion in the numerical solution. Upwind differencing was tried with both explicit and ADI forms of the finite difference equation. Both performed satisfactorily, producing nearly identical results and requiring time steps of the same order of magnitude. The ADI execution, however, required more CPU time as well as additional storage. Explicit upwind differencing was used for solution of the species equation.

3.2 System of Grid Points

A system of grid points was established in two-dimensional rectangular coordinates for solution of the finite difference equations. Reference Figure 3.1. There are "M" grid points in the horizontal direction and "N" grid

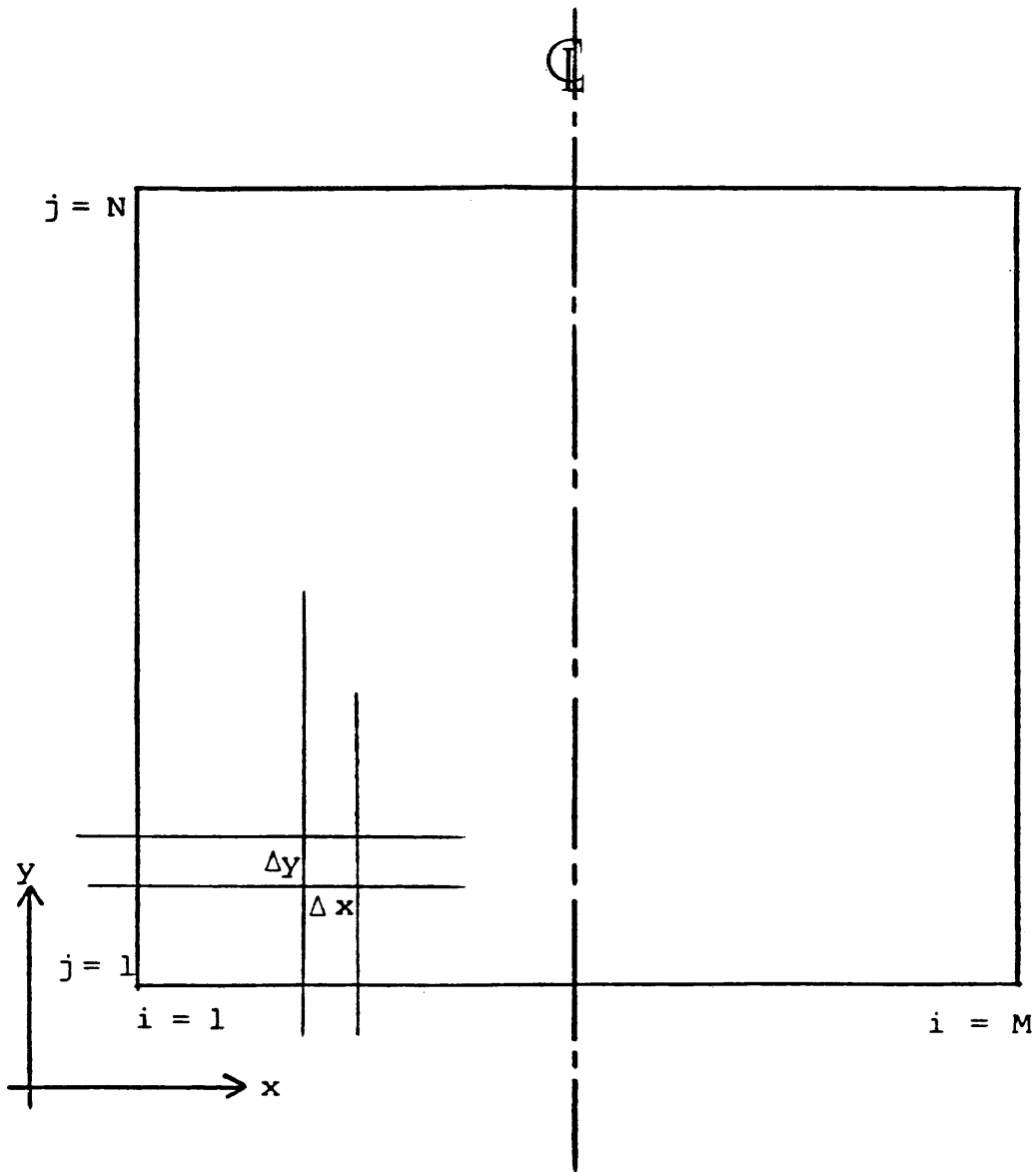


Figure 3.1
Two-Dimensional System of Grid Points

points in the vertical direction. Consistent with the development of the initial and boundary conditions, symmetry about the centerline was not imposed.

Gradients in the vertical and horizontal dimensions were expected to be of the same order of magnitude, suggesting a common spatial increment with Δx equal to Δy , could be used. This expedient results in less complicated finite difference equations. The increment was designated h . Common practice is to define this increment based on height, yielding

$$h = \frac{1}{(N-1)} \quad (3.2-1)$$

Because the horizontal to vertical ratio was a variable in this paper it was desired to standardize the increment, retaining the same step size for all calculations. A value of twenty, the minimum number of grid points used in any dimension, was chosen so that

$$h = \frac{1}{(20-1)} \quad (3.2-2)$$

Now the number of grid points, rather than the size of the spatial increment, is variable. The height-to-width ratio is varied by changing the ratio of M to N . The accuracy of the execution is increased by increasing M and N proportionately, thereby increasing the number of grid points.

For Δx equal to Δy the aspect ratio may be defined as

the ratio of M to N. An aspect ratio of one corresponds to a square grid, greater than one indicates an increase in width relative to height, and less than one signifies a two-dimensional vessel taller than it is wide.

Subscripts for the horizontal and vertical directions are "i" and "j", respectively. A superscript "n", is used for the time step, $\Delta\tau$, when required.

3.3 Finite Difference Form of the Governing Equations

3.3.1 Stream Function Equation

Solution of the stream function equation by SOR takes the finite difference form [6,7,8]:

$$\begin{aligned} \psi_{i,j}^n = & \psi_{i,j}^{n-1} + \left(\frac{\text{OPTOM}}{4} \right) \left[\psi_{i-1,j}^{n-1} + \psi_{i+1,j}^{n-1} + \psi_{i,j+1}^{n-1} \right. \\ & \left. + \psi_{i,j-1}^{n-1} - 4\psi_{i,j}^{n-1} + h^2 \omega_{i,j}^n \right] \end{aligned} \quad (3.3-1)$$

where OPTOM, the relaxation factor is equal to [7]

$$\text{OPTOM} = \frac{8 - 4\sqrt{4 - (\cos \pi/M - \cos \pi/N)}}{(\cos \pi/M - \cos \pi/N)} \quad (3.3-2)$$

Previous values of the stream function, and current values of the vorticity are required. The solution is iterative at the time step with convergence to a maximum allowable error.

3.3.2 Vorticity Transport Equation

Vorticity is directly proportional to the horizontal temperature gradient. The central difference form is:

$$\omega_{i,j} = Ra \left(\frac{\theta_{i+1,j} - \theta_{i-1,j}}{2h} \right) \quad (3.3-3)$$

Current values of the temperature are used to generate the current vorticity values.

3.3.3 Thermal Energy Equation

Temperatures at the new time step are generated by solving the thermal energy equation using an ADI technique [5,6]. The general x-implicit equation is

$$\begin{aligned} & \left(-\frac{U_{i-1,j}^n}{2h} - \frac{1}{h^2} \right) \theta_{i-1,j}^* + \left(\frac{2}{\gamma \Delta \tau} + \frac{2}{h^2} \right) \theta_{i,j}^* \\ & + \left(\frac{U_{i+1,j}^n}{2h} - \frac{1}{h^2} \right) \theta_{i+1,j}^* = \left(\frac{2}{\gamma \Delta \tau} \right) \theta_{i,j}^n + \\ & \left[\frac{v_{i,j-1}^n \theta_{i,j-1}^n - v_{i,j+1}^n \theta_{i,j+1}^n}{2h} \right] + \left[\frac{\theta_{i,j+1}^n - 2\theta_{i,j}^n + \theta_{i,j-1}^n}{h^2} \right] \end{aligned} \quad (3.3-4)$$

Similarly, the general y-implicit equation is

$$\begin{aligned} & \left(-\frac{v_{i,j-1}^n}{2h} - \frac{1}{h^2} \right) \theta_{i,j-1}^{n+1} + \left(\frac{2}{\gamma \Delta \tau} + \frac{2}{h^2} \right) \theta_{i,j}^{n+1} \\ & + \left(\frac{v_{i,j+1}^n}{2h} - \frac{1}{h^2} \right) \theta_{i,j+1}^{n+1} = \left(\frac{2}{\gamma \Delta \tau} \right) \theta_{i,j}^* + \\ & \left[\frac{U_{i-1,j}^n \theta_{i-1,j}^* - U_{i+1,j}^n \theta_{i+1,j}^*}{2h} \right] + \left[\frac{\theta_{i+1,j}^* - 2\theta_{i,j}^* + \theta_{i-1,j}^*}{h^2} \right] \end{aligned} \quad (3.3-5)$$

where superscript "*" denotes a time half step, $n+1/2$.

As illustrated in the above finite difference equations, the non-linear term was handled by using values of velocity from the current time step rather than from the new time step. (New velocity values do not exist at this point. They could be estimated by linear extrapolation or determined by iteration at the time step. Neither approach was believed necessary.) Values of the temperature at the current time step are also required.

3.3.4 Velocity Equations

Velocity is obtained from the stream function by applying central differencing to the stream function definition. The resulting equations are

$$U_{i,j} = \left(\frac{\Psi_{i,j+1} - \Psi_{i,j-1}}{2h} \right), \quad (3.3-6)$$

$$V_{i,j} = - \left(\frac{\Psi_{i+1,j} - \Psi_{i-1,j}}{2h} \right)$$

Current values of the stream function are required, yielding current values of the velocity components.

3.3.5 Species Equation for Tracer

The Species equation for tracer was solved for new values of the tracer concentration using explicit upwind

differencing [7,8]. The selection of the upwind differencing technique was made to introduce a damping factor that would eliminate oscillations and negative concentrations generated with the implicit method.

Using the steady state velocity field the upwind differencing velocities are defined as follows:

$$UF = (U_{i+1,j} + U_{i,j})/2 \quad (3.3-7)$$

$$UB = (U_{i-1,j} + U_{i,j})/2$$

$$VF = (V_{i,j+1} - V_{i,j})/2$$

$$VB = (V_{i,j-1} + V_{i,j})/2$$

the explicit form of the species equation for tracer becomes

$$E_{i,j}^{n+1} = E_{i,j}^n - P1 - P2 + (\Delta\tau/\epsilon L e h^2) \{ E_{i+1,j}^n + E_{i-1,j}^n + E_{i,j+1}^n + E_{i,j-1}^n - 4E_{i,j}^n \} \quad (3.3-8)$$

where the parameters P1 and P2 are given by

$$P1 = (\Delta\tau/2\epsilon h) (UF - |UF|) E_{i+1,j}^n + (UF + |UF| - UB + |UB|) E_{i,j}^n - (UB + |UB|) E_{i-1,j}^n \quad (3.3-9)$$

$$P2 = (\Delta\tau/2\epsilon h) (VF - |VF|) E_{i,j+1}^n + (VF + |VF| - VB + |VB|) E_{i,j}^n - (VB + |VB|) E_{i,j-1}^n \quad (3.3-10)$$

Current values of tracer concentration are used in conjunction with the upwind differencing velocities to generate the new tracer concentration values.

3.4 Finite Difference form of the Initial Conditions

3.4.1 Velocity

The initial conditions for velocity are given by

$$U_{i,j} = 0 \quad \text{for all } i, j \quad (3.4-1)$$

$$V_{i,j} = V_0 \quad \text{for all } i, j$$

V_0 , the initial velocity is calculated from

$$V_0 = -\text{RePr} \left(\frac{20-1}{N-1} \right) \quad (3.4-2)$$

where RePr is the product of a Reynolds number based on actual height and a Prandtl number employing the effective thermal diffusivity.

3.4.2 Stream Function

Requirements on the initial stream function profile are that it be linear with respect to x , and constant with respect to y . Imposing the additional constraint that the stream function be zero at the centerline, the following form can be deduced

$$\psi_{i,j} = V_0 \left(\frac{M-1}{20-1} \right) \left[\frac{1}{2} - \left(\frac{i-1}{M-1} \right) \right] \quad \text{for all } i, j \quad (3.4-3)$$

3.4.3 Temperature

The initial temperature profile is constant with

respect to x and varies with respect to y as a function of V_0 . In terms of $RePr$ it may be expressed as

$$\theta_{i,j} = 1 - (j-1)[1/(N-1)] \quad (3.4-4)$$

for no flow and

$$\theta_{i,j} = \frac{\exp[RePr[1 - (j-1)(1/(N-1))]] - 1}{\exp(RePr) - 1} \quad (3.4-5)$$

for net through-flow. These forms are consistent with the normalized initial conditions

$$\theta_{i,1} = 1 \quad \text{for all } i \quad (3.4-6)$$

$$\theta_{i,N} = 0 \quad \text{for all } i$$

3.4.4 Vorticity

The initial vorticity is zero.

$$\omega_{i,j} = 0 \quad \text{for all } i, j \quad (3.4-7)$$

3.4.5 Tracer Concentration

Tracer was introduced with the flow in a narrow rectangular pulse, approximating the impulse function.

Reference Figure 3.2.

The initial condition for tracer concentration is

$$E_{i,N} = E_{\text{initial}} \quad \text{for all } i, \tau < \delta \quad (3.4-8)$$

$$E_{i,N} = 0 \quad \text{for all } i, \tau \geq \delta$$

and

$$E_{i,j} = 0 \quad \text{for all } i, j \neq N$$

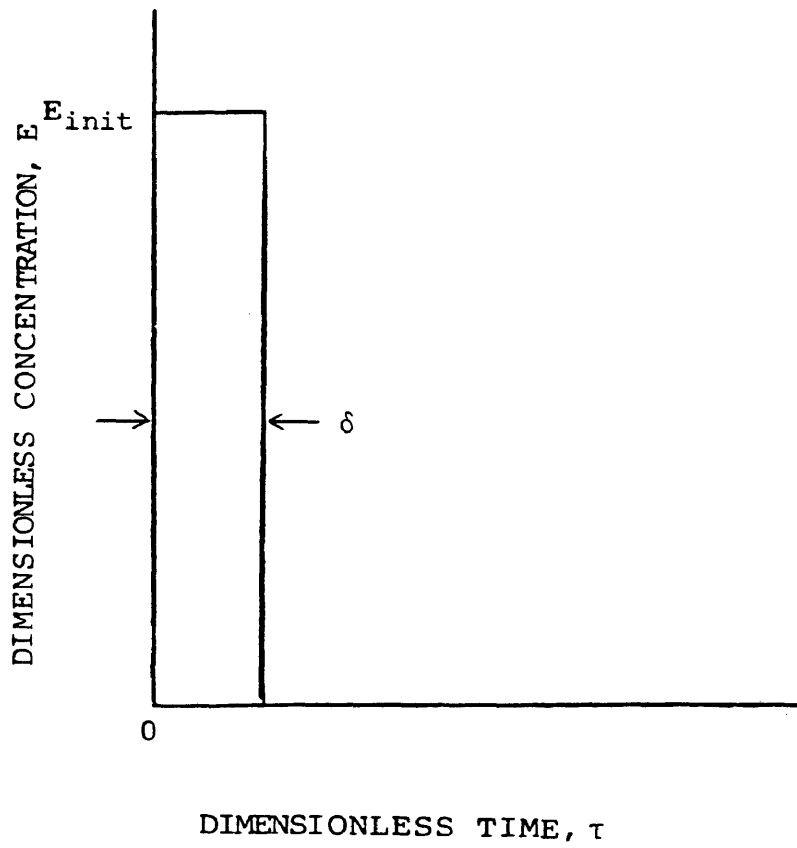


Figure 3.2
Rectangular Pulse

3.5 Finite Difference form of the Boundary Conditions

3.5.1 Velocity

Components of velocity retain their initial value at the entrance and exit

$$U_{i,j} = 0 \quad \text{for all } i, j=1 \text{ or } N \quad (3.5-1)$$

$$V_{i,j} = V_0 \quad \text{for all } i, j=1 \text{ or } N$$

At the side walls the following conditions must be satisfied

$$U_{i,j} = 0 \quad \text{for } i=1 \text{ or } M, \text{ all } j \quad (3.5-2)$$

$$\left. \frac{\partial V}{\partial X} \right|_{i=1 \text{ or } M} = 0 \quad \text{for all } j$$

The condition on velocity component V at the walls may be expressed as a first order boundary condition

$$V_{1,j} = V_{2,j} \quad \text{for all } j \quad (3.5-3)$$

$$V_{M,j} = V_{M-1,j} \quad \text{for all } j$$

First order boundary conditions are used for first order derivatives throughout this paper despite using second order finite difference equations for the following reason presented by Roache [7]. When using the vorticity stream function scheme second order forms can cause instability. The first order form is the safest to use and often gives results essentially equal to higher order forms.

3.5.2 Stream Function

The stream function retains its initial condition at all boundaries.

3.5.3 Temperature

As previously stated the boundary conditions at the entrance and exit are

$$\begin{aligned}\theta_{i,1} &= 1 && \text{for all } i && (3.5-4) \\ \theta_{i,N} &= 0 && \text{for all } i\end{aligned}$$

At the side walls

$$\left. \frac{\partial \theta}{\partial X} \right|_{i=1 \text{ or } M} = 0 \quad \text{for all } j \quad (3.5-5)$$

is expressed as the first order boundary condition

$$\begin{aligned}\theta_{1,j} &= \theta_{2,j} && \text{for all } j && (3.5-6) \\ \theta_{M,j} &= \theta_{M-1,j} && \text{for all } j\end{aligned}$$

3.5.4 Vorticity

A vorticity boundary condition is not explicitly required for solution of the finite difference form of the governing system of equations.

3.5.5 Tracer Concentration

Concentration of tracer at the inlet is specified by

the concentration and duration of the impulse. The boundary condition at the side walls

$$\left. \frac{\partial E}{\partial X} \right|_{i=1 \text{ or } M} = 0 \quad \text{for all } j \quad (3.5-7)$$

is expressed as

$$E_{1,j} = E_{2,j} \quad \text{for all } j \quad (3.5-8)$$

$$E_{M,j} = E_{M-1,j} \quad \text{for all } j$$

The condition at the exit

$$\left. \frac{\partial E}{\partial Y} \right|_{j=N} = 0 \quad \text{for all } i \quad (3.5-9)$$

becomes

$$E_{i,N} = E_{i,N-1} \quad \text{for all } i \quad (3.5-11)$$

3.6 Execution

3.6.1 Overview

The execution was carried out in two successive steps: solution of the flow equations for the steady state velocity field, followed by solution of the species equation for tracer. The former provided stream function and temperature contours in addition to the velocity field. The later result was used to generate the RTD and tracer concentration contours.

A criterion was needed to establish when steady state had been reached. It was believed that a function of

vorticity could be used: when vorticity ceased to increase with time the steady state would be attained. Inspection of preliminary results suggested using the natural logarithm of the root mean square (rms) average vorticity as it varied with time.

3.6.2 Flow Calculations

The numerical approach to the flow calculations was as follows:

- 1) Iterative solution of the stream function Poisson's equation with SOR.
- 2) Calculation of the velocity components by central difference.
- 3) Solution of the time-dependent thermal energy equation by an ADI technique.
- 4) Calculation of vorticity by central difference.
- 5) Repetition of steps (1) through (4) until the steady state is reached.

Reference figure 3.3 for the flow diagram.

A time step of $\Delta\tau = 5$ and a nominal value for the ratio of specific heats, $\gamma = 2 \times 10^{-4}$, were used in all executions. Note that the ratio of specific heats occurs only in conjunction with the time step. Modifying its value has the same effect as changing the time step.

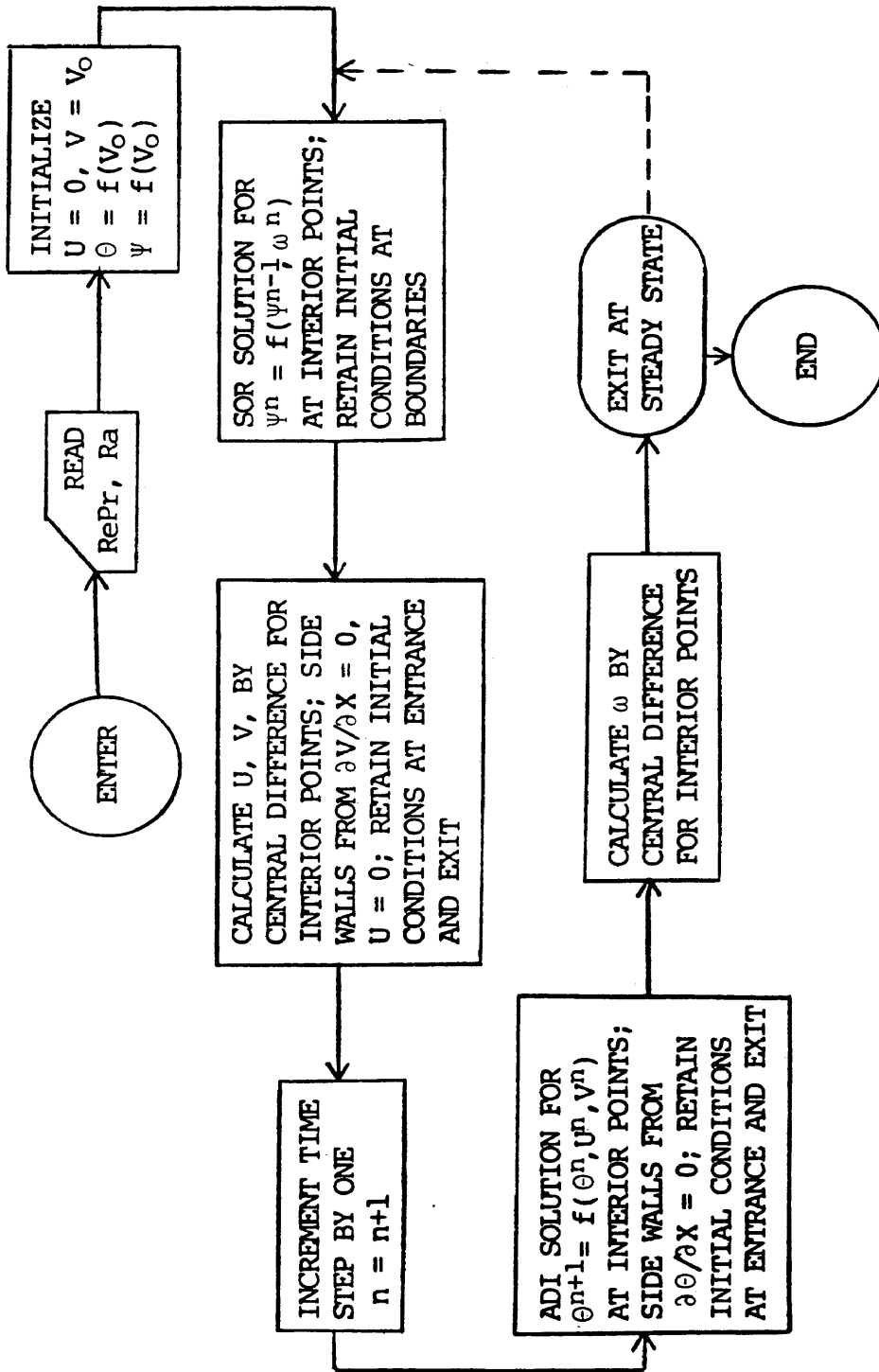


Figure 3.3
Flow Diagram for Flow Calculations

3.6.3 Tracer Concentration Calculation

Solution of the time dependent species equation for tracer using the steady state velocities was with an explicit upwind differencing technique. Nominal values of porosity, the Lewis number, and pulse duration were selected. They were: $\epsilon = 0.35$, $Le = 40$, $N_{trace} = 10$. The time step, for most executions, was $\Delta\tau = 0.0001$. In a result similar to that for the flow calculations, porosity is always associated with the time step and modifications to its value have the effect of modifying the time step.

Results are presented in a form suitable for comparison with previous work. The RTD used was the average dimensionless concentration of tracer at the exit versus a dimensionless residence time. The average concentration at the exit is comparable to the five point cup mixing average concentration used by Feuerherm.

The dimensionless residence time, τ^* is the dimensionless time, τ divided by the residence time for the vessel in dimensionless terms, τ_{res}

$$\tau^* = \frac{\tau}{\tau_{res}} \quad (3.6-1)$$

The residence time for the vessel, t_{res} , is the void volume divided by the volumetric flow rate, where for a

vessel of unit depth the void volume is the product of height, width and porosity, and the volumetric flow rate is the product of width and the superficial velocity. Expressing the superficial velocity in terms of RePr

$$v_o = \frac{\text{RePr } \alpha'}{\text{height}} \quad (3.6-2)$$

the residence time for the vessel is

$$t_{\text{res}} = \frac{\text{height}^2 \epsilon}{\text{RePr } \alpha'} \quad (3.6-3)$$

In dimensionless terms, the height is

$$\text{height} = \left(\frac{N-1}{20-1} \right) H \quad (3.6-4)$$

and the dimensionless residence time for the vessel is

$$\tau_{\text{res}} = \frac{\epsilon}{\text{RePr}} \left(\frac{N-1}{20-1} \right)^2 \quad (3.6-5)$$

Finally, the dimensionless residence time is

$$\tau^* = \frac{\tau \text{ RePr}}{\epsilon} \left(\frac{20-1}{N-1} \right)^2 \quad (3.6-6)$$

The dimensionless time τ was used in executing the program. τ^* was calculated for presentation of RTDs only.

One last step remains to allow full comparison of the RTDs: the dimensionless concentration of the pulse must be standardized. This was done by requiring a standard mass of tracer to be introduced with the flow. This mass is given by

$$\text{mass} = \frac{\text{volumetric flow rate}}{\text{flow rate}} \times \frac{\text{pulse duration}}{\text{duration}} \times C_{\text{initial}} \quad (3.6-7)$$

In terms of RePr the mass is

$$\text{mass} = \frac{\text{RePr } \alpha'}{\text{height}} \times \text{width} \times C_{\text{initial}} \times \text{pulse duration} \quad (3.6-8)$$

To obtain a dimensionless initial concentration the mass must be expressed in terms of the reference concentration C_{A0} , as well. Defining C_{A0} as the initial concentration in a perfectly mixed vessel, the mass may be obtained from the relationship

$$C_{A0} = \frac{\text{mass}}{\text{void volume}} \quad (3.6-9)$$

Substituting and rearranging,

$$\text{mass} = C_{A0} \times \text{height} \times \text{width} \times \epsilon \quad (3.6-10)$$

The result of equating the two expressions for mass is

$$E_{\text{initial}} = \frac{C_{\text{initial}}}{C_{A0}} = \frac{\epsilon \text{ height}^2}{\text{RePr } \alpha' \text{ pulse duration}} \quad (3.6-11)$$

The pulse duration in dimensionless terms is

$$\text{pulse duration} = \Delta\tau N_{\text{trace}} \left(\frac{H^2}{\alpha'} \right) \quad (3.6-12)$$

where $\Delta\tau$ is the dimensionless time step and N_{trace} is the number of time steps. The initial concentration becomes

$$E_{\text{initial}} = \frac{\epsilon}{\text{RePr } \Delta\tau N_{\text{trace}}} \left(\frac{N-1}{20-1} \right)^2 \quad (3.6-13)$$

Figure 3.2 may be reconstructed in terms of the dimensionless concentration and dimensionless residence time defined in this section. Rewriting E_{initial} as

$$E_{\text{initial}} = \frac{\tau_{\text{res}}}{\Delta\tau N_{\text{trace}}} \quad (3.6-14)$$

and the pulse duration δ as

$$\delta = \Delta\tau \cdot N_{\text{trace}} \quad (3.6-15)$$

or,

$$\delta^* = \frac{\Delta\tau N_{\text{trace}}}{\tau_{\text{res}}} \quad (3.6-16)$$

Figure 3.4 results. It is apparent that the area under the pulse is equal to one. Applying conservation of mass, the following relationship for the average exit concentration may be deduced

$$\int_0^{\infty} E(\tau^*) d\tau^* = 1 \quad (3.6-17)$$

Hence, the area beneath the RTD curve will always be one.

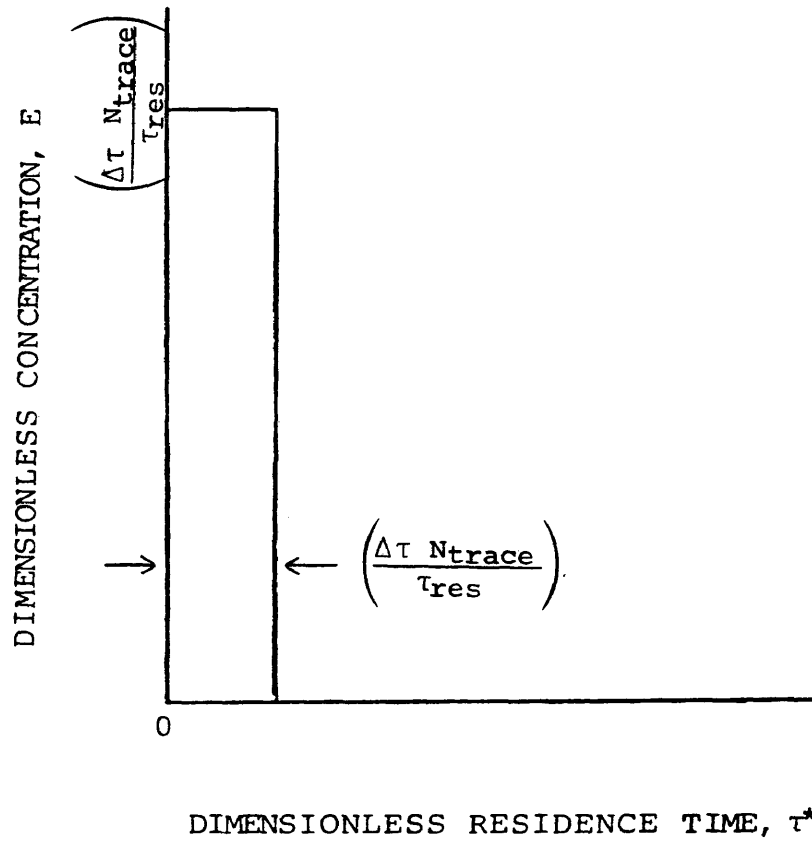


Figure 3.4
Rectangular Pulse in Dimensionless Variables

4. THE PERFECTLY MIXED VESSEL AND PLUG FLOW

As discussed in the introduction, tracer response theory presents two limiting cases: the perfectly mixed vessel, and plug flow. For comparison with results of computations, these will be developed in the dimensionless variables of this paper: E and τ^* .

The response of a perfectly mixed vessel to a unit impulse is given by

$$E = \exp^{-}(\tau^*) \quad (4.0-1)$$

Applying equation (3.6-17) the predictable result is

$$\int_0^{\infty} \exp^{-}(\tau^*) d\tau^* = 1 \quad (4.0-2)$$

Having set the reference concentration equal to the initial concentration in the perfectly mixed vessel the initial concentration in dimensionless terms must be

$$E = \frac{C_A}{C_{A0}} = 1 \quad (4.0-3)$$

For plug flow, the species equation for tracer becomes

$$\epsilon \frac{\partial E}{\partial \tau} = \frac{1}{Le} \left[\frac{\partial^2 E}{\partial Y^2} - v \frac{\partial E}{\partial Y} \right] \quad (4.0-4)$$

following the solution presented by Friedley [15] we use the boundary conditions

$$E = \delta \quad \text{at } j=N \quad (4.0-5)$$

$$\frac{\partial E}{\partial Y} = 0 \quad \text{at } j=1$$

The Laplace transform solution for a unit impulse is given by

$$E(Y,s) = \overline{G(Y,s)} \cdot \delta = G(Y,s) \quad (4.0-6)$$

where $G(Y,s)$ is the transfer function. Taking the limit as the bed height approaches infinity, the inverse of the transfer function, and hence the exit concentration is

$$E(Y,\tau^*) = \frac{1}{2\sqrt{\pi}} \left(\frac{Pe}{\tau^{*3}} \right)^{1/2} \exp \left[\frac{-Pe}{4\tau^*} (\tau^* - 1)^2 \right] \quad (4.0-7)$$

Results for plug flow are characterized by a Peclet number for mass dispersion, reference Friedley.

$$Pe = \frac{\text{height } v_0}{D} \quad (4.0-8)$$

Since

$$RePr = \frac{\text{height } v_0}{\alpha'} \quad (4.0-9)$$

and

$$Le = \frac{\alpha'}{D} \quad (4.0-10)$$

The Peclet number may be reconstructed as

$$Pe = RePr \cdot Le \quad (4.0-11)$$

5. PRESENTATION OF RESULTS

5.1 Increase in Vorticity with Time

The first task was to recognize the presence of free convection and detect when the steady state had been achieved. As previously discussed, preliminary tests suggested using the natural logarithm of the rms average vorticity as it varied with time. Graphs of the natural log of the dimensionless vorticity versus dimensionless time are presented in Figures 5.1 through 5.4 for various $RePr$ and Ra numbers. Convecting cases are easily identified by a linear growth in the log of vorticity which abruptly ceases when the steady state is reached. The overshoot and oscillation observed at the juncture is typical of an implicit method. Non-convecting cases were also easily identified: discounting the initial start-up, no growth in vorticity was discerned. In summary, the vorticity criterion tells unambiguously when steady state is reached.

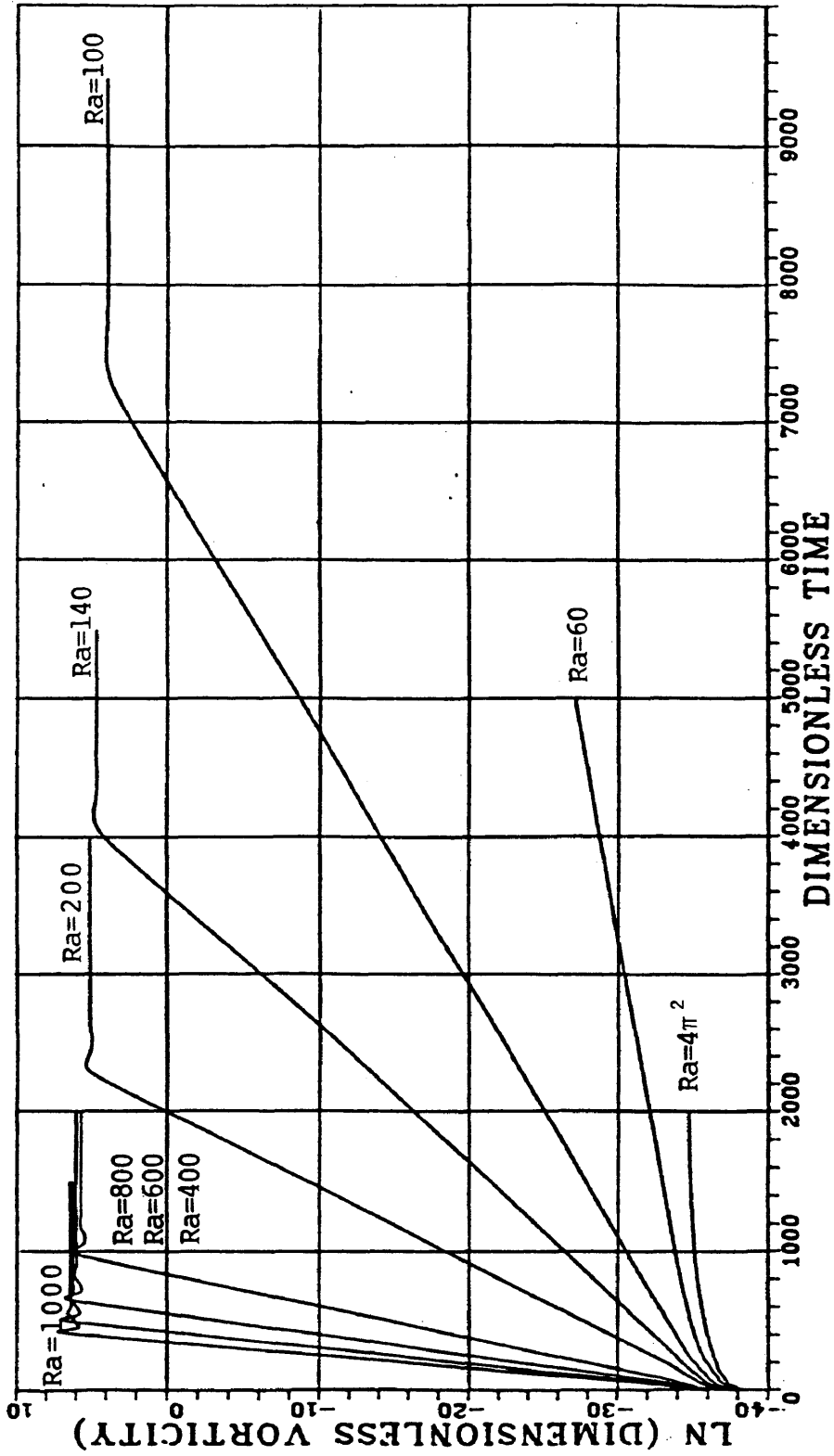


Figure 5.1
Increase in Vorticity
RePr=0, M/N=20/20

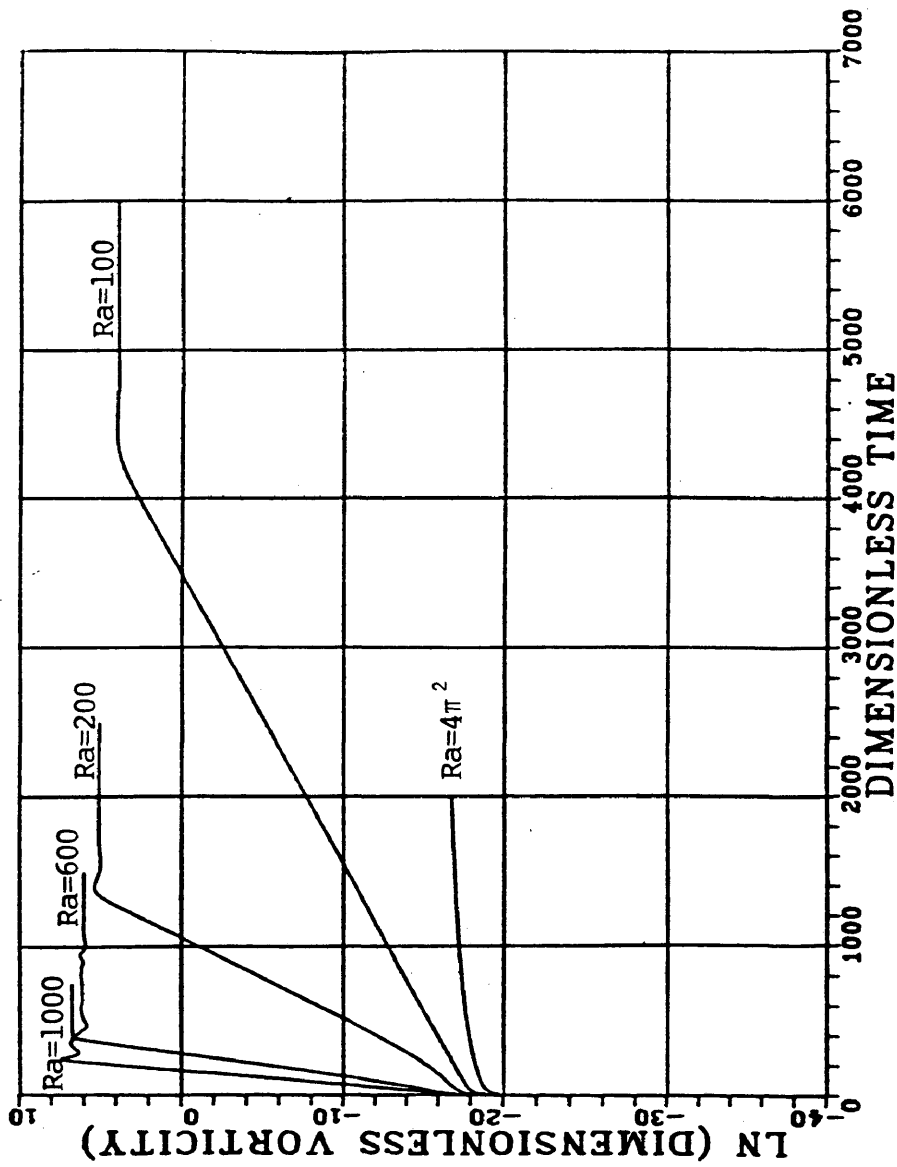


Figure 5.2
Increase in Vorticity
 $RePr=1, M/N=20/20$

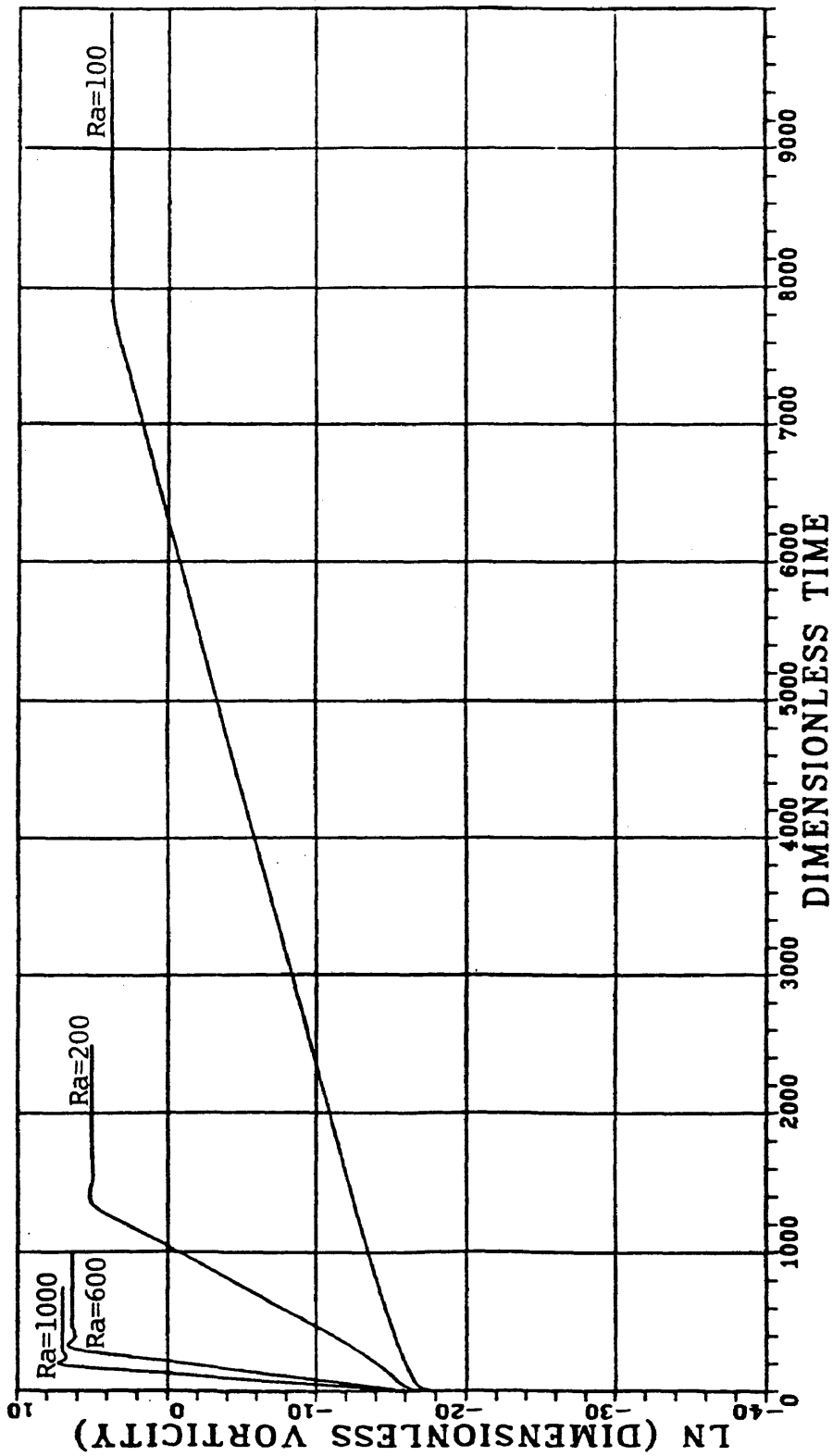


Figure 5.3
Increase in Vorticity
 $RePr=4, M/N=20/20$

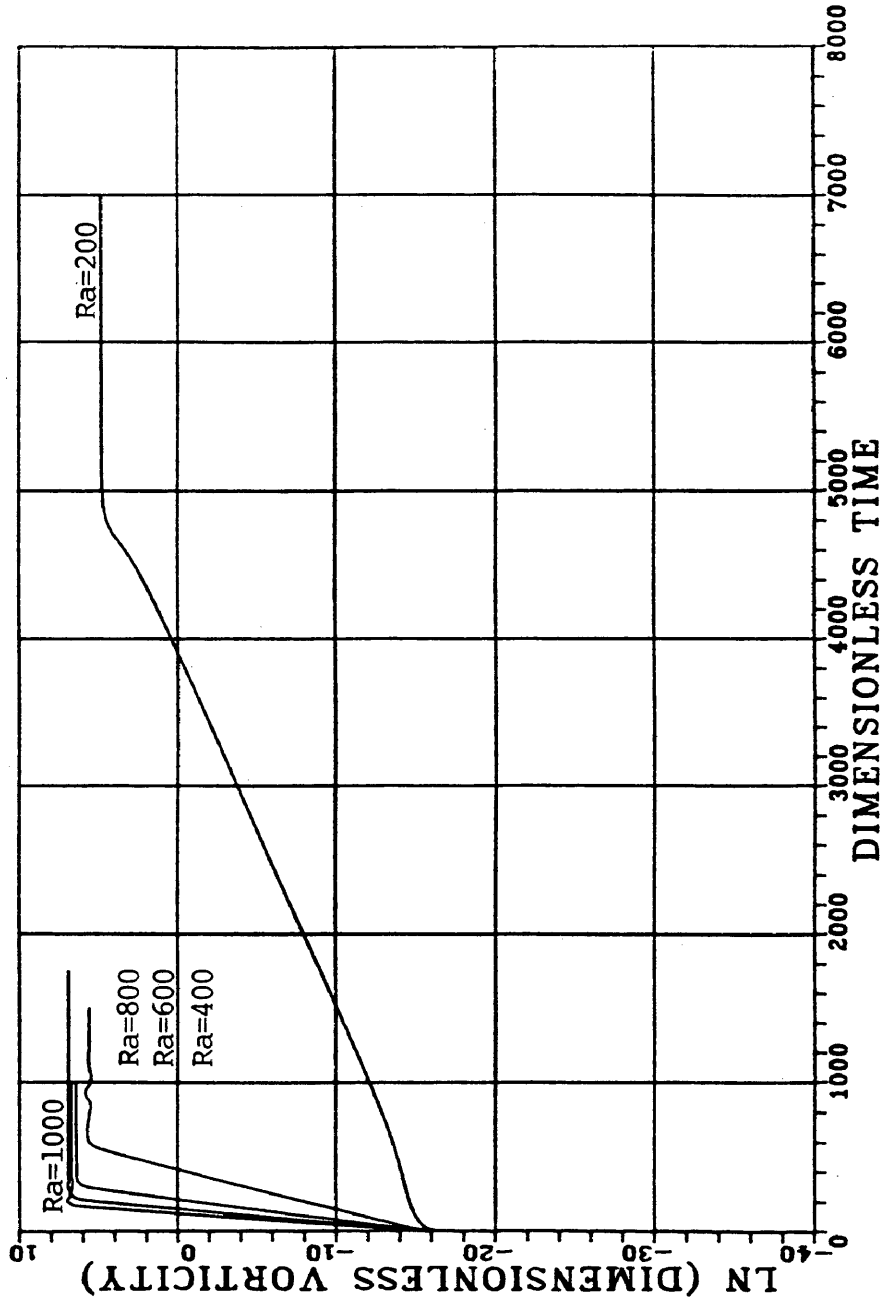


Figure 5.4
Increase in Vorticity
RePr=10, M/N=20/20

5.2 Stream Function and Temperature Contours

Confirmation that free convection was occurring was readily obtained by viewing contour plots of the stream function and temperature at steady state. Cell patterns with one, two, three, and four cells were observed. Results for a square grid, aspect ratio equal to one ($M/N = 20/20$), are summarized in Table 5.1. Figure 5.5 presents a sample initial temperature profile for $RePr = 0$. Representative examples of paired stream function and temperature contours for convecting flow are presented in Figures 5.6 through 5.15. Additional flow contours for various aspect ratios are presented in Figures 5.16 through 5.23 for $RePr = 4$, $Ra = 200$ and in Figures 5.24 and 5.25 for $RePr = 4$, $Ra = 600$.

Table 5.1

Number of Convecting Cells, $M/N = 20/20$

RePr \ Ra	0	1	4	10
100	1	1	1	-
140	2	-	-	-
200	2	2	2	2
400	2	-	-	2
600	2	2	3	4
800	2	-	-	4
1000	2	3	4	4

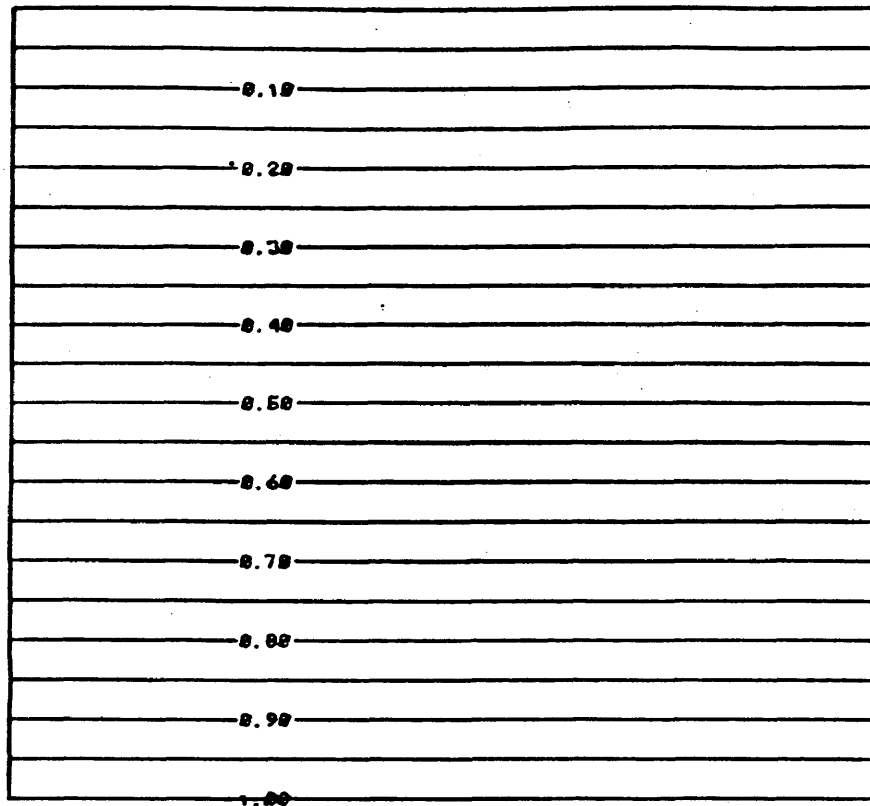


Figure 5.5
Initial Temperature Contour
RePr=0, M/N=20/20

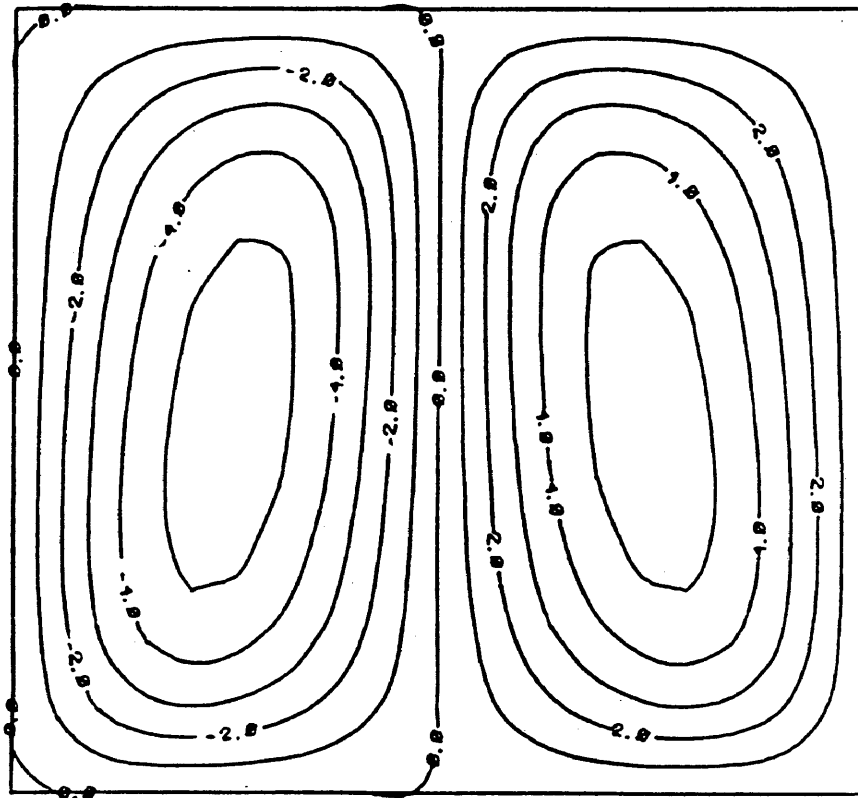


Figure 5.6
Stream Function Contour
 $RePr=0$, $Ra=200$, $M/N=20/20$

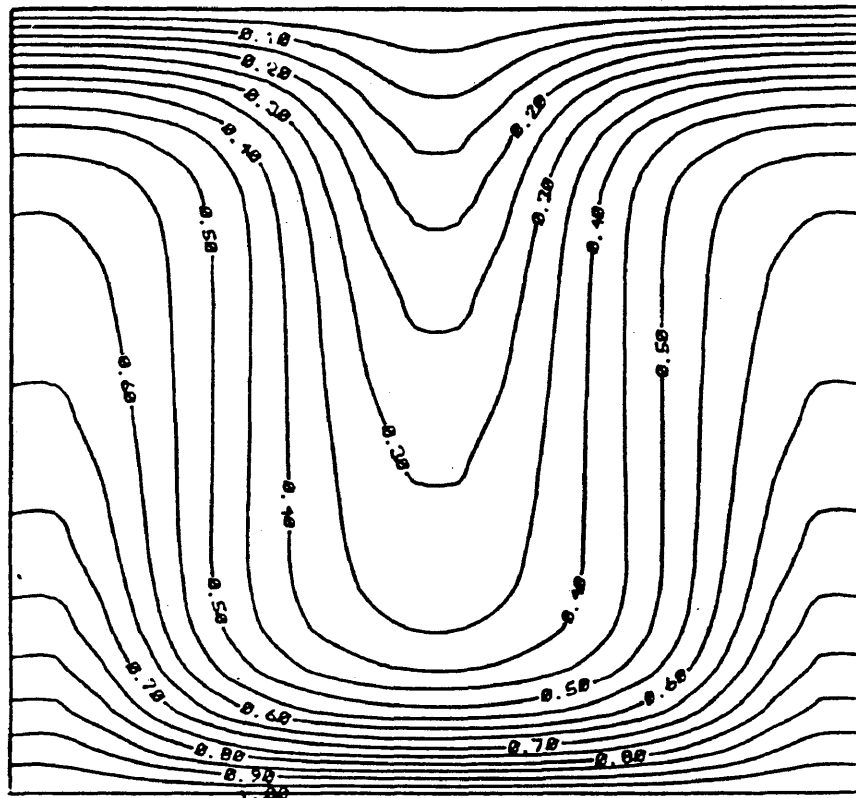


Figure 5.7
Temperature Contour
 $RePr=0$, $Ra=200$, $M/N=20/20$

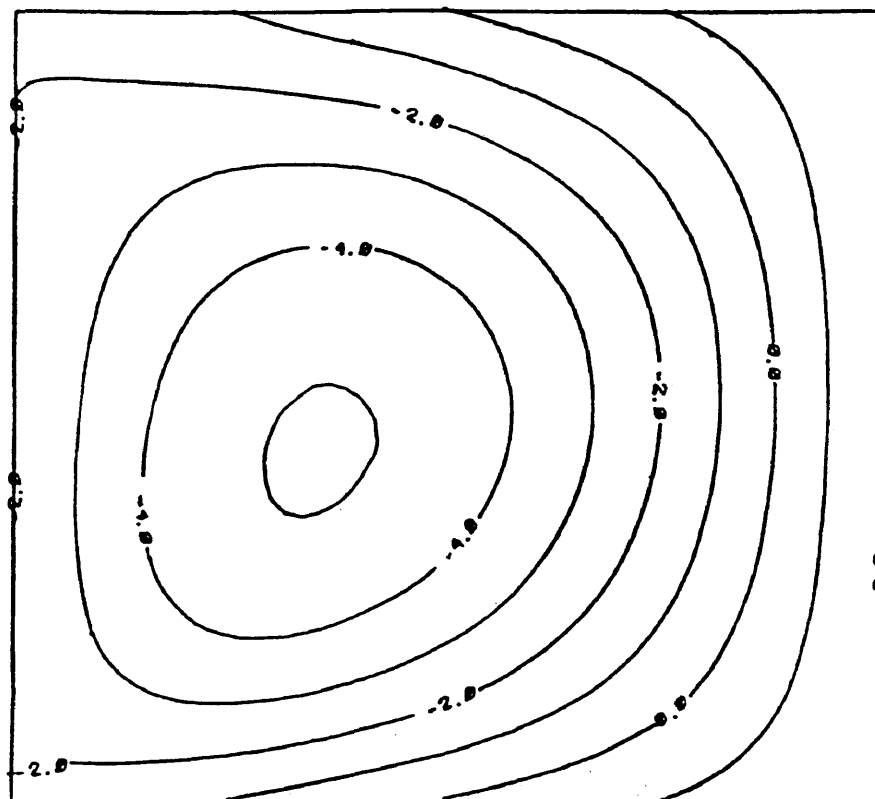


Figure 5.8
Stream Function Contour
 $RePr=4$, $Ra=100$, $M/N=20/20$

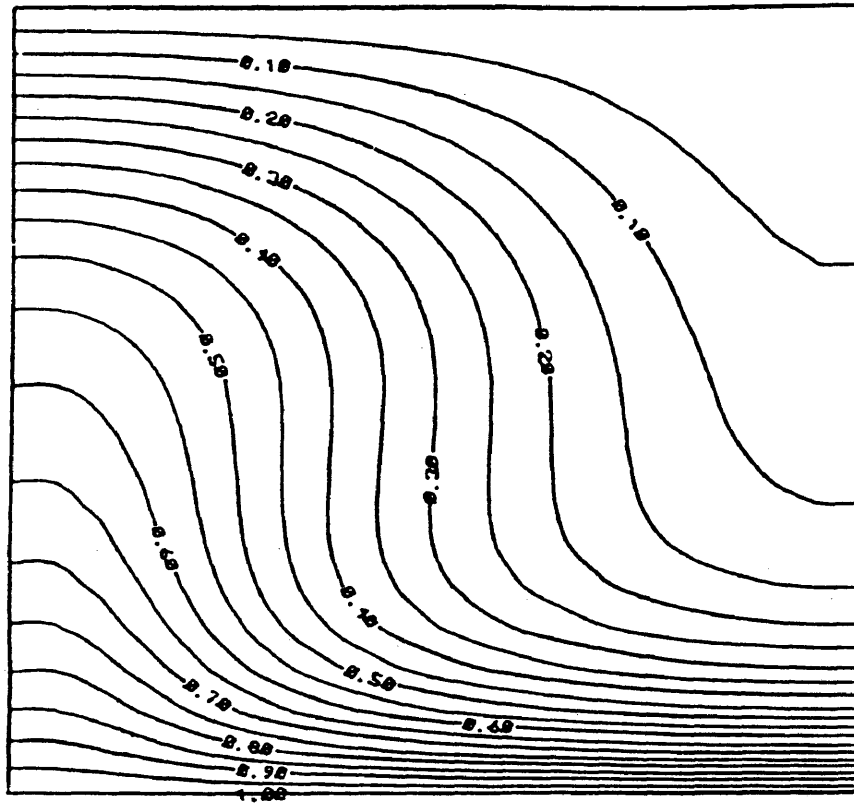


Figure 5.9
Temperature Contour
 $RePr=4$, $Ra=100$, $M/N=20/20$

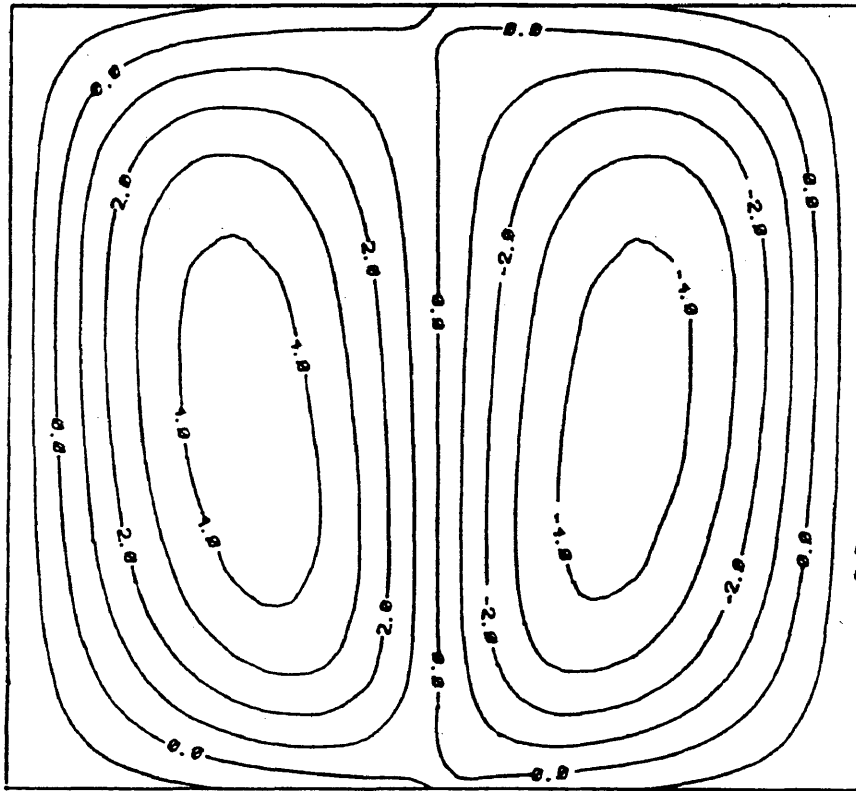


Figure 5.10
Stream Function Contour
 $RePr=4, Ra=200, M/N=20/20$

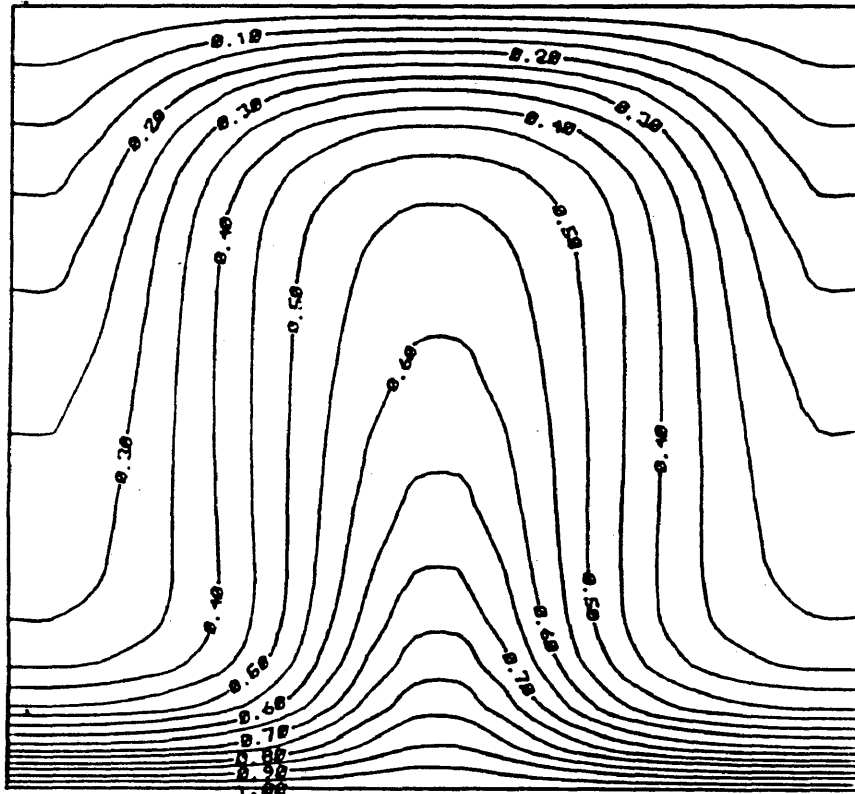


Figure 5.11
Temperature Contour
 $RePr=4$, $Ra=200$, $M/N=20/20$

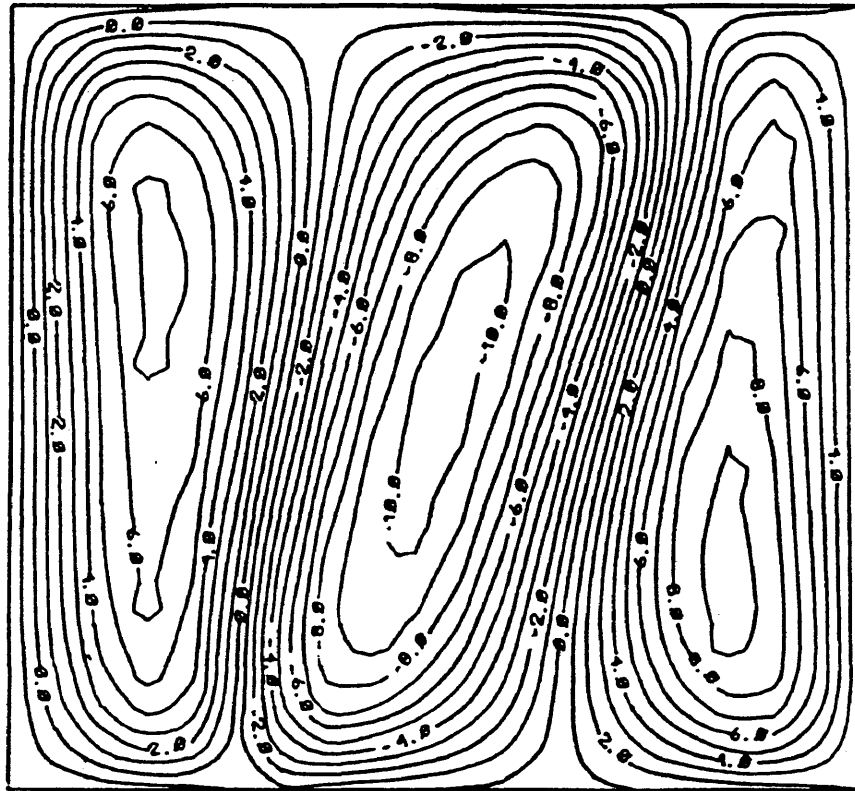


Figure 5.12
Stream Function Contour
 $RePr=4, Ra=600, M/N=20/20$

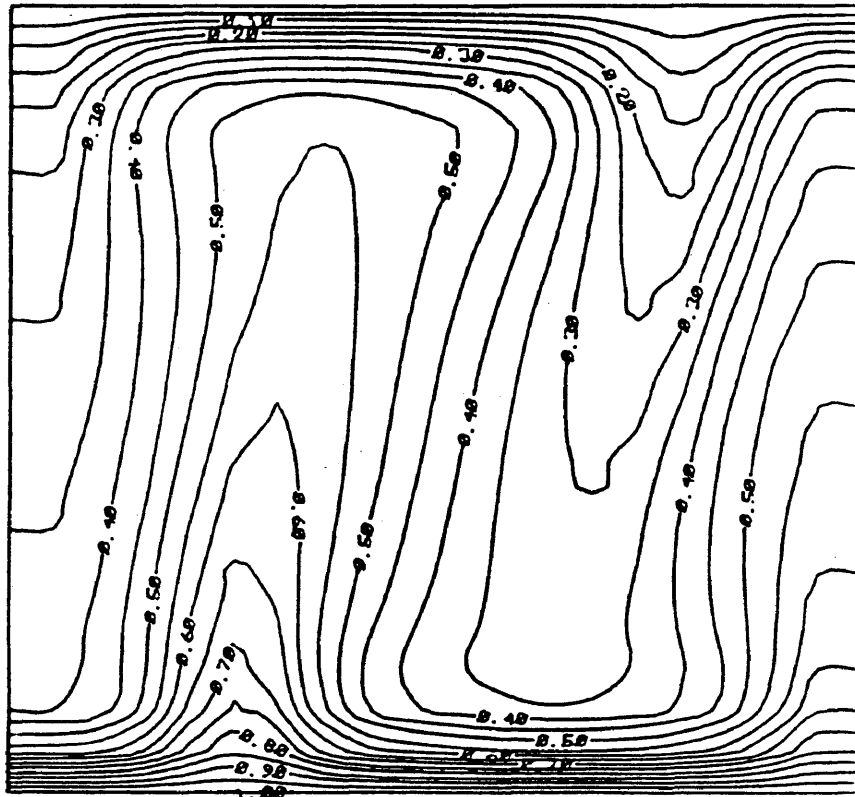


Figure 5.13
Temperature Contour
 $RePr=4$, $Ra=600$, $M/N=20/20$

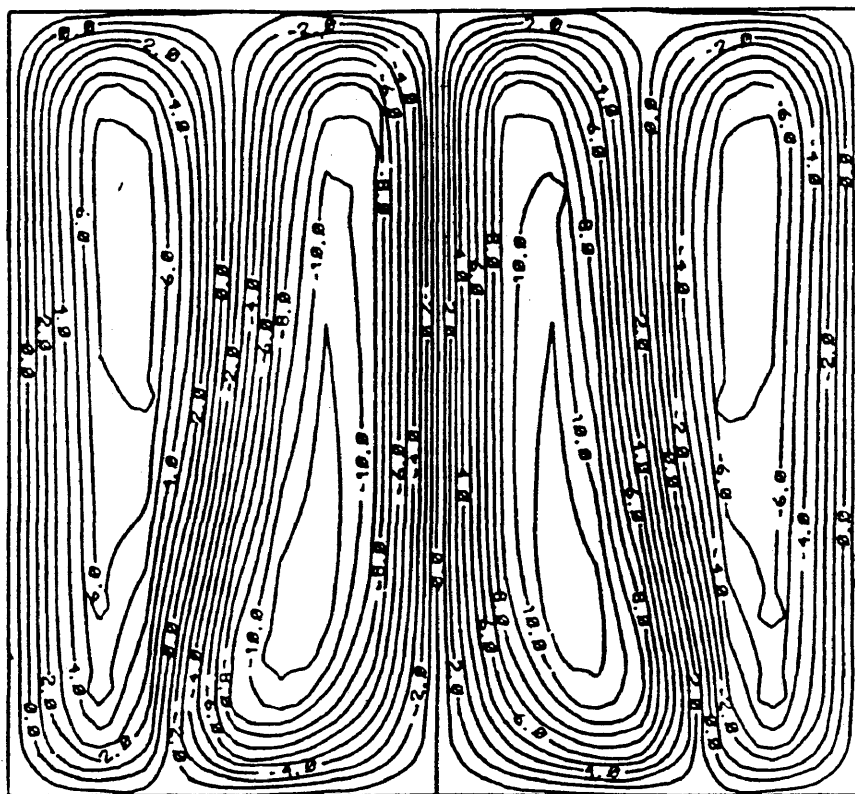


Figure 5.14
Stream Function Contour
 $RePr=4$, $Ra=1000$, $M/N=20/20$

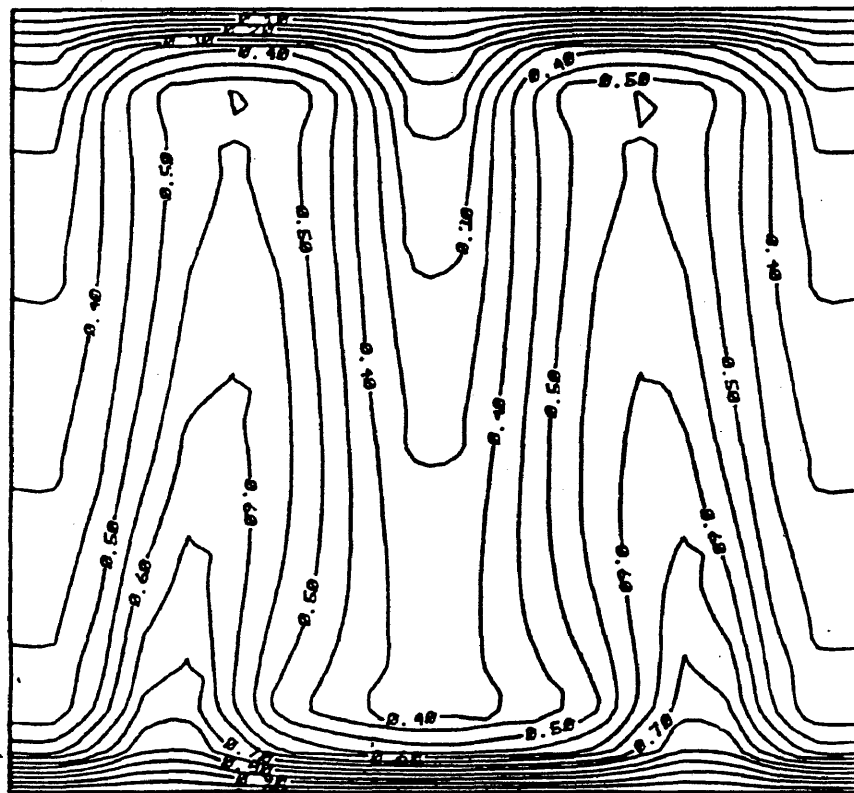


Figure 5.15
Temperature Contour
 $RePr=4$, $Ra=1000$, $M/N=20/20$

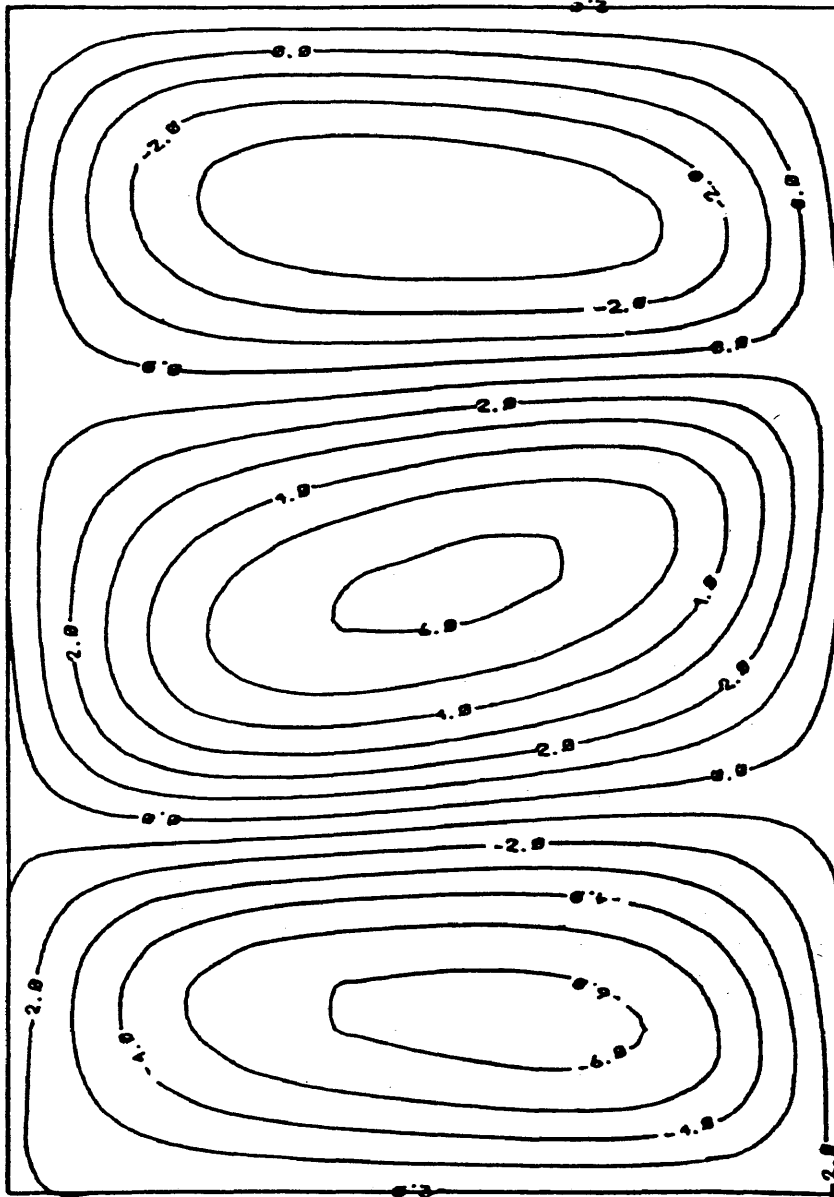


Figure 5.16
Stream Function Contour
RePr=4, Ra=200, M/N=30/20

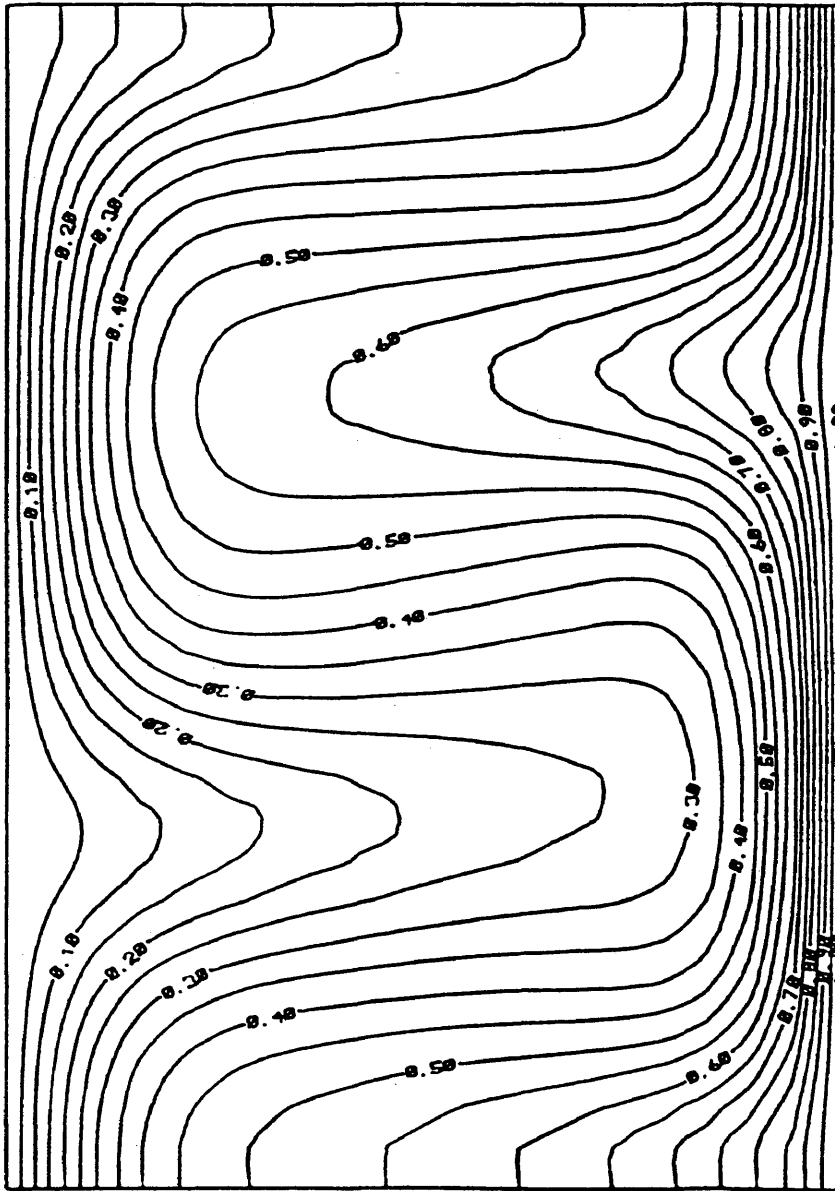


Figure 5.17
Temperature Contour
RePr=4, Ra=200, M/N=30/20

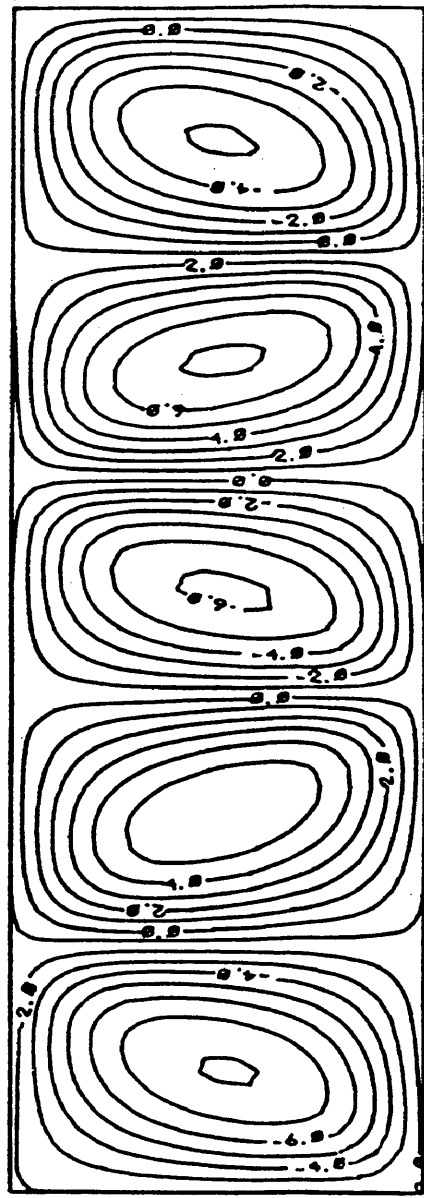


Figure 5.18
Stream Function Contour
RePr=4, Ra=200, M/N=60/20

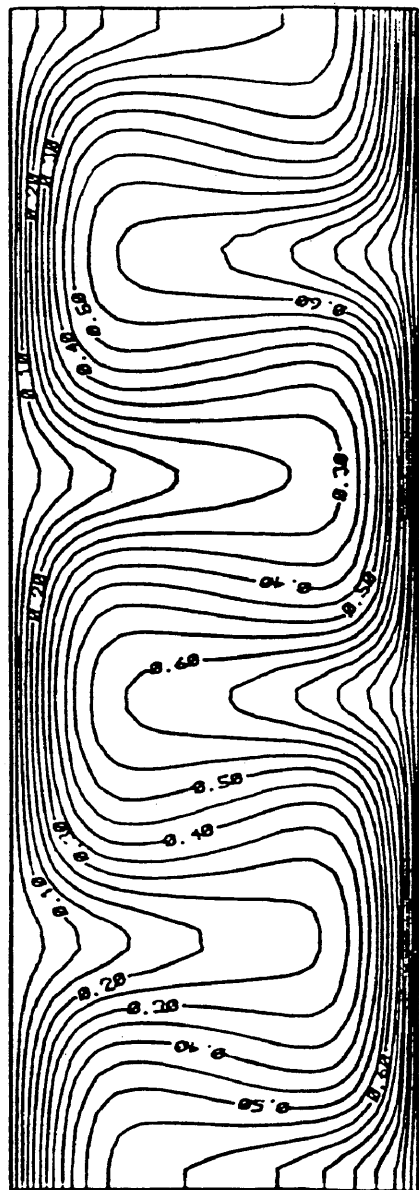


Figure 5.19
Temperature Contour
RePr=4, Ra=200, M/N=60/20

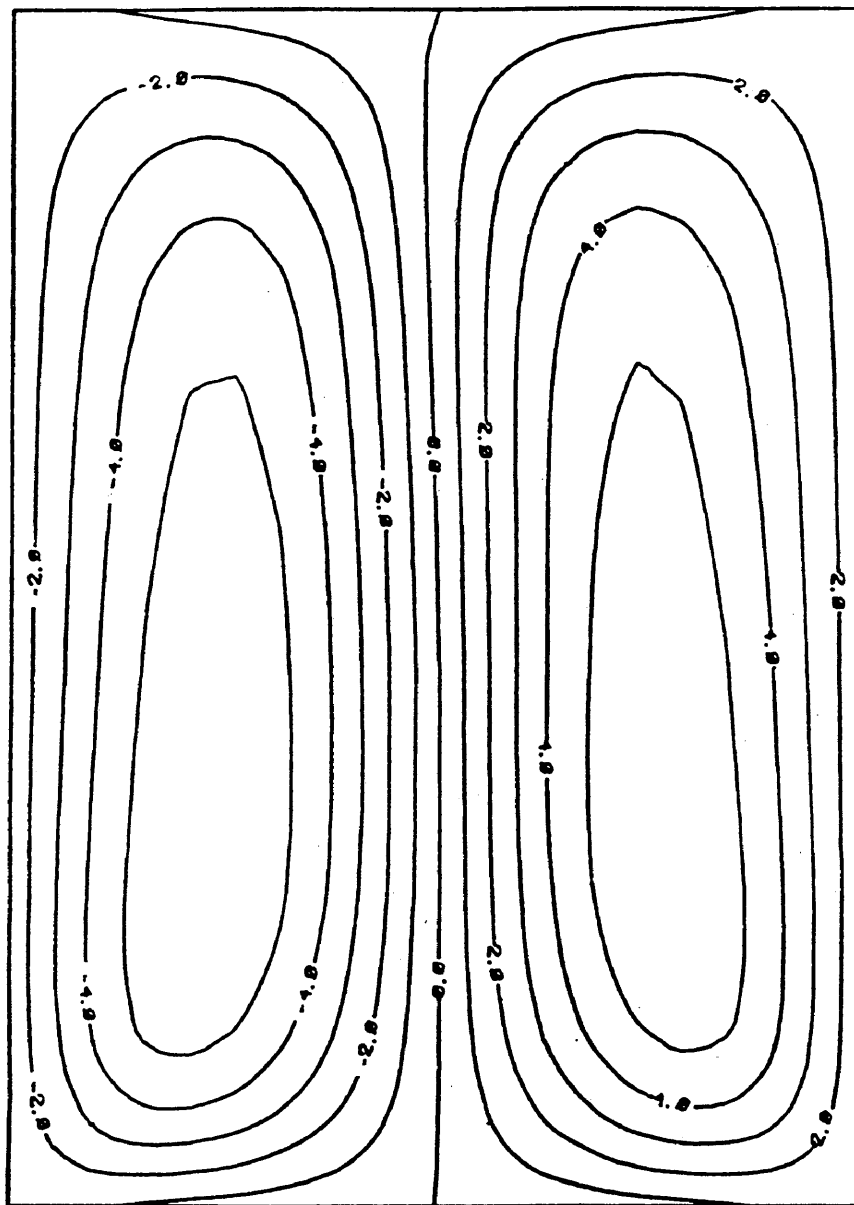


Figure 5.20
Stream Function Contour
 $RePr=4$, $Ra=200$, $M/N=20/30$

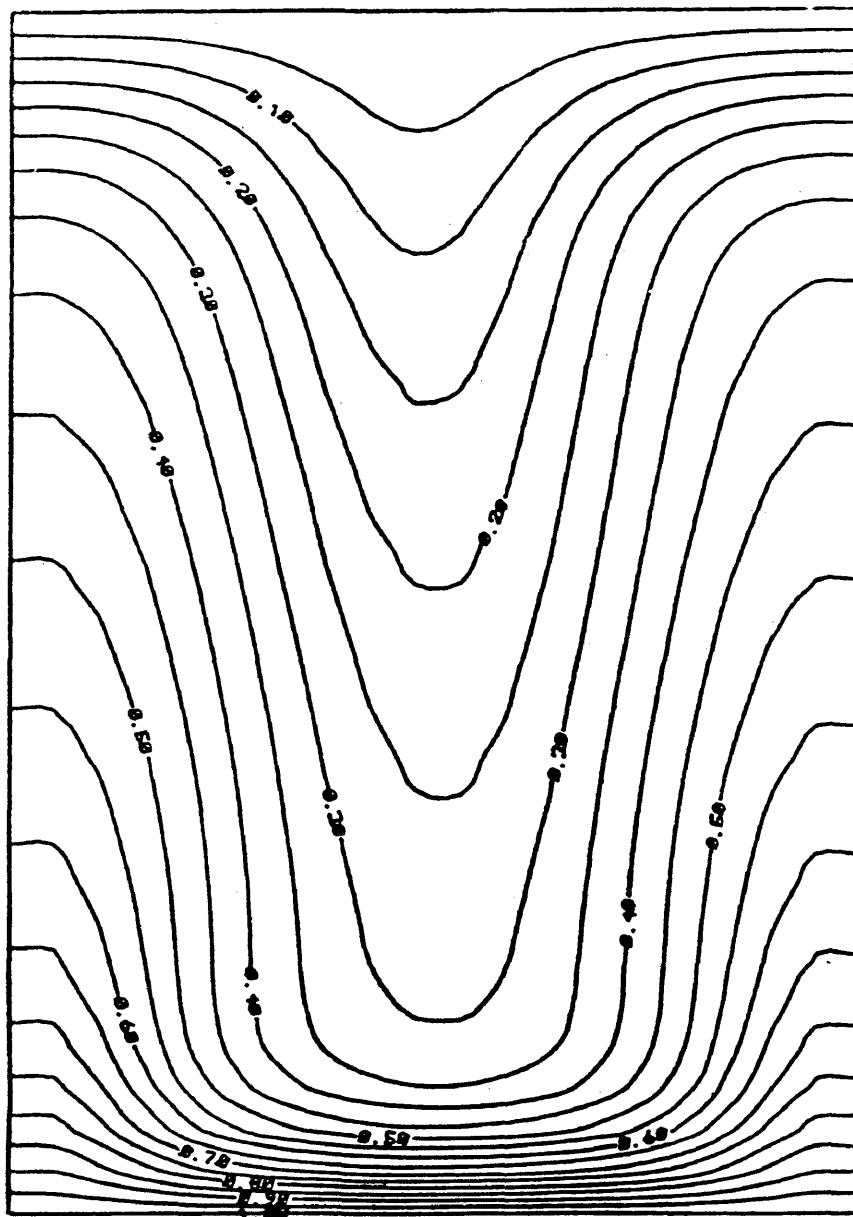


Figure 5.21
Temperature Contour
 $RePr=4$, $Ra=200$, $M/N=20/30$

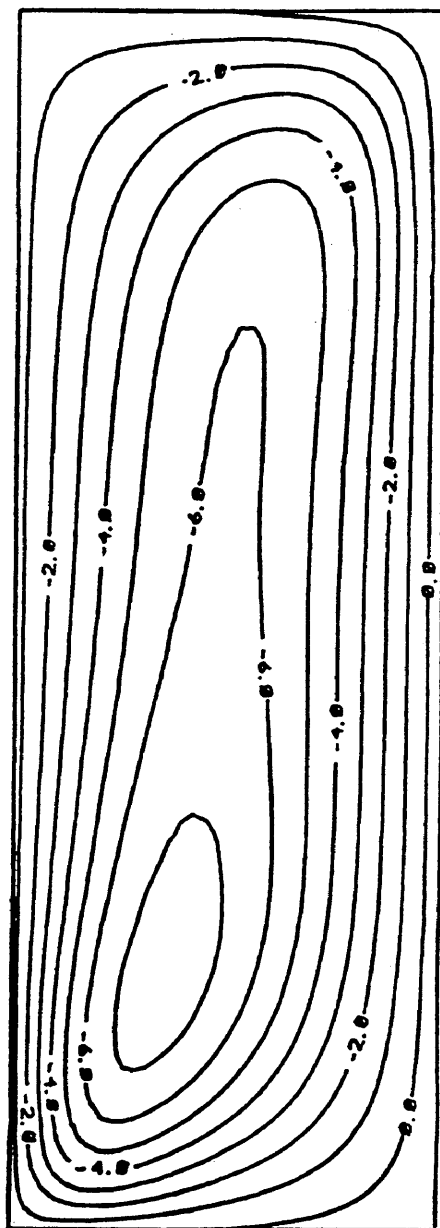


Figure 5.22
Stream Function Contour
 $RePr=4$, $Ra=200$, $M/N=20/60$

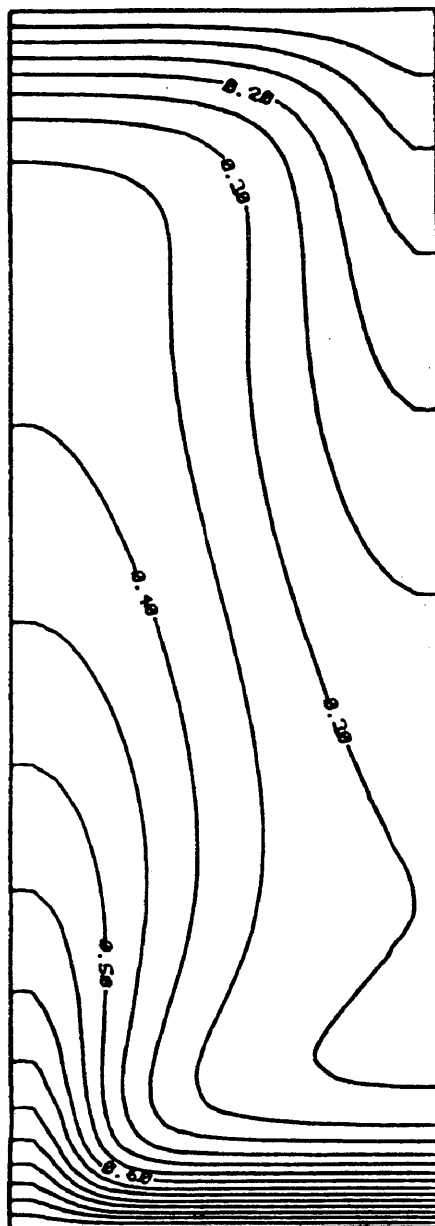


Figure 5.23
Temperature Contour
 $RePr=4$, $Ra=200$, $M/N=20/60$

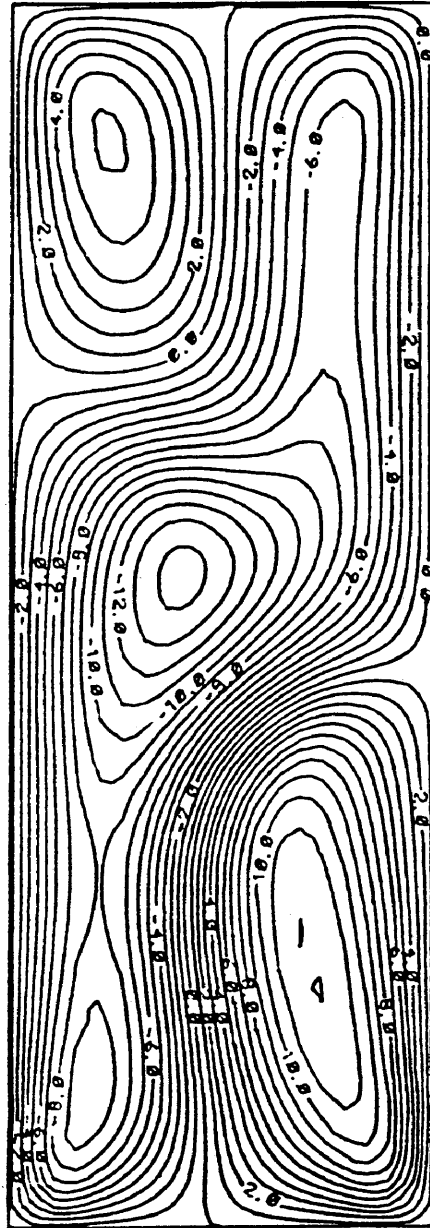


Figure 5.24
Stream Function Contour
 $RePr=4$, $Ra=600$, $M/N=20/60$

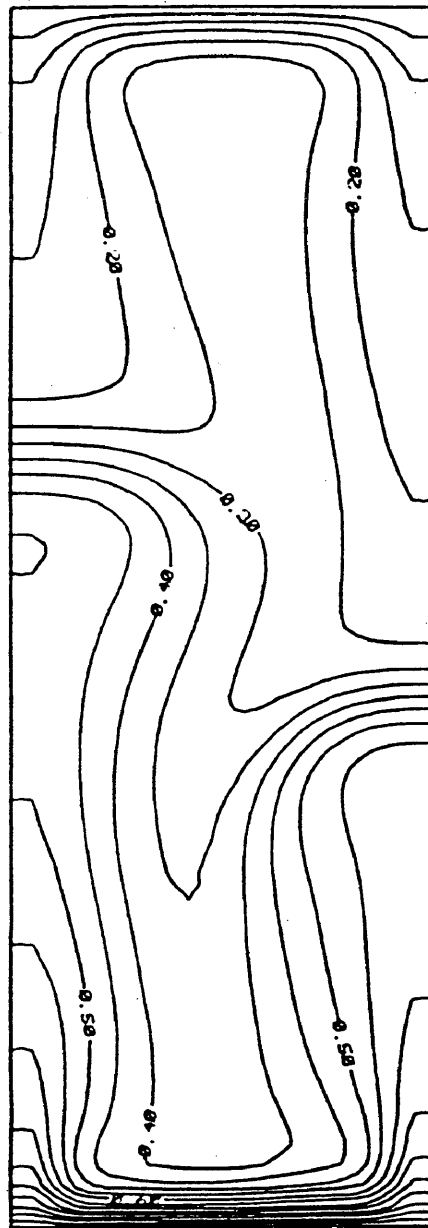


Figure 5.25
Temperature Contour
 $Re_P=4$, $Ra=600$, $M/N=20/60$

5.3 Tracer RTDs and Contours

The response of the various steady state flows to a rectangular pulse of tracer was observed for through-flow cases. It was desired to correlate variations in the number of cells, $RePr$, and Ra number with the form of the RTD. RTDs for various cases, aspect ratio equal to one, are presented in Figures 5.26 through 5.35.

Tracer concentration contours corresponding to the RTD of Figure 5.29, $RePr = 4$, $Ra = 200$, $M/N = 20/20$ are presented at successive times in Figures 5.36 through 5.47; these contours allow the movement of tracer through the flow to be followed. (Refer to Figures 5.10 and 5.11 for the applicable stream function and temperature contours.) Additional RTDs for variations in the aspect ratio are presented in Figures 5.48 through 5.52.

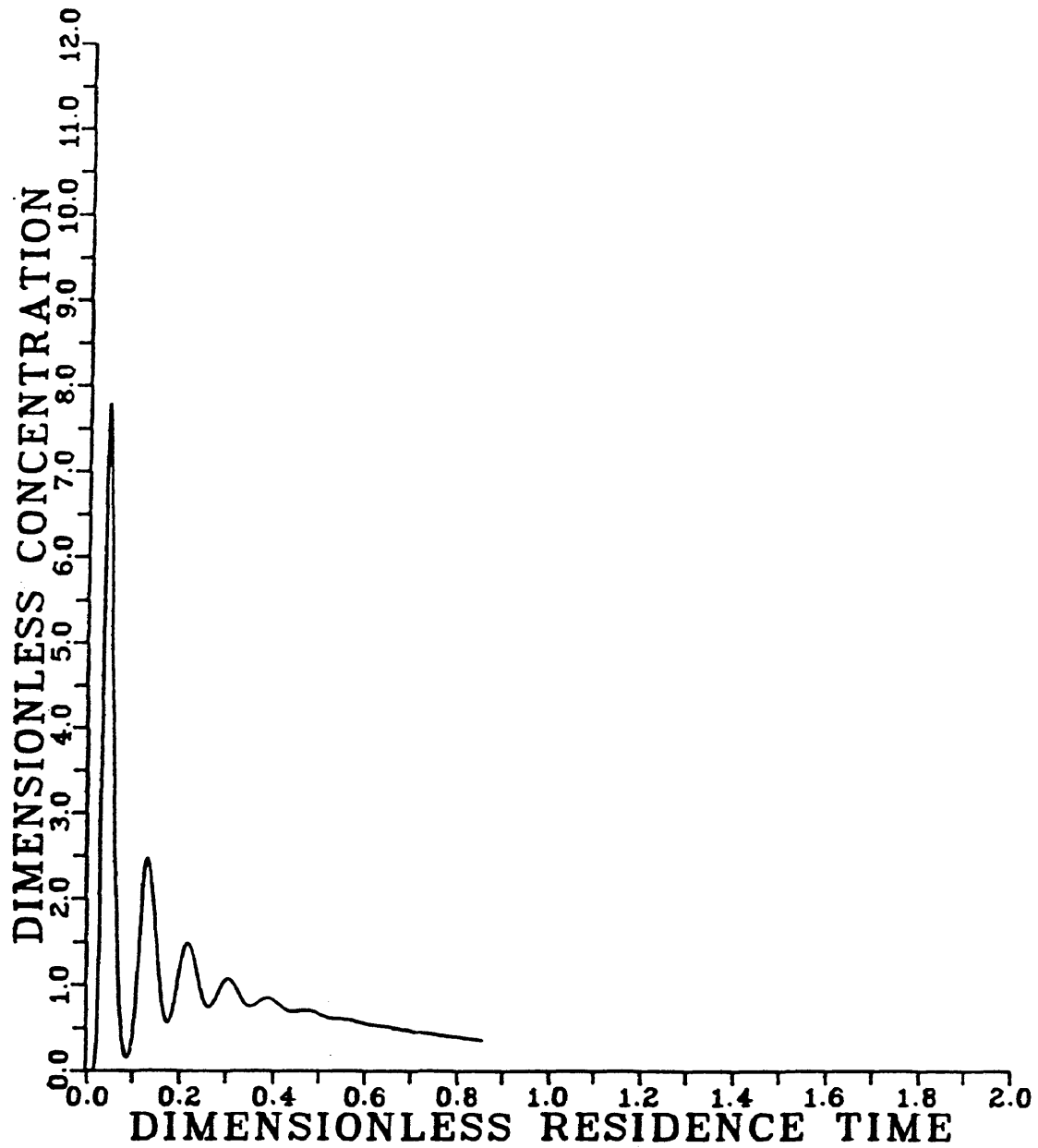


Figure 5.26
Residence Time Distribution
 $RePr=1$, $Ra=200$ $M/N=20/20$, $\Delta\tau = .0001$

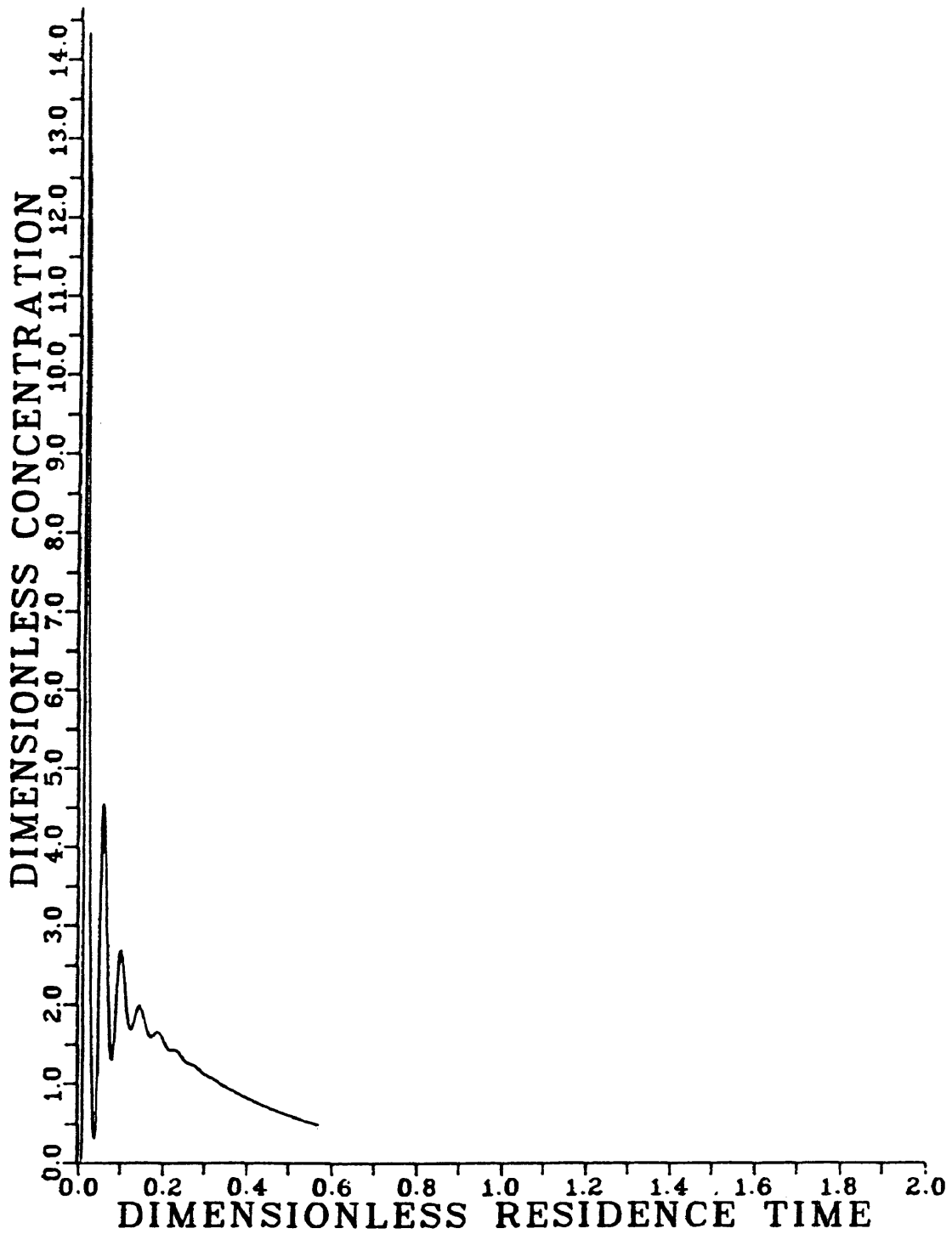


Figure 5.27
Residence Time Distribution
 $RePr=1$, $Ra=600$, $M/N=20/20$, $\Delta\tau=.0001$

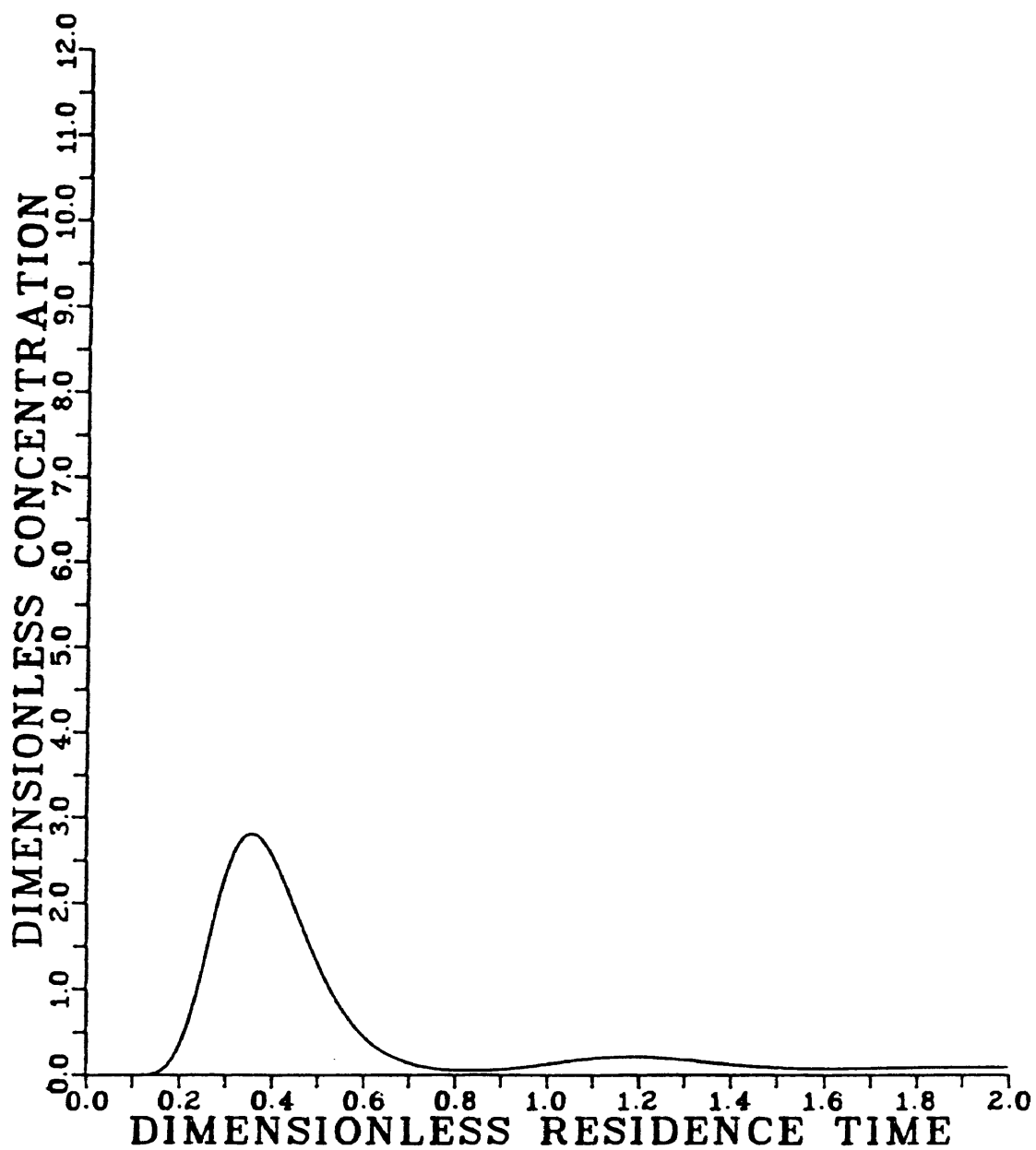


Figure 5.28
Residence Time Distribution
 $RePr=4$, $Ra=100$, $M/N=20/20$, $\Delta\tau=.0001$

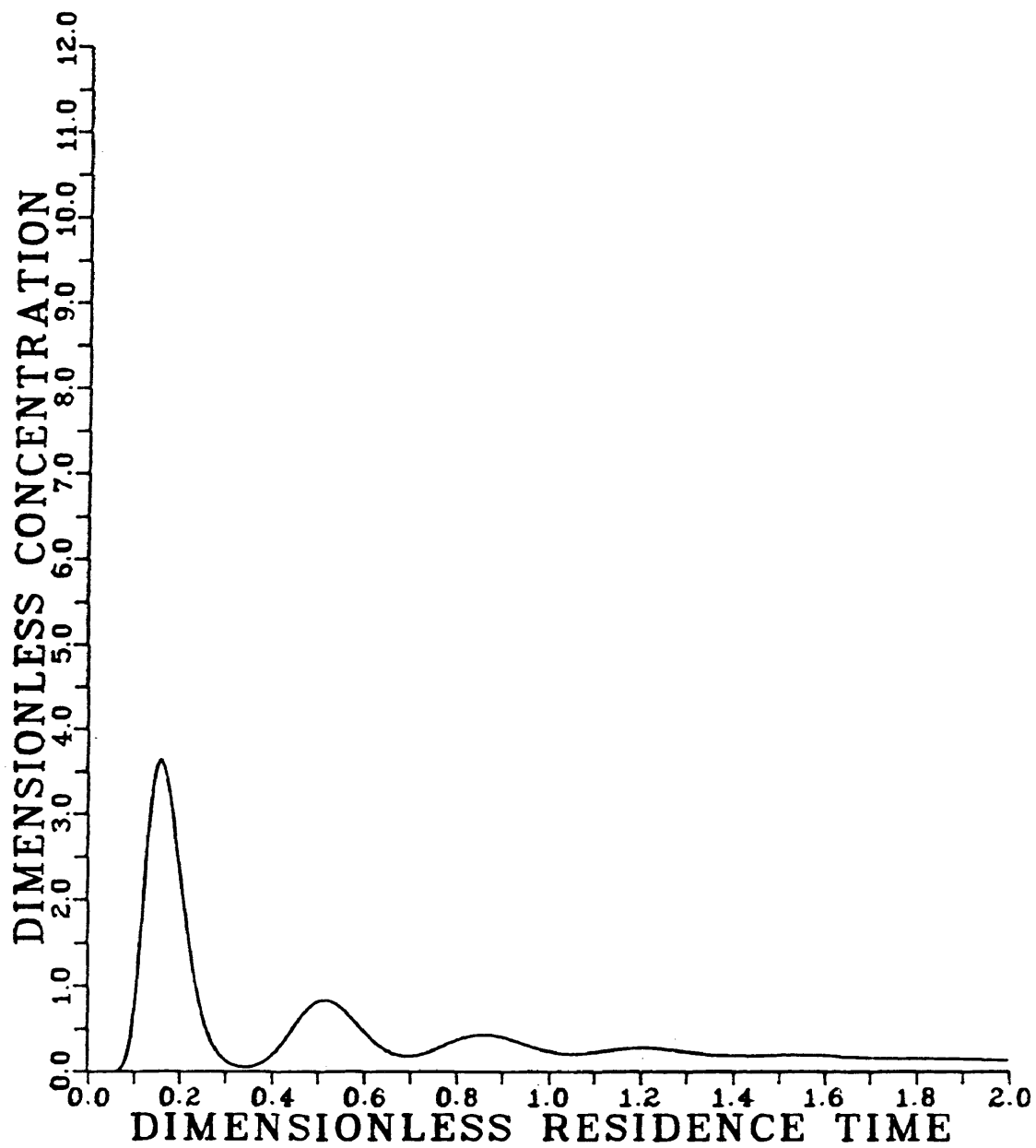


Figure 5.29
Residence Time Distribution
 $RePr=4$, $Ra=200$, $M/N=20/20$, $\Delta\tau=.0001$

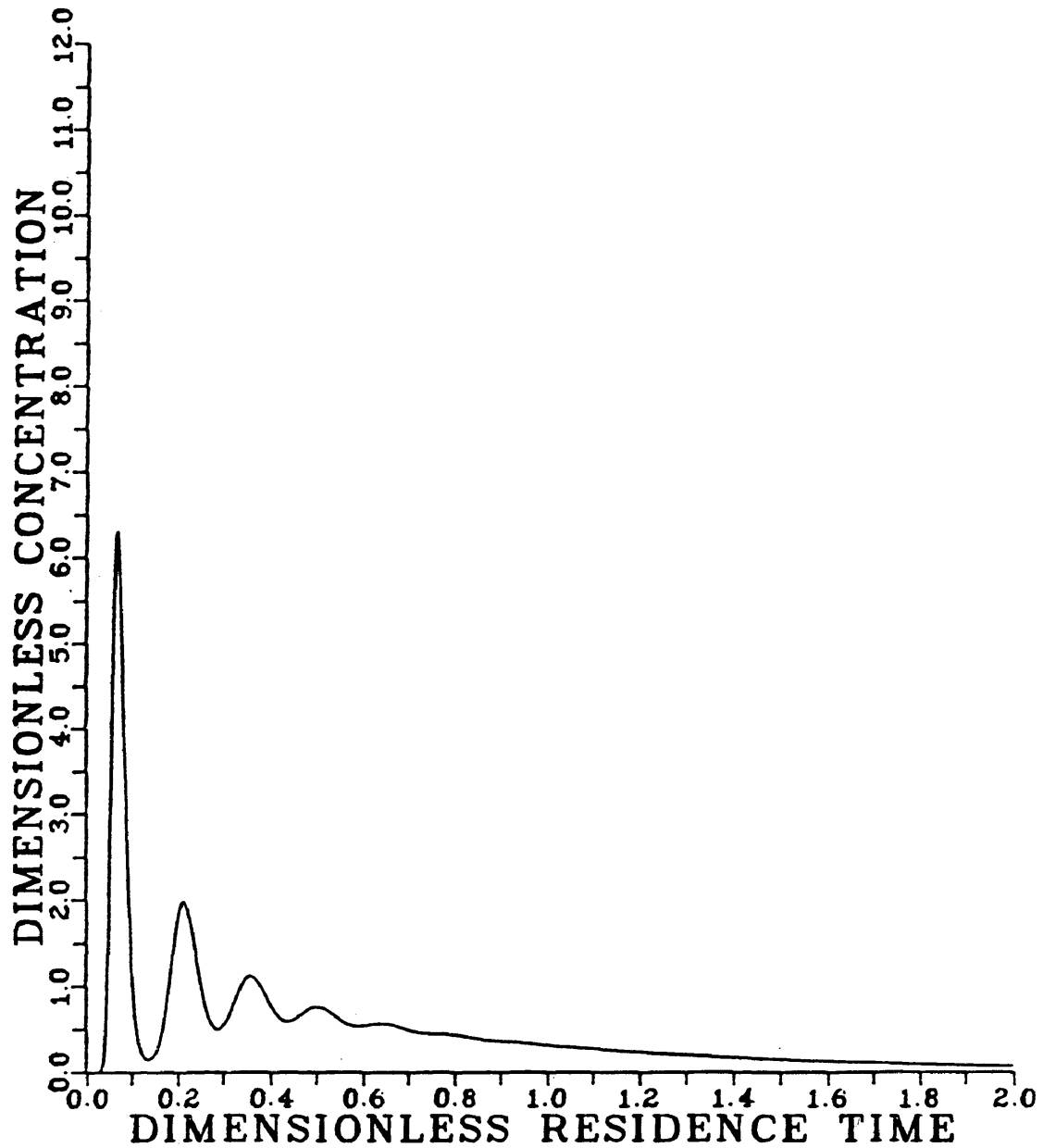


Figure 5.30
Residence Time Distribution
 $RePr=4$, $Ra=600$, $M/N=20/20$, $\Delta\tau=.0001$

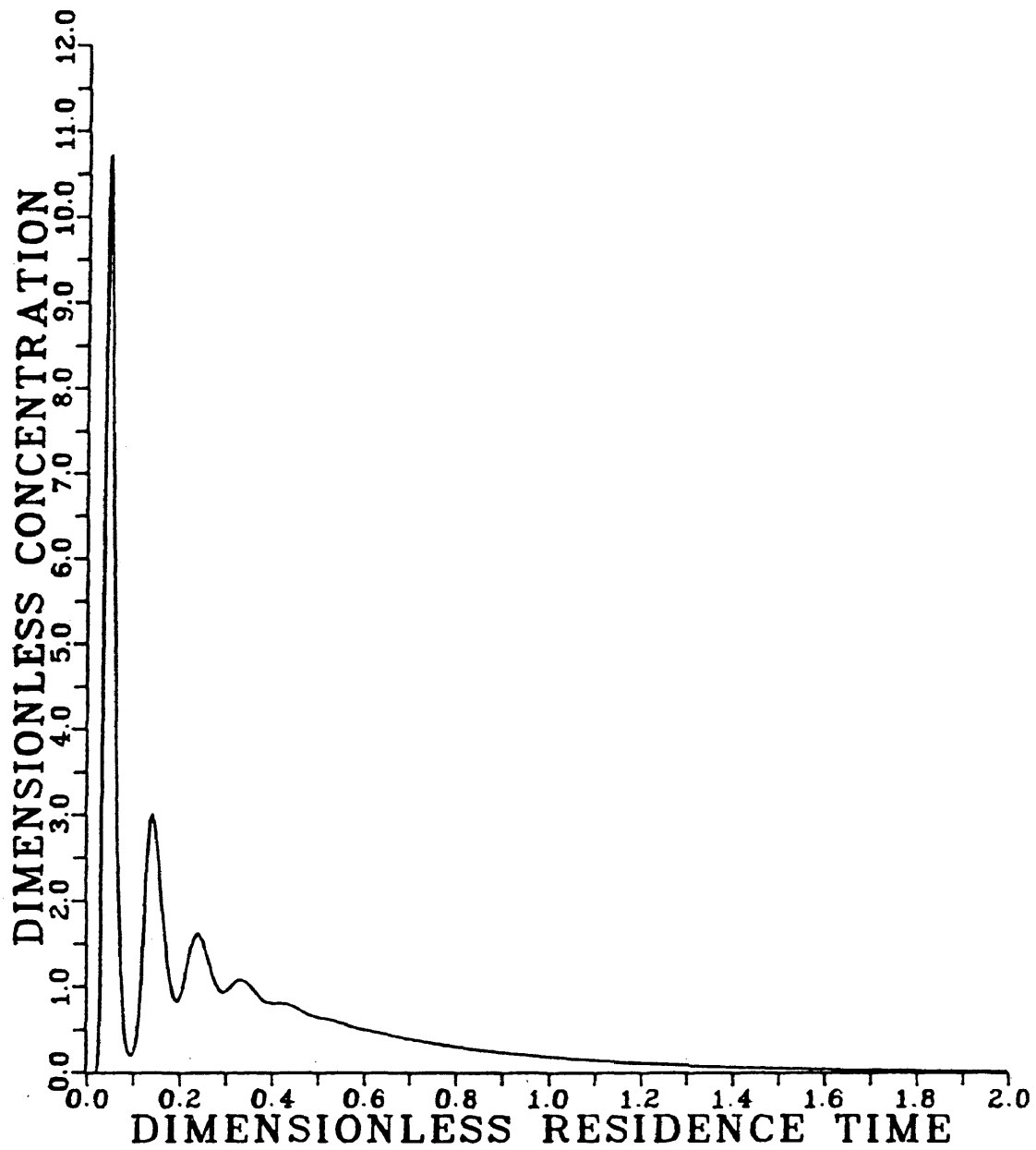


Figure 5.31
Residence Time Distribution
 $RaPr=4$, $Ra=1000$, $M/N=20/20$, $\Delta\tau = .0001$

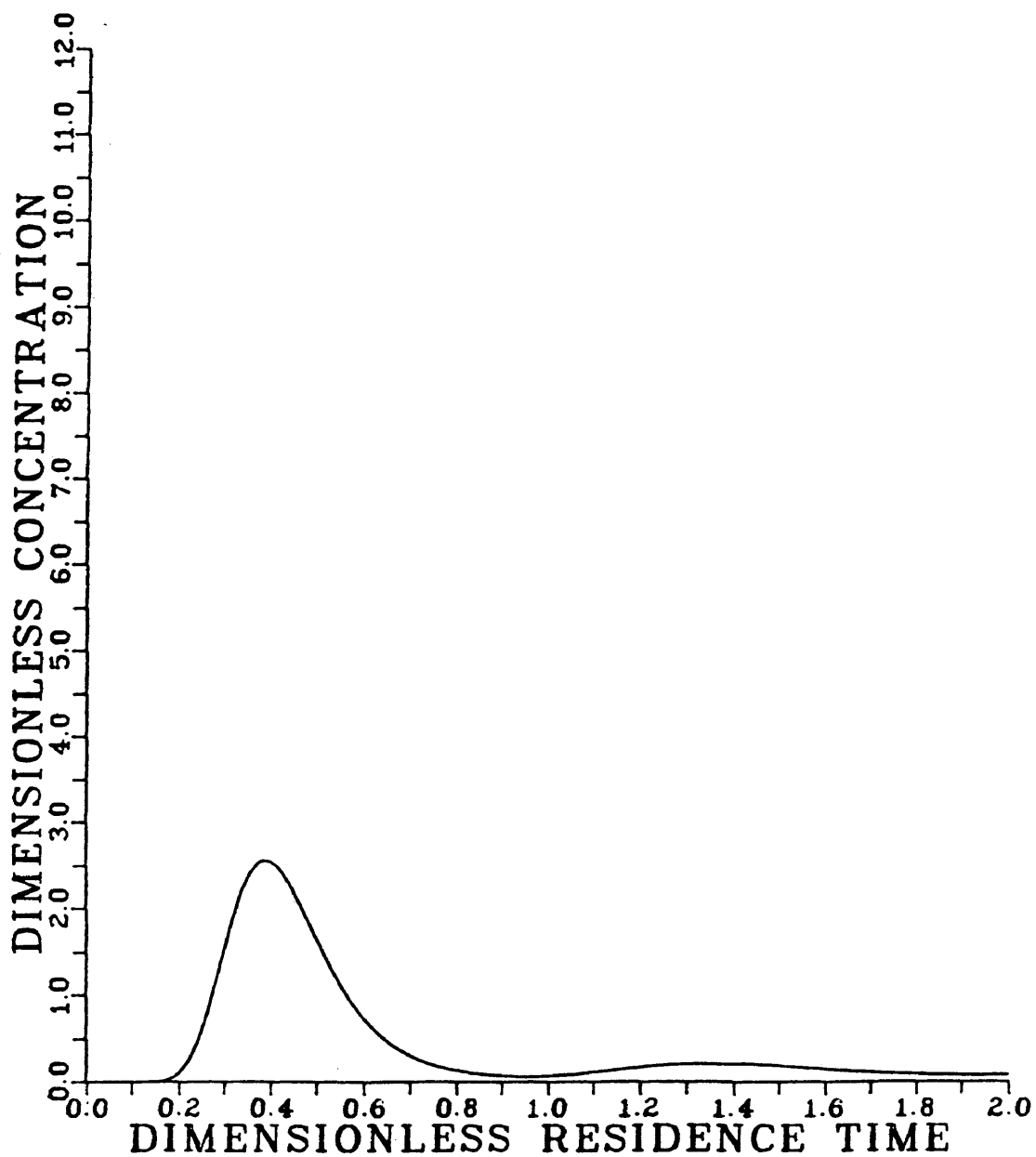


Figure 5.32
Residence Time Distribution
 $RePr=10$, $Ra=200$, $M/N=20/20$, $\Delta\tau = .0001$

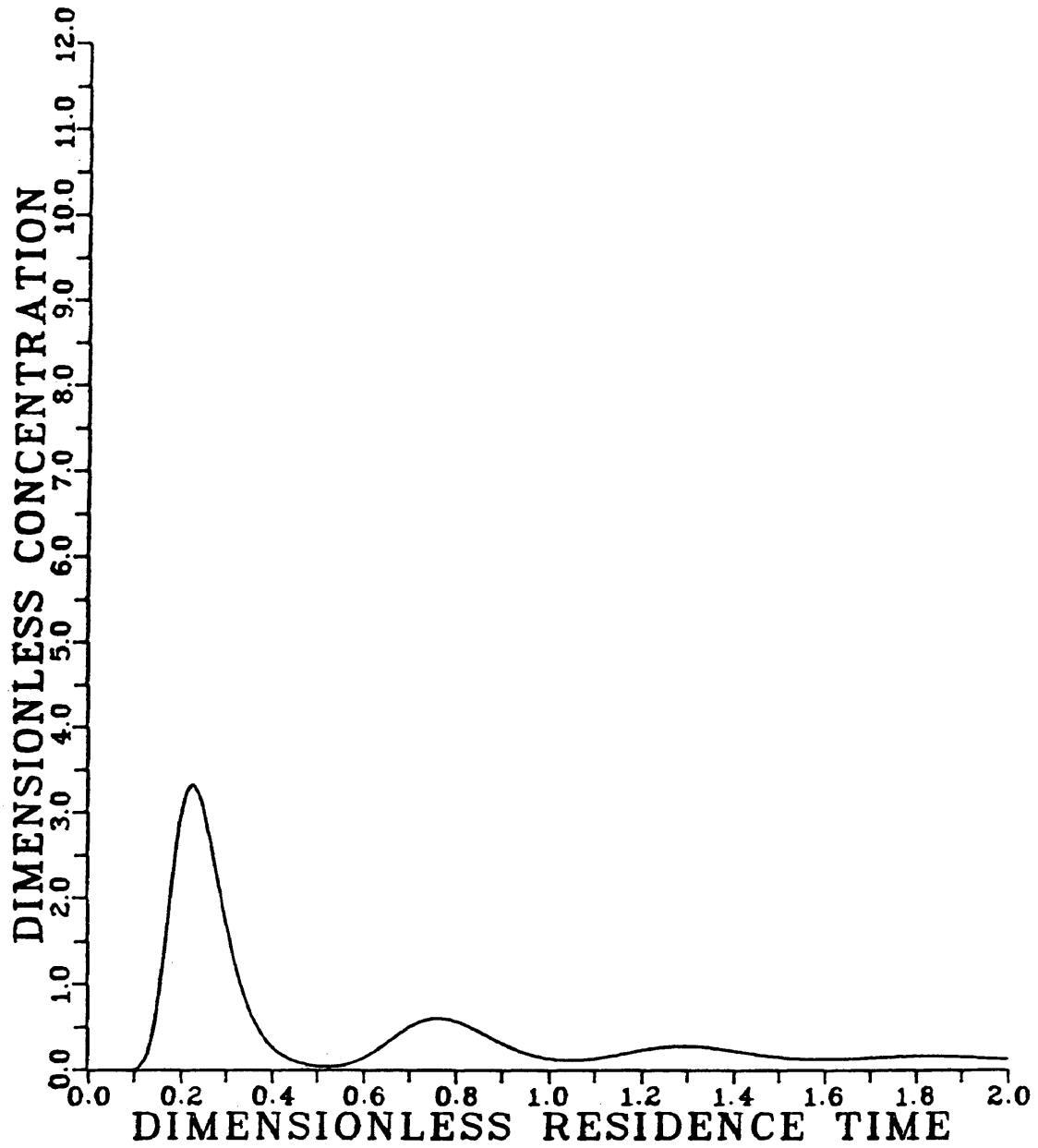


Figure 5.33
Residence Time Distribution
 $RePr=10$, $Ra=400$, $M/N=20/20$, $\Delta\tau=.0001$

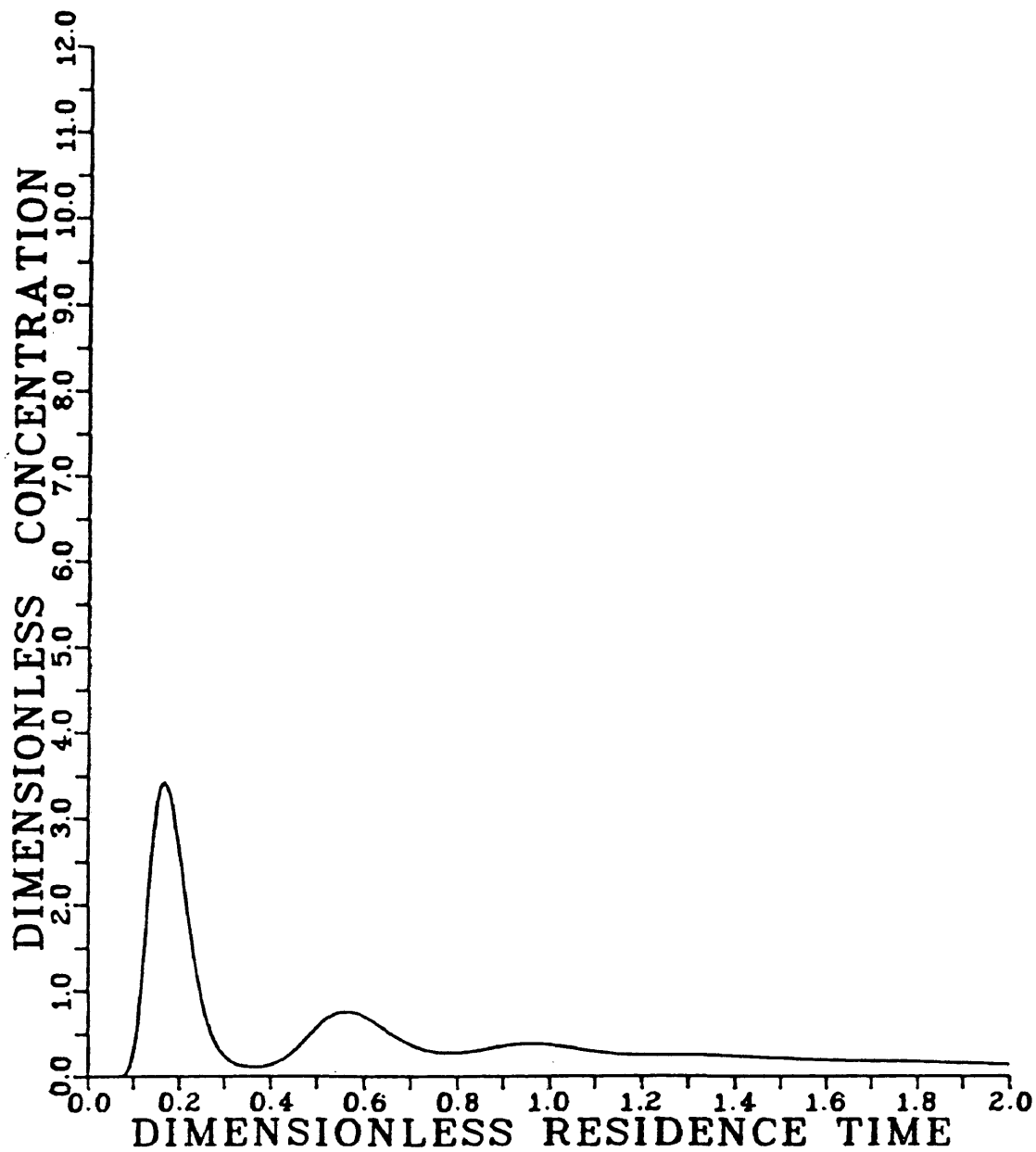


Figure 5.34
Residence Time Distribution
 $RePr=10$, $Ra=600$, $M/N=20/20$, $\Delta\tau = .0001$

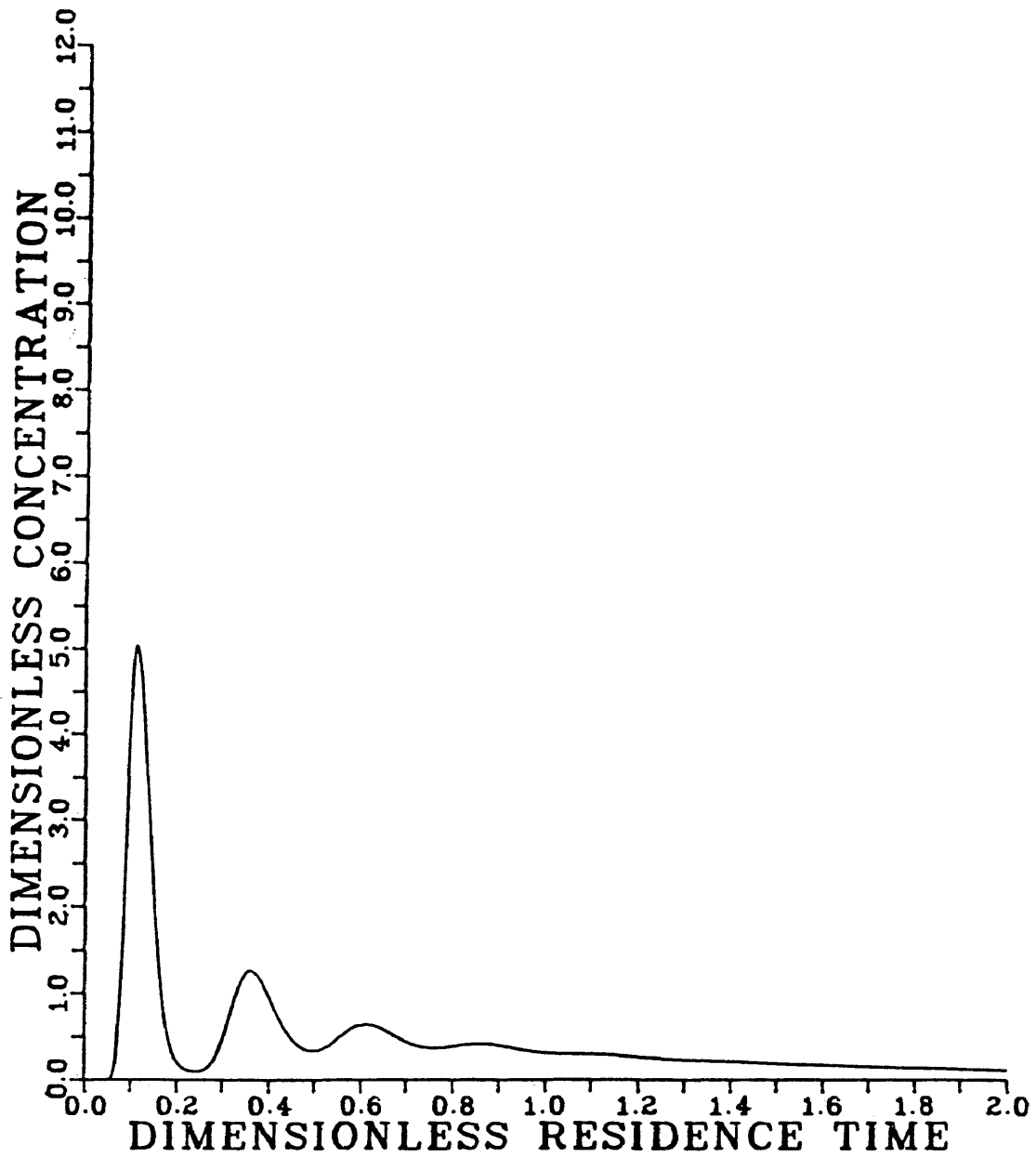


Figure 5.35
Residence Time Distribution
 $RePr=10$, $Ra=1000$, $M/N=20/20$, $\Delta\tau=.0001$

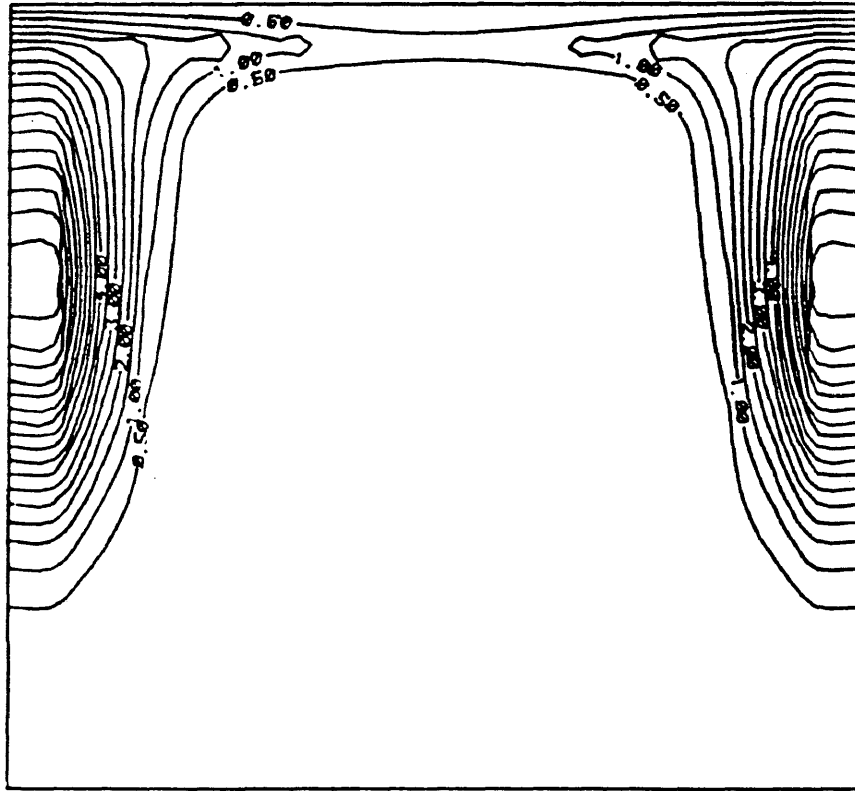


Figure 5.36
Tracer Concentration Contour
 $\tau^* = .057$, $RePr=4$, $Ra=200$, $M/N=20/20$

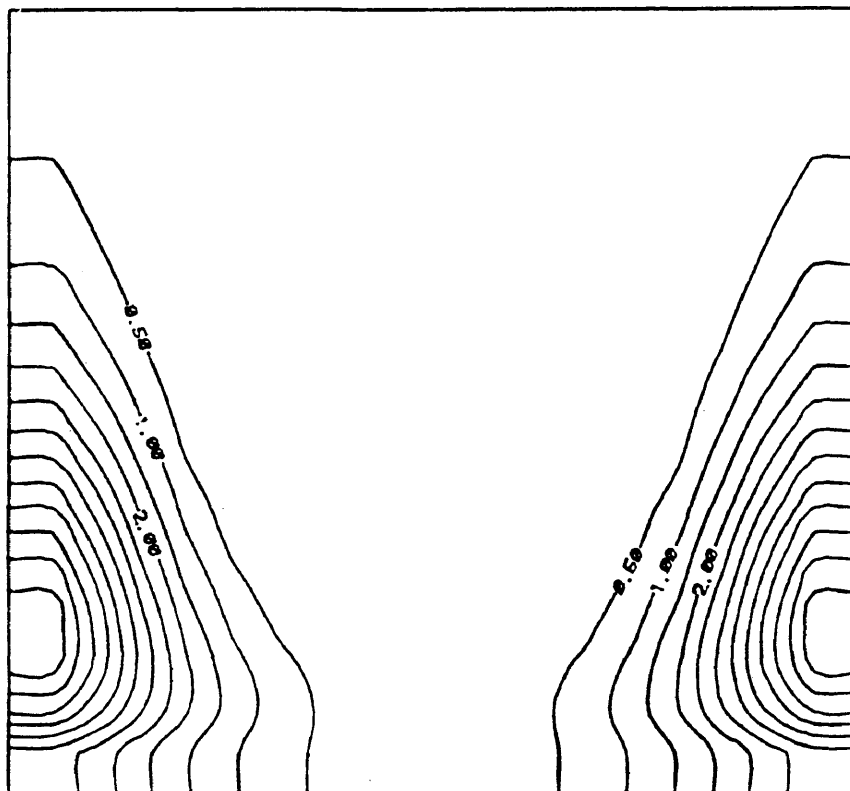


Figure 5.37
Tracer Concentration Contour
 $\tau^* = .114$, $RePr = 4$, $Ra = 200$, $M/N = 20/20$

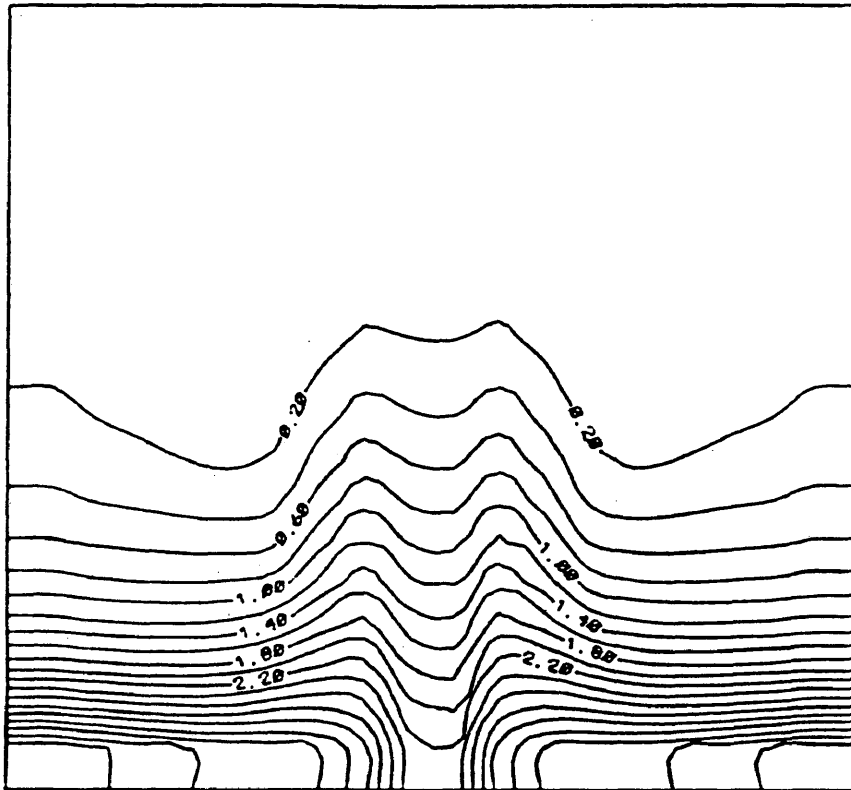


Figure 5.38
Tracer Concentration Contour
 $\tau^* = .171$, $RePr = 4$, $Ra = 200$, $M/N = 20/20$

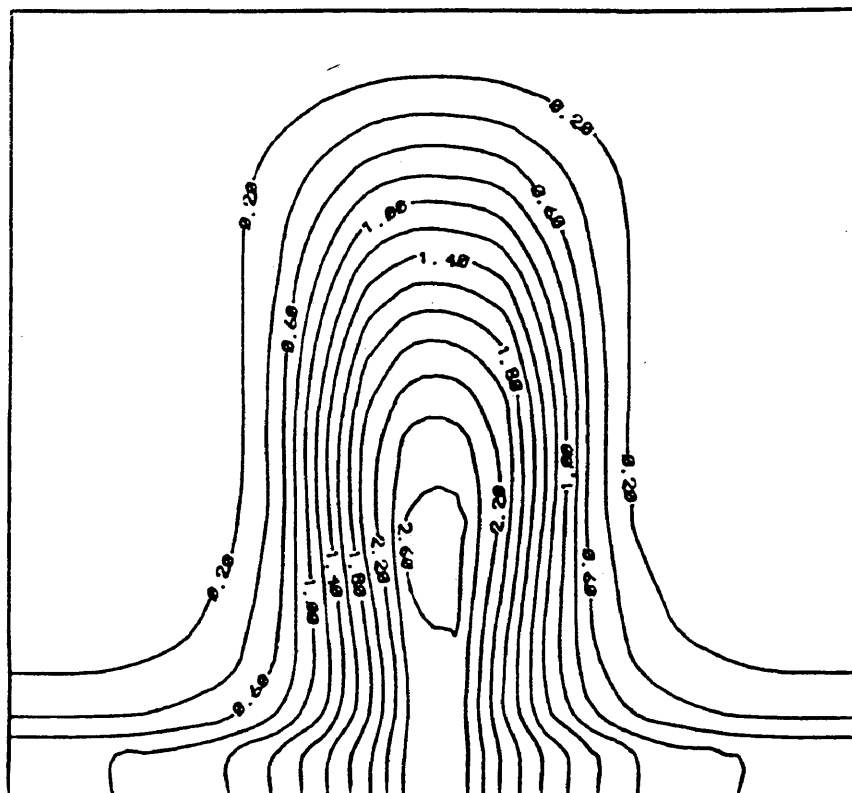


Figure 5.39
Tracer Concentration Contour
 $\tau^* = .229$, $RePr = 4$, $Ra = 200$, $M/N = 20/20$

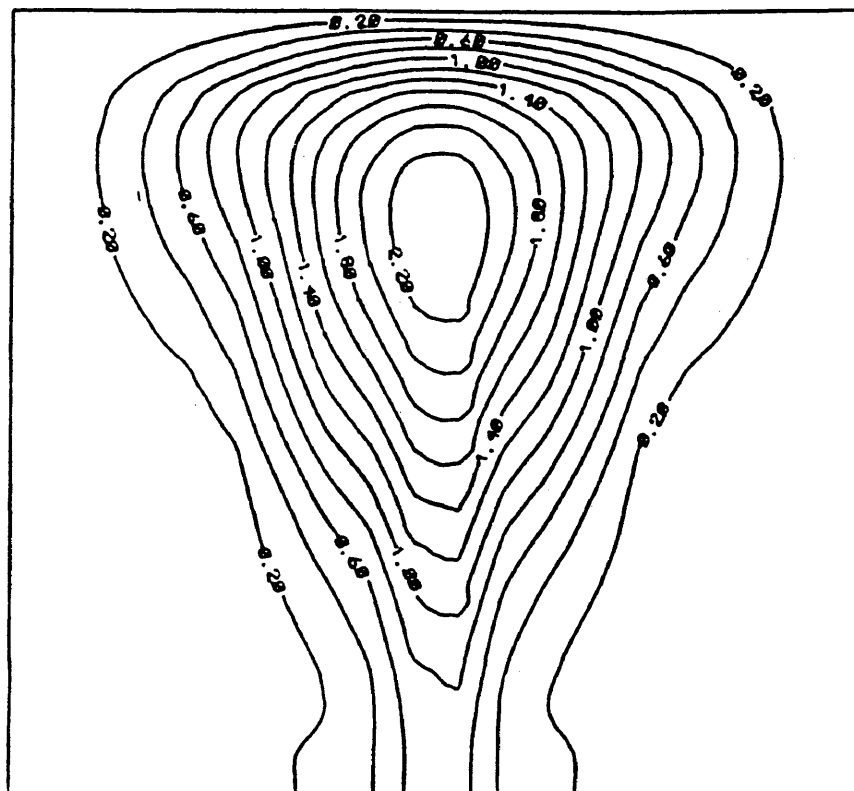


Figure 5.40
Tracer Concentration Contour
 $\tau^* = .286$, $RePr=4$, $Ra=200$, $M/N=20/20$

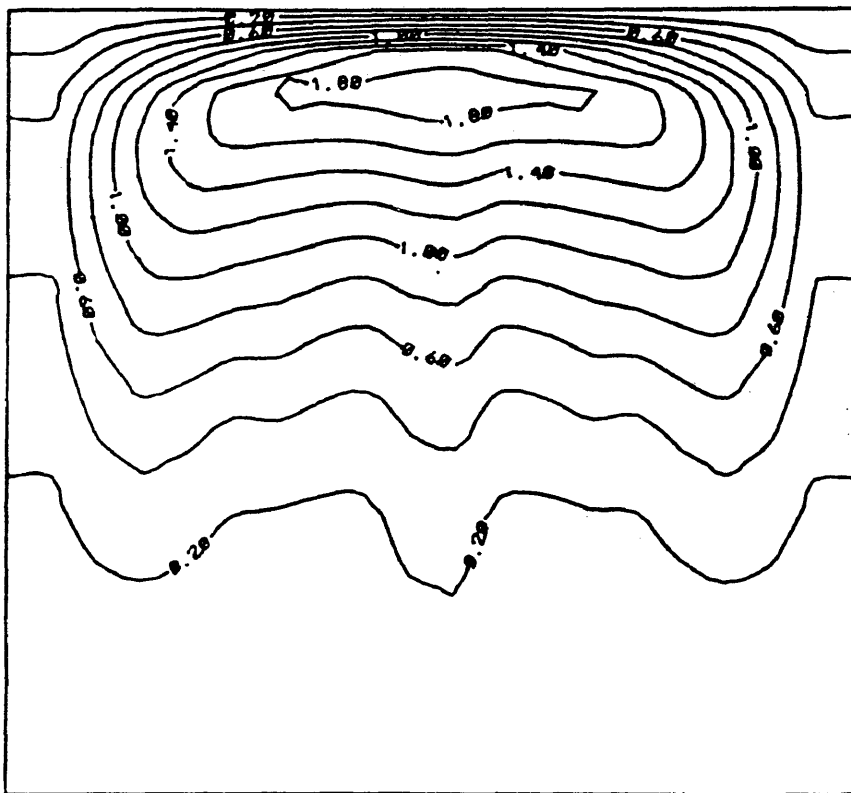


Figure 5.41
Tracer Concentration Contour
 $\tau^* = .343$, $RePr=4$, $Ra=200$, $M/N=20/20$

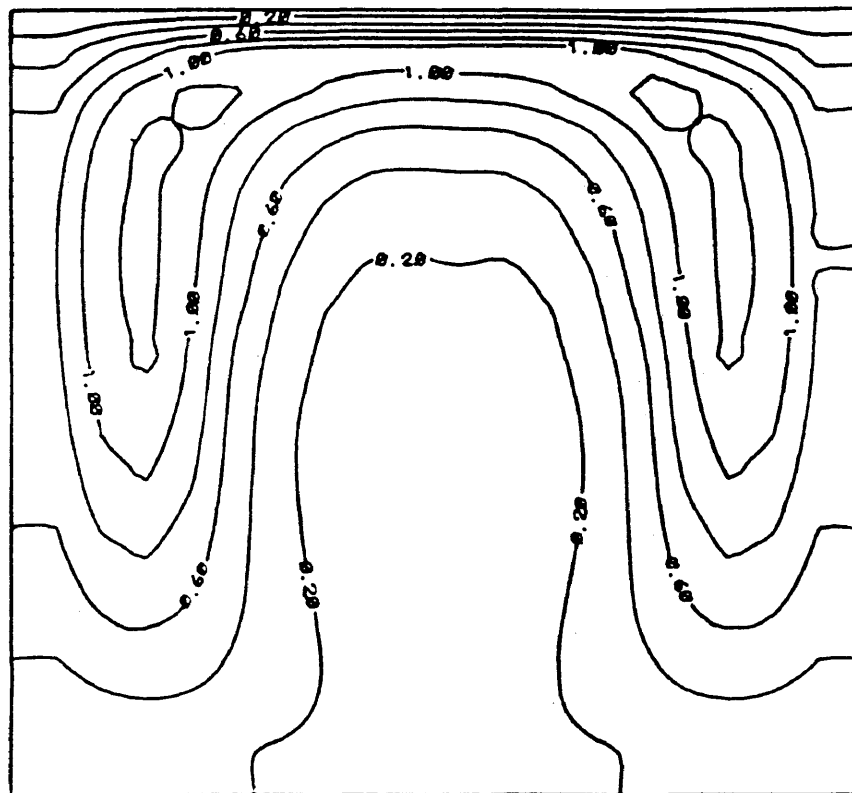


Figure 5.42
Tracer Concentration Contour
 $\tau^* = .400$, $RePr = 4$, $Ra = 200$, $M/N = 20/20$

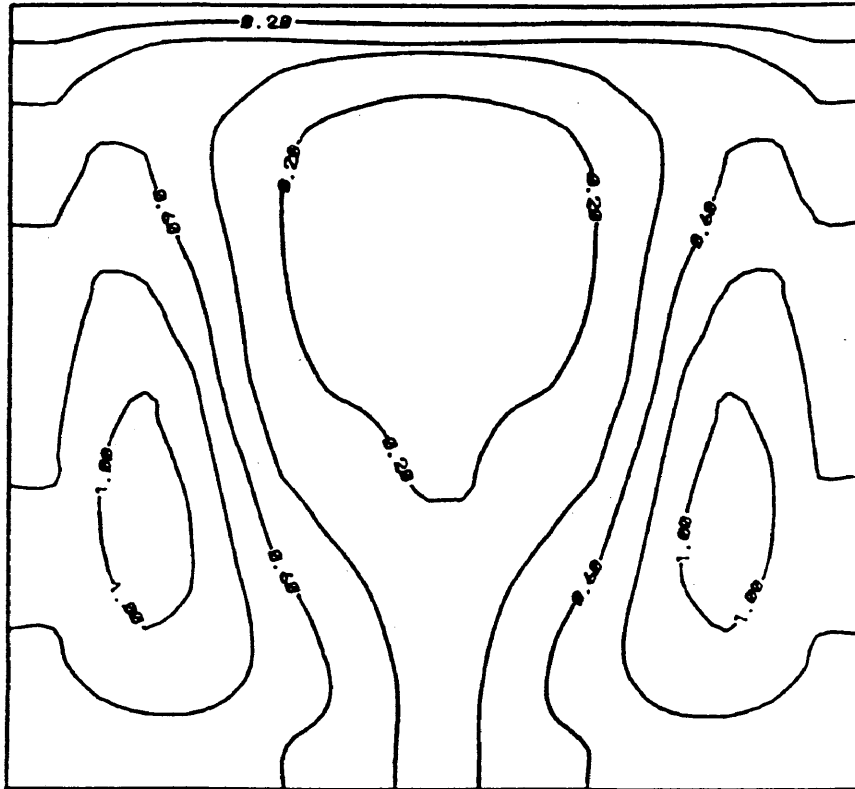


Figure 5.43
Tracer Concentration Contour
 $\tau^* = .457, RePr=4, Ra=200, M/N=20/20$

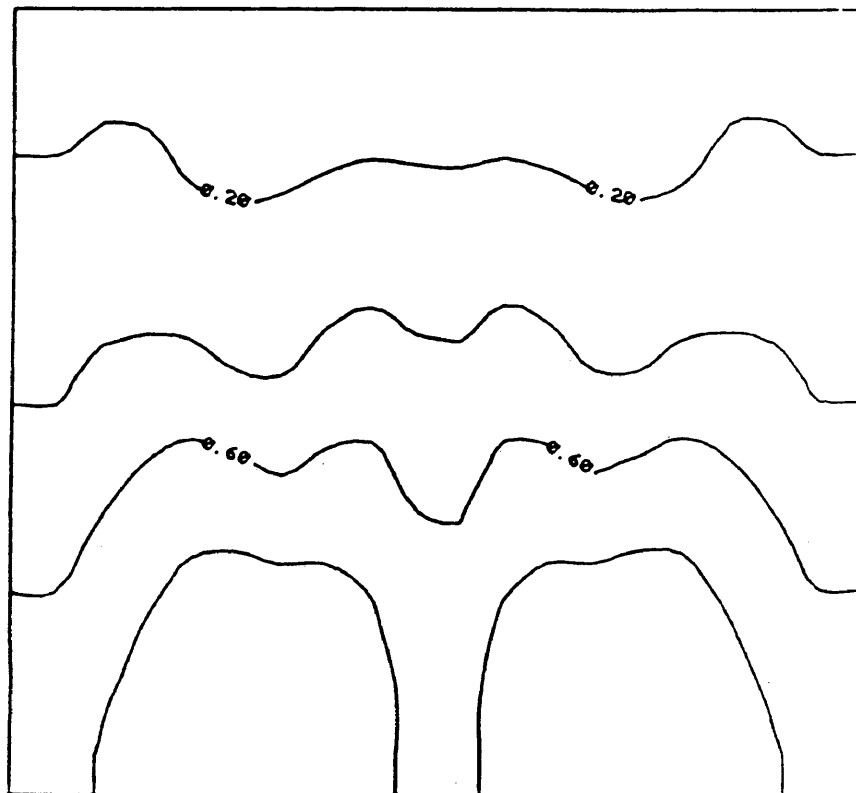


Figure 5.44
Tracer Concentration Contour
 $\tau^* = .514$, $RePr=4$, $Ra=200$, $M/N=20/20$

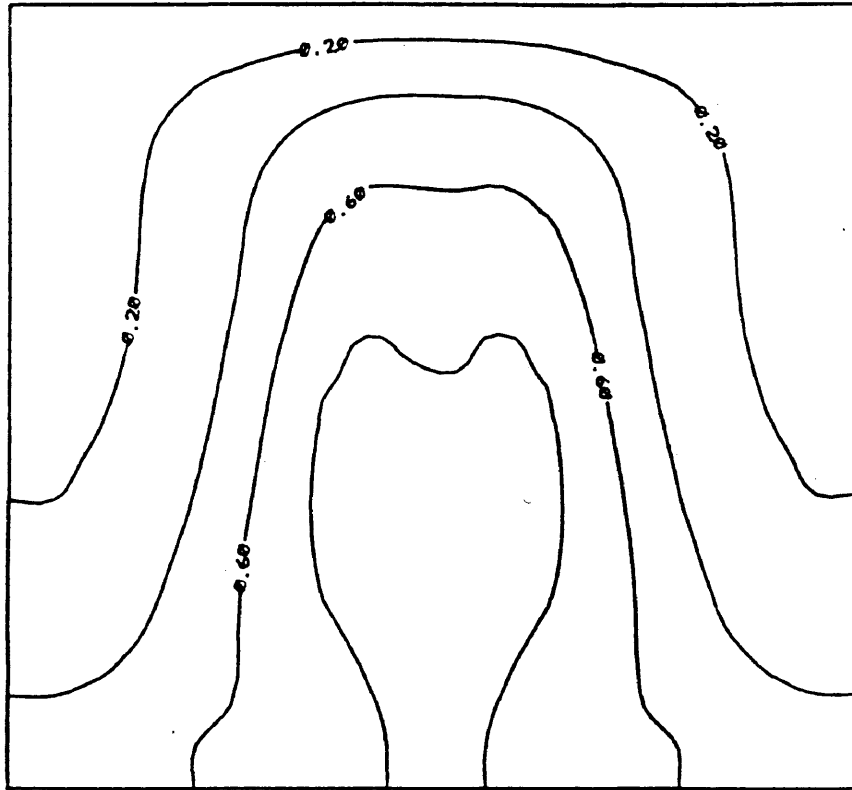


Figure 5.45
Tracer Concentration Contour
 $\tau^* = .571, RePr=4, Ra=200, M/N=20/20$

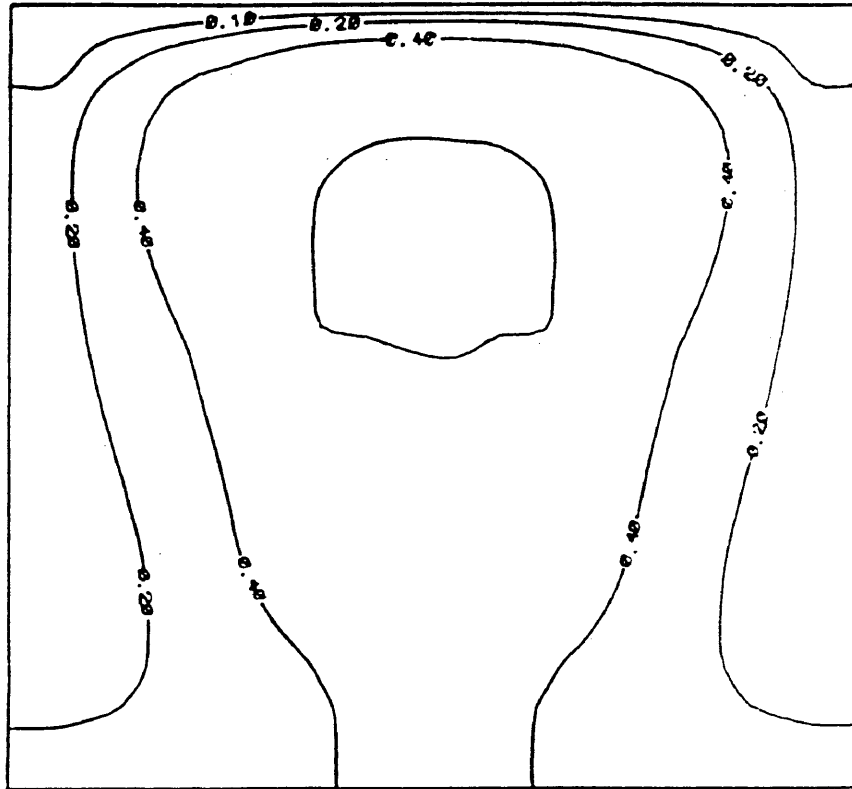


Figure 5.46
Tracer Concentration Contour
 $\tau^* = .629, RePr=4, Ra=200, M/N=20/20$

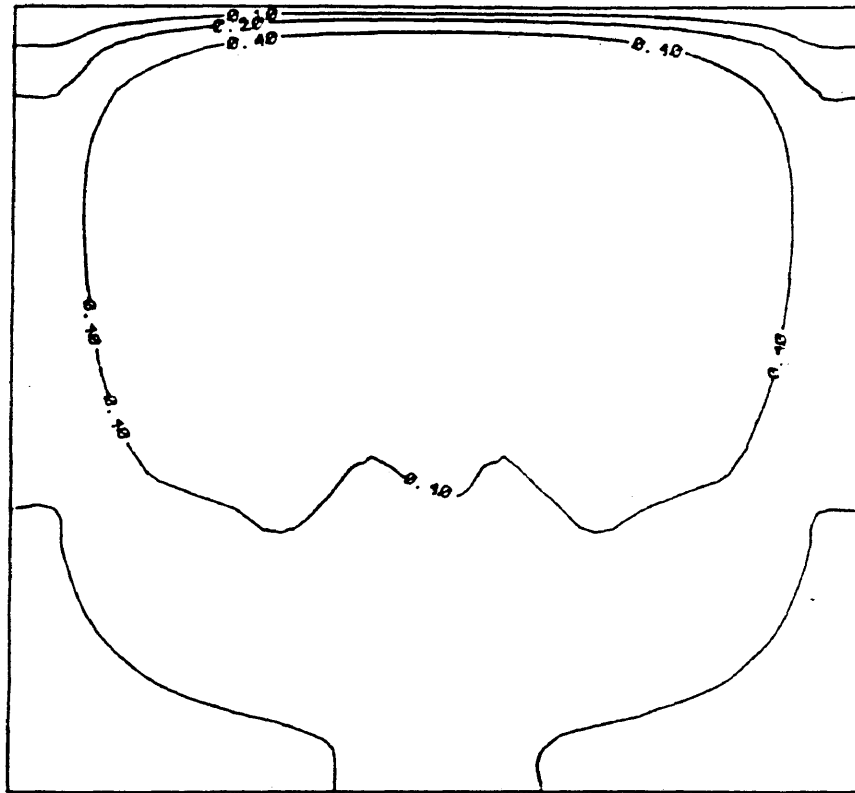


Figure 5.47
Tracer Concentration Contour
 $\tau^* = .686$, $RePr=4$, $Ra=200$, $M/N=20/20$

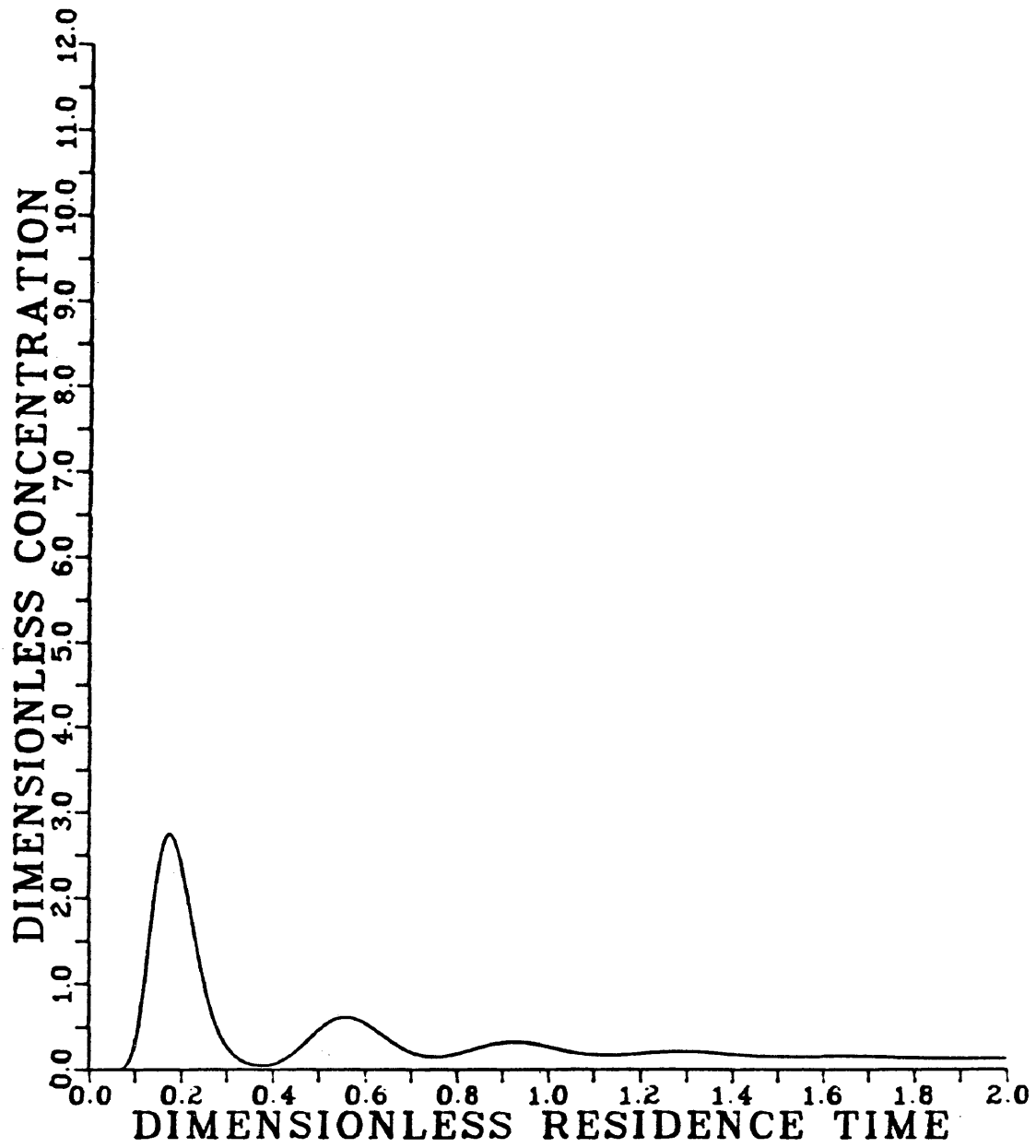


Figure 5.48
Residence Time Distribution
 $RePr=4$, $Ra=200$, $M/N=60/20$, $\Delta\tau=.0001$

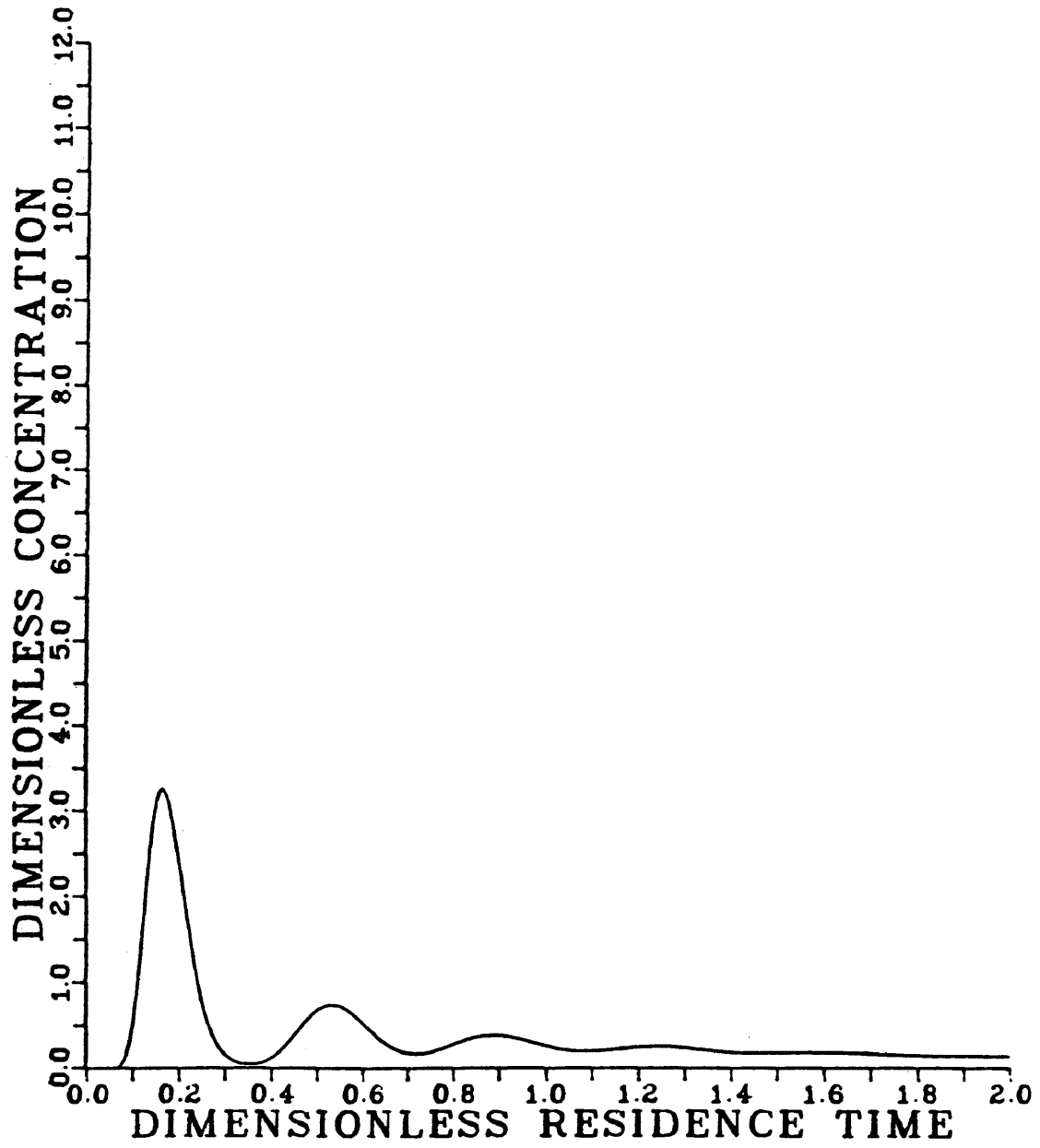


Figure 5.49
Residence Time Distribution
RePr=4, Ra=200, M/N=30/20, $\Delta\tau=.0001$

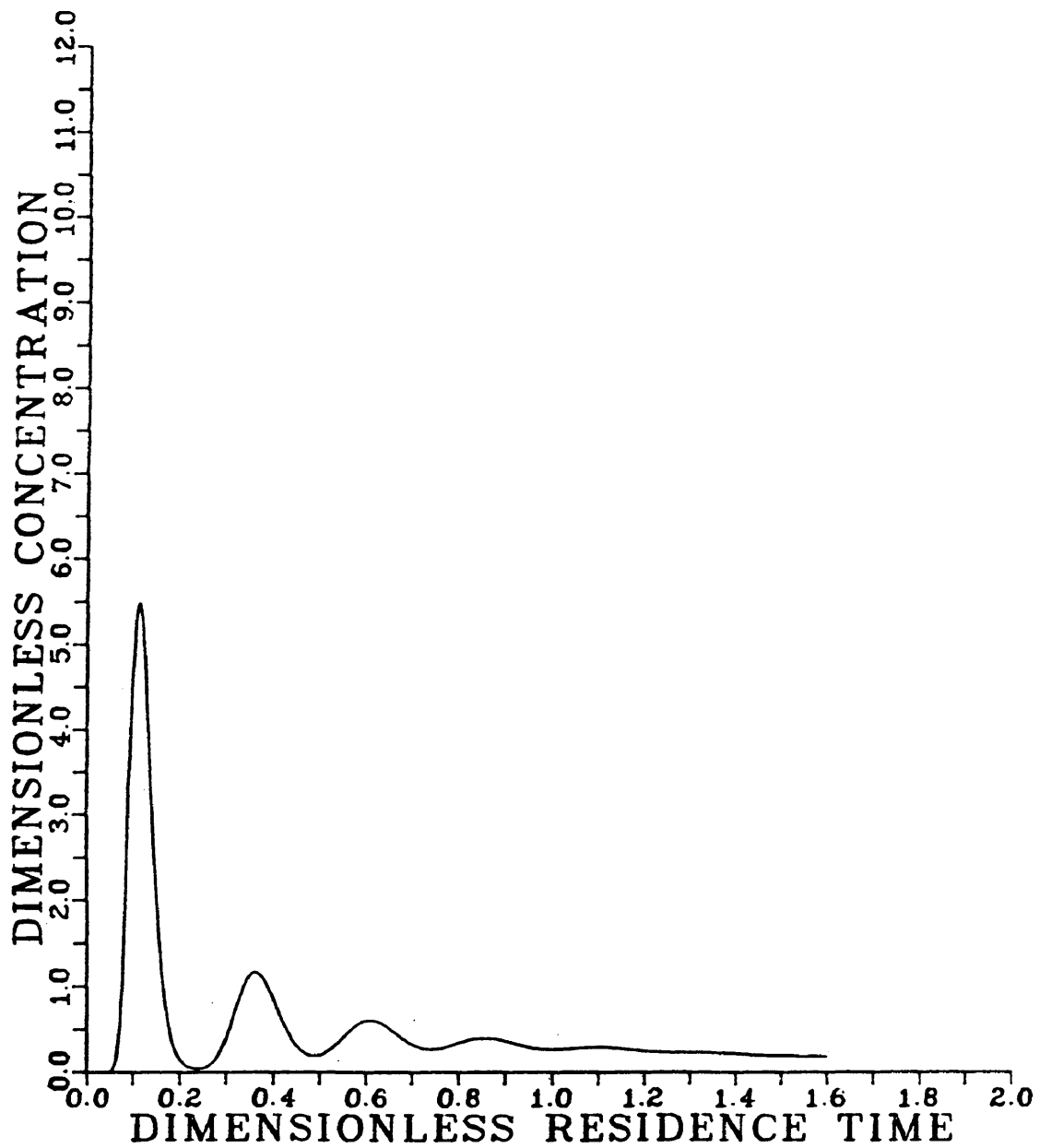


Figure 5.50
Residence Time Distribution
 $RePr=4$, $Ra=200$, $M/N=20/30$, $\Delta\tau=.0001$

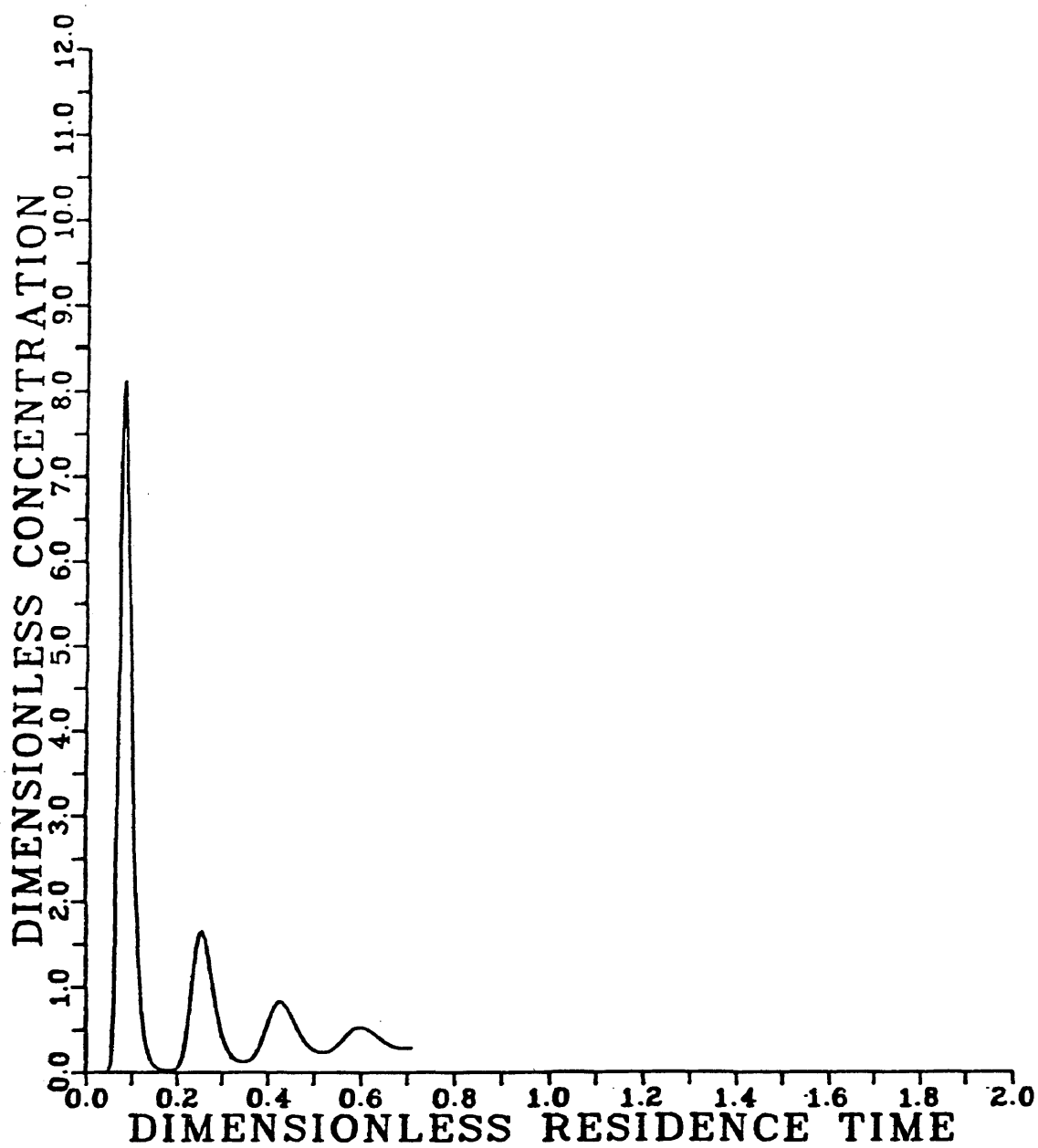


Figure 5.51
Residence Time Distribution
 $RePr=4$, $Ra=200$, $M/N=20/60$, $\Delta\tau=.0002$

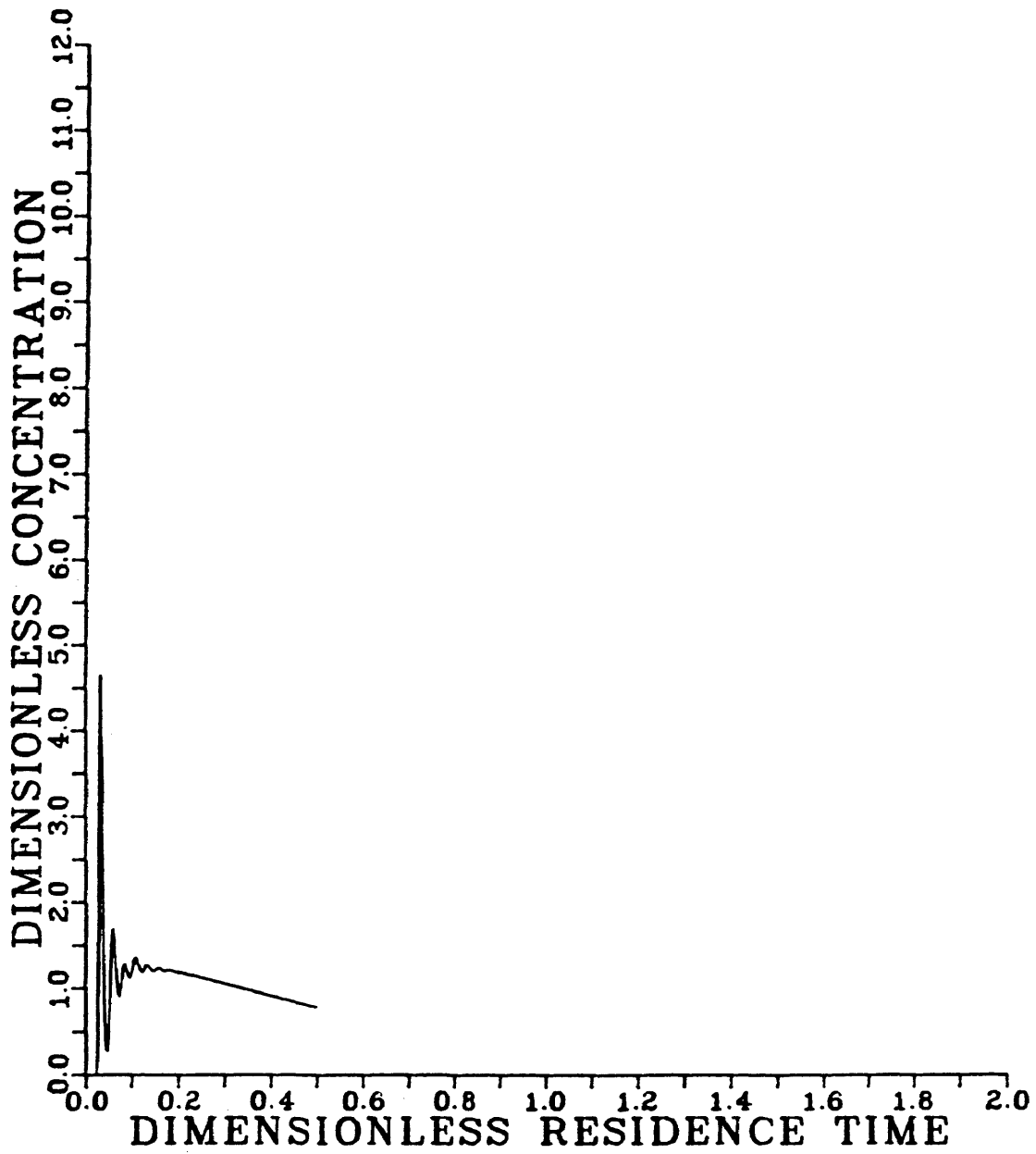


Figure 5.52
Residence Time Distribution
 $RePr=4$, $Ra=600$, $M/N=20/60$, $\Delta\tau=.0002$

5.4 Verification of RTD Results

5.4.1 Plug Flow

Plug flow results calculated by numerical techniques can be compared to those predicted by theory. A graph of the theoretical results for mass dispersion Peclet numbers of 40, 160 and 400, corresponding to $RePr = 1, 4$ and 10 is presented in Figure 5.53. Figure 5.54 presents the results for the explicit upwind differencing method with a 20×20 grid. Figure 5.55 shows the improvement in going to a 40×40 grid for $RePr = 10$. Figure 5.56 shows the result of using an ADI method for a 20×20 grid.

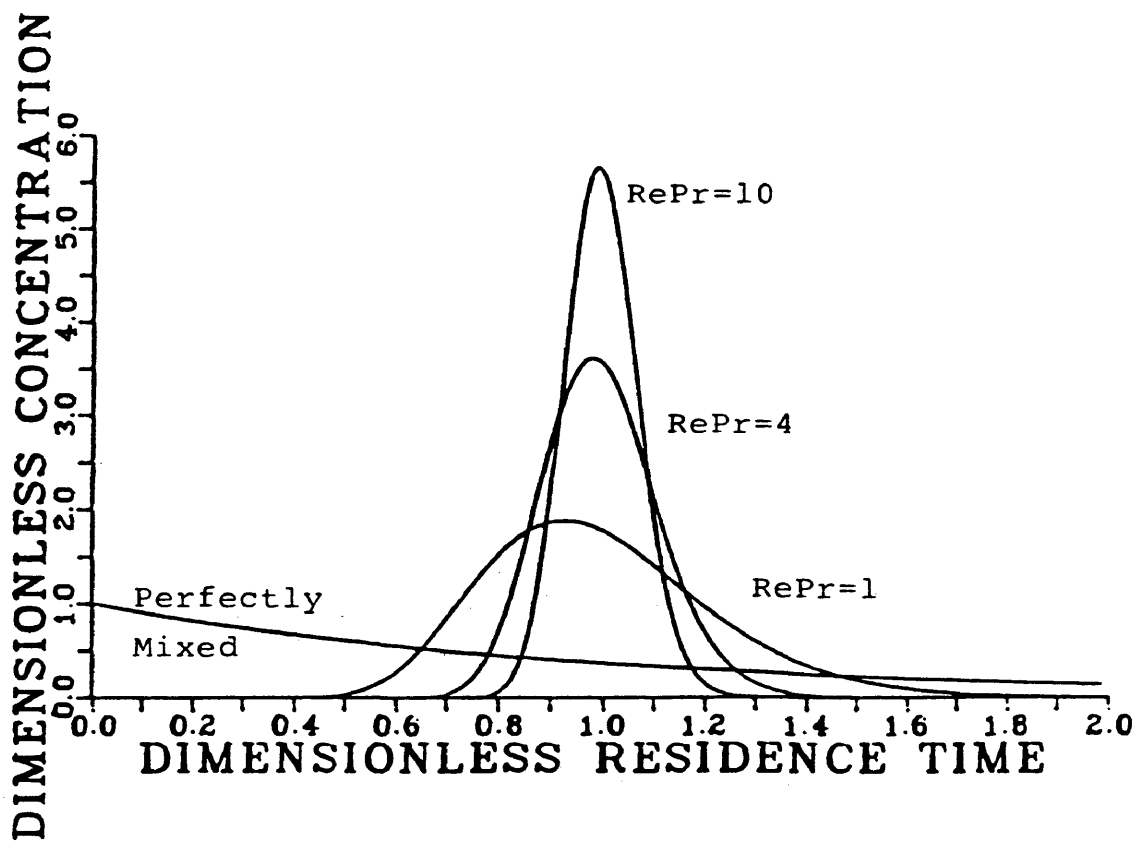


Figure 5.53
Theoretical Residence Time Distributions
Plug Flow and Perfectly Mixed Vessel

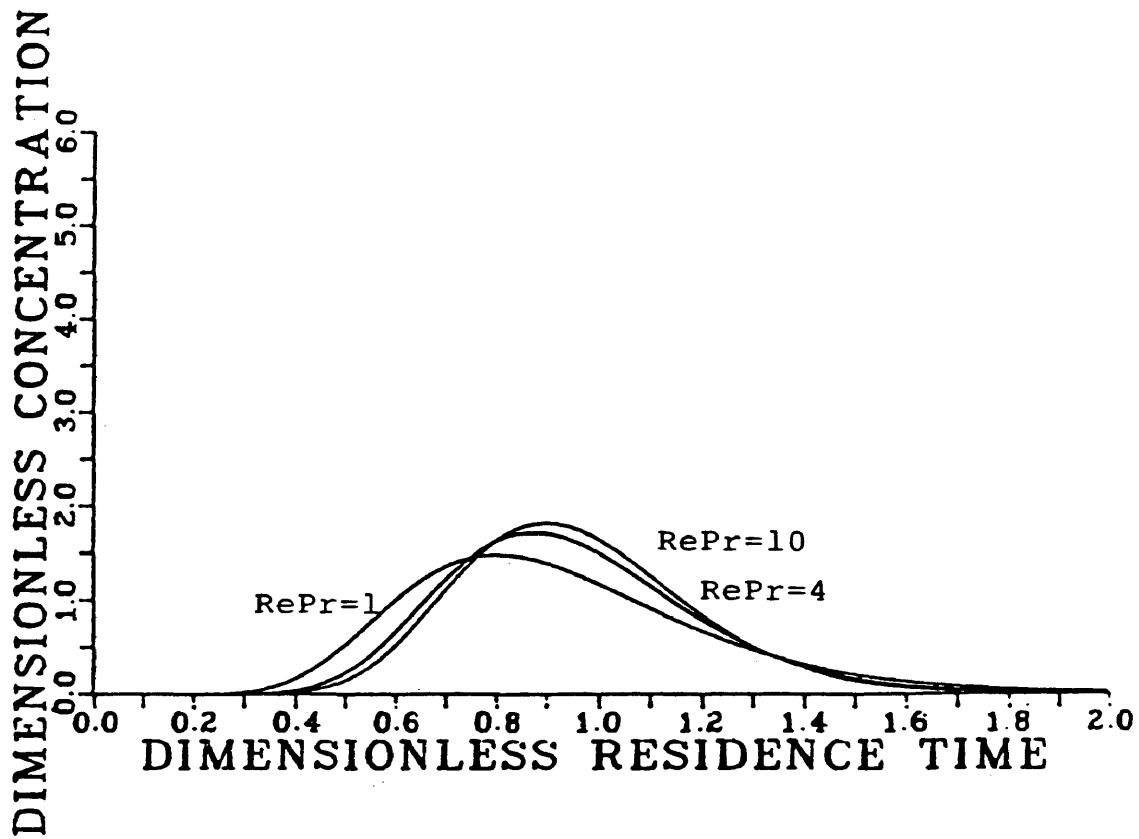


Figure 5.54
Residence Time Distributions
Plug Flow, Explicit Upwind Differencing, $M/N=20/20$

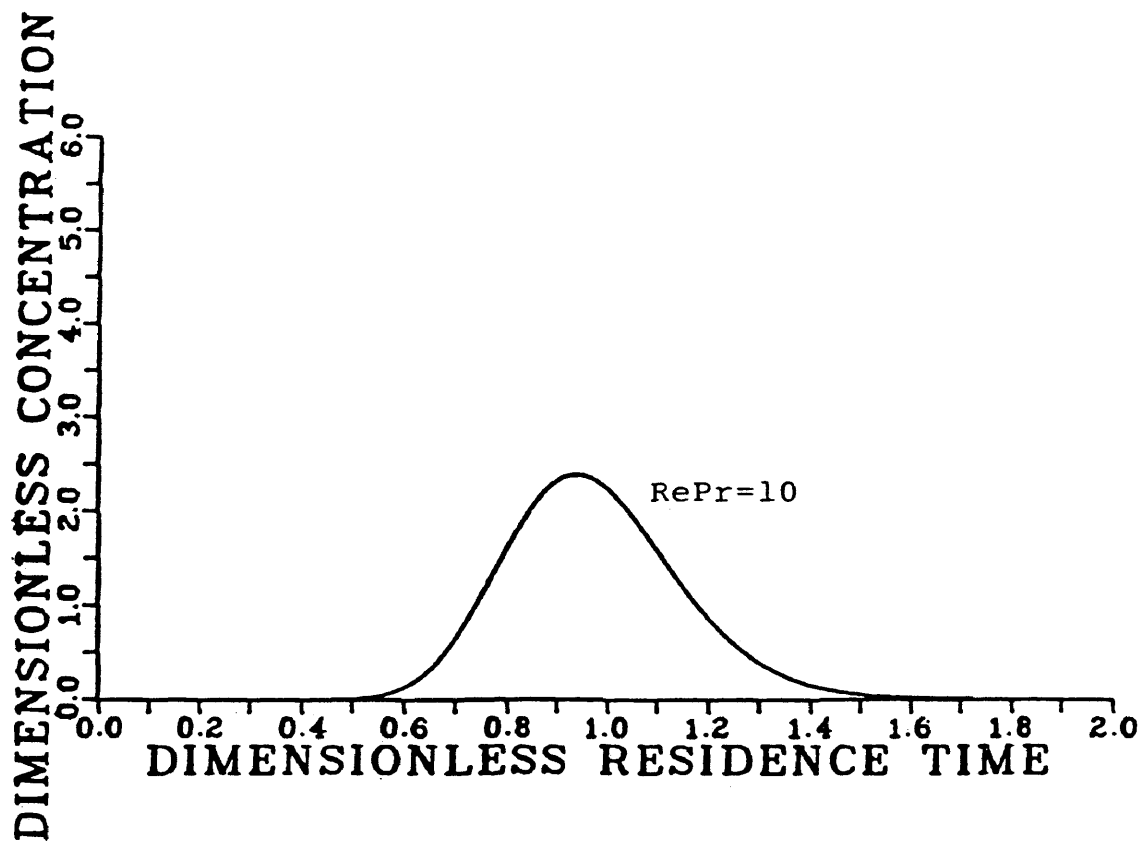


Figure 5.55
Residence Time Distribution
Plug Flow, Explicit Upwind Differencing, M/N=40/40

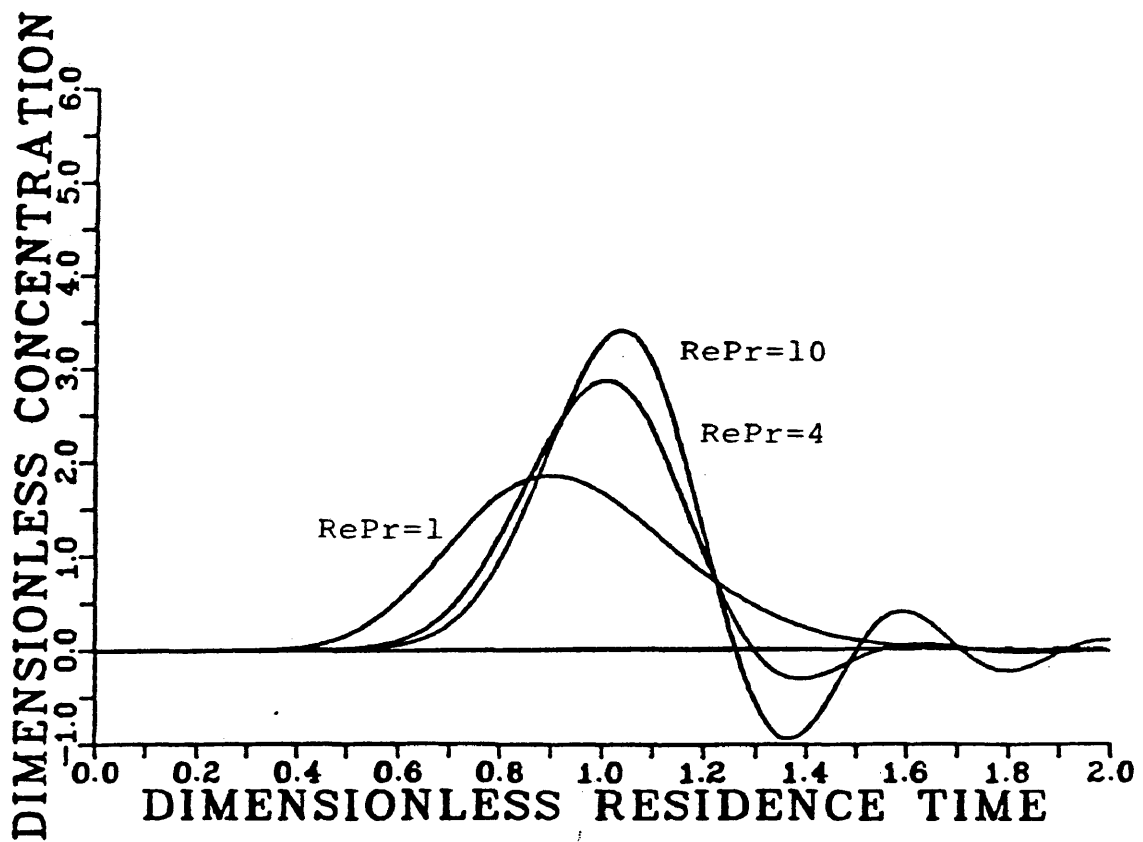


Figure 5.56
Residence Time Distributions
Alternating Direction Implicit, $M/N=20/20$

5.4.2 Convecting Flows

This section is included to illustrate the effects of various parameters and numerical techniques on convecting flow RTDs. Figures 5.57 and 5.58, together with Figure 5.31, show the effect of varying time and spatial steps for a square grid, $RePr=4$, $Ra=1000$. Figures 5.59 and 5.60 show the results using an ADI technique for two cases. The cases are $RePr=4$, $Ra=200$ (reference Figure 5.29 for the explicit upwind differencing result) and $RePr=4$, $Ra=1000$ (Figure 5.31). Use of a larger grid, 30×30 , for $RePr=4$, $Ra=1000$ was necessary with the ADI calculation as it was critically unstable for a grid size of 20×20 .

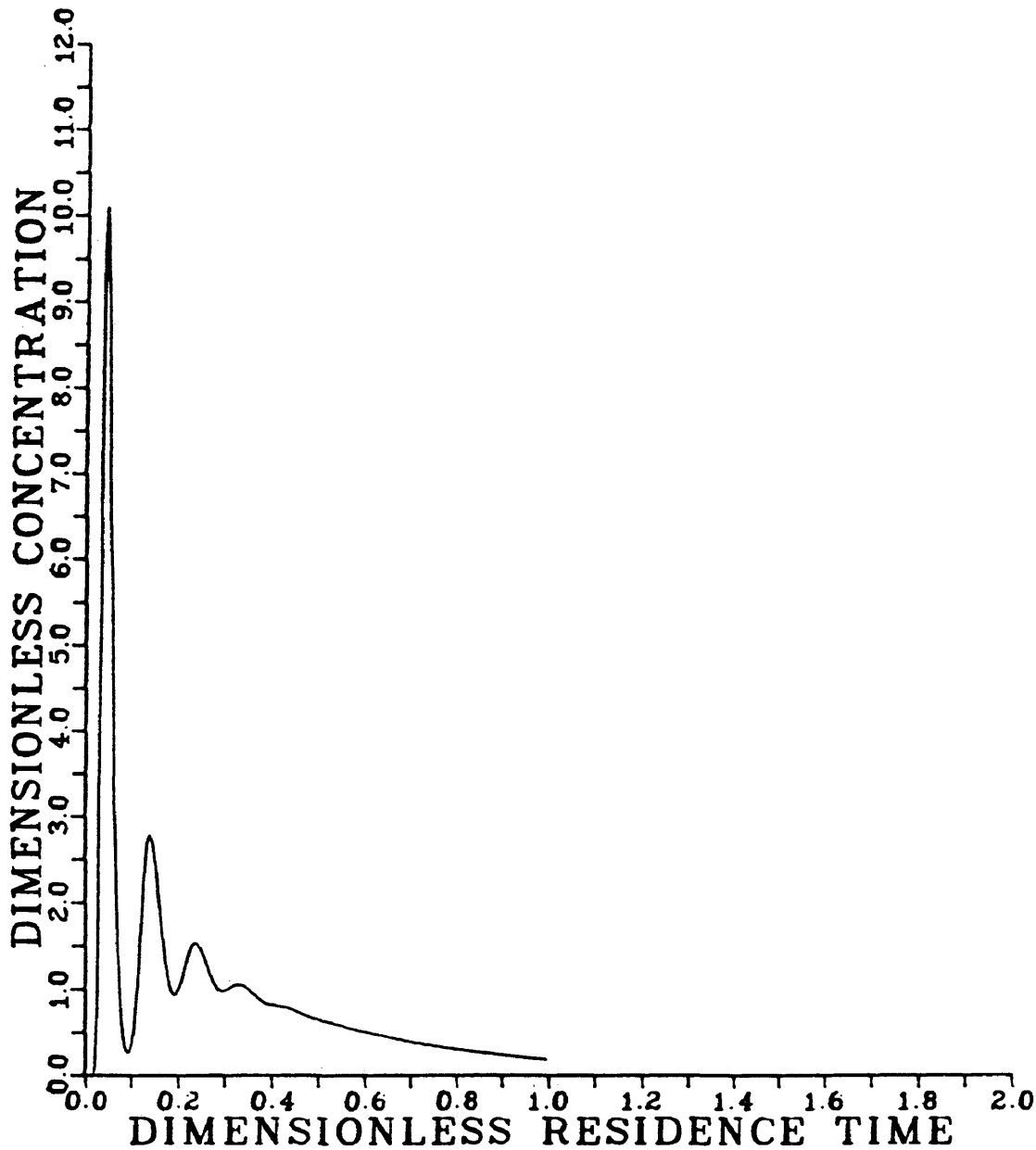


Figure 5.57
Residence Time Distribution
 $RePr=4, Ra=1000, M/N=20/20, \Delta\tau = .00005$

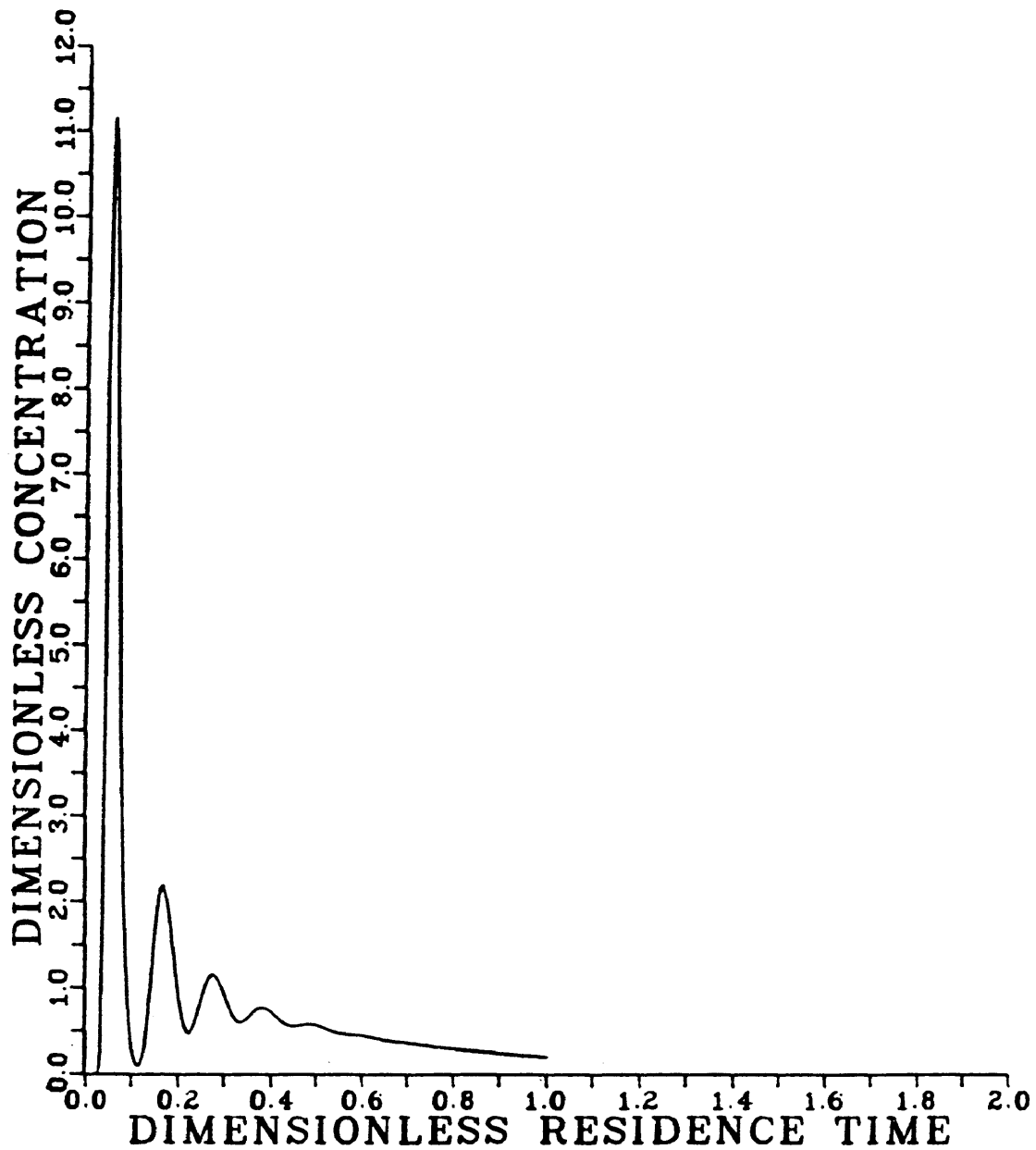


Figure 5.58
Residence Time Distribution
 $RePr=4$, $Ra=1000$, $M/N=40/40$, $\Delta\tau = .0002$

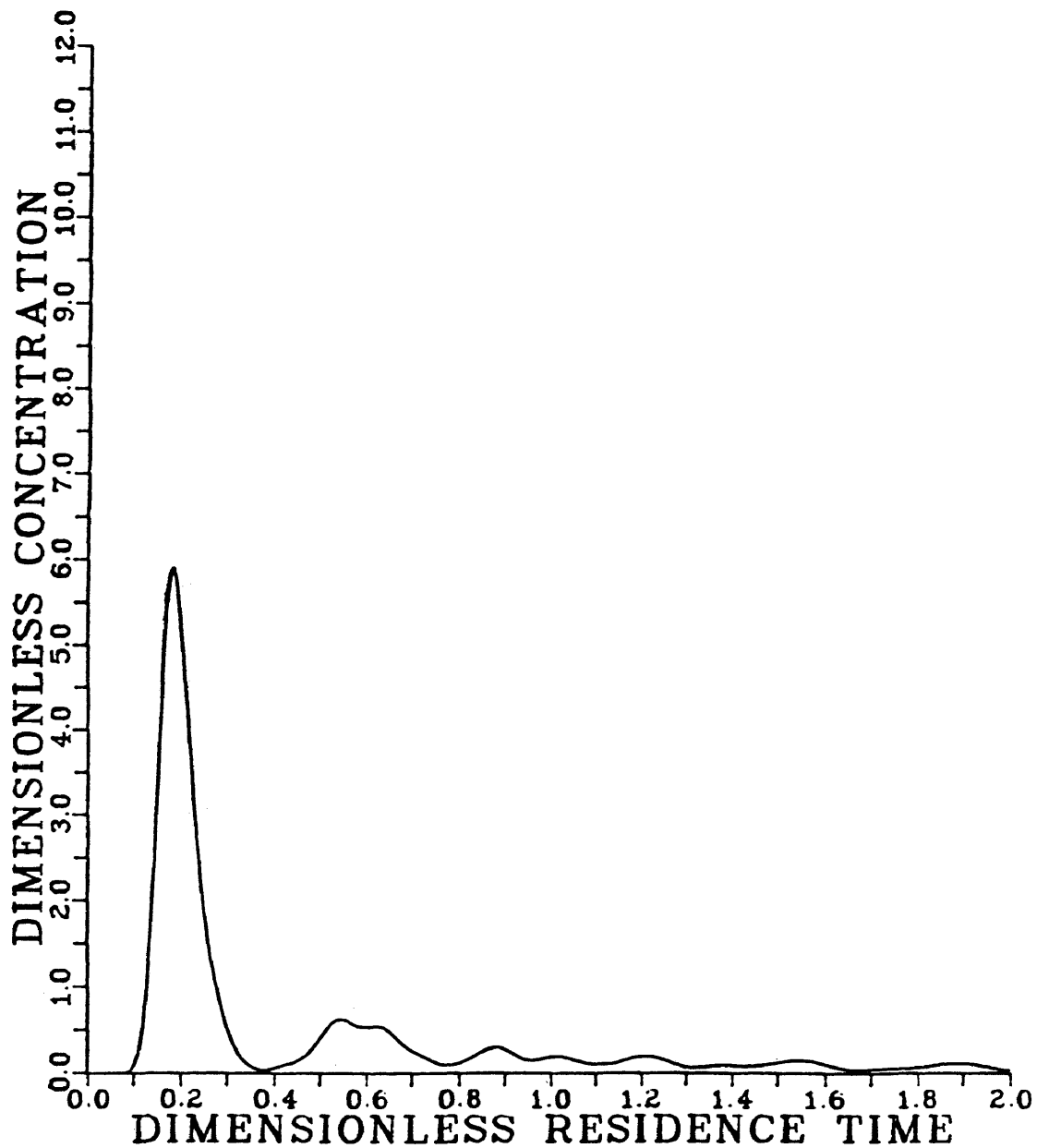


Figure 5.59
ADI Residence Time Distribution
 $RePr=4$, $Ra=200$, $M/N=20/20$, $\Delta\tau=.0001$

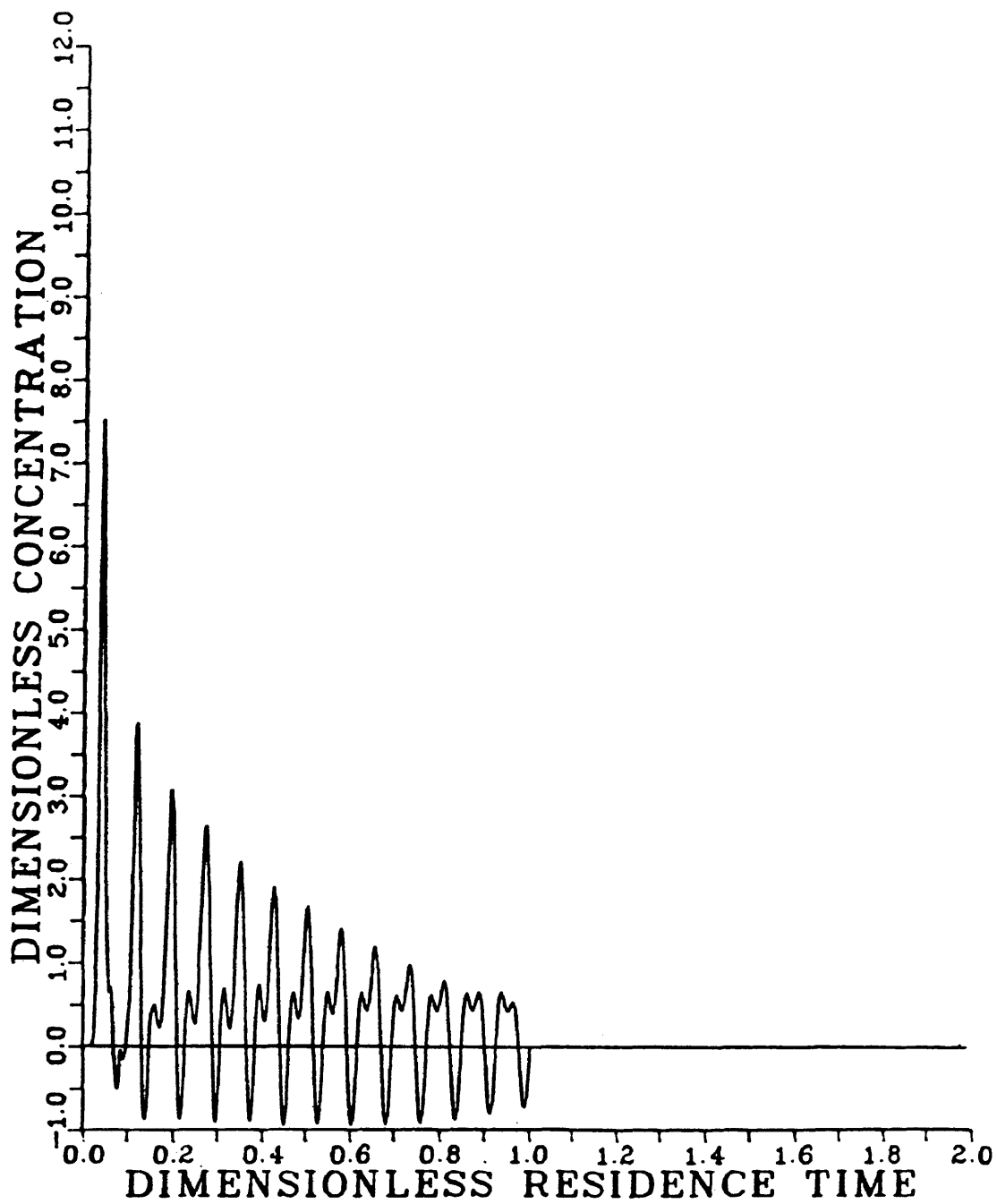


Figure 5.60
ADI Residence Time Distribution
 $RePr=4, Ra=1000, M/N=30/30, \Delta\tau = .0001$

6. DISCUSSION OF RESULTS

6.1 Detection of Free Convection and the Steady State

Plotting the log of the rms vorticity against time provides a reliable indicator of when the steady state has been attained. Combined with contours of the stream function and temperature the presence or absence of free convection can be ascertained. The time taken to achieve steady free convection can also be found.

6.2 The Critical Rayleigh Number

A brief comparison of linear and energy theory with the calculated results is presented to verify the numerical method is substantially accurate. Theory predicts that the onset of free convection in porous media is characterized by a critical Rayleigh number, Ra_{cr} , for a given $RePr$. The theoretical results of Homsy and Sherwood were graphically presented in Figure 1.1 of the Introduction. The graph is duplicated in Figure 6.1 with points plotted for the cases studied. All calculated convecting cases are in the theoretical free convection region. All calculated non-convecting cases are below the linear limit for the onset of convection. Calculated results are in agreement with theory.

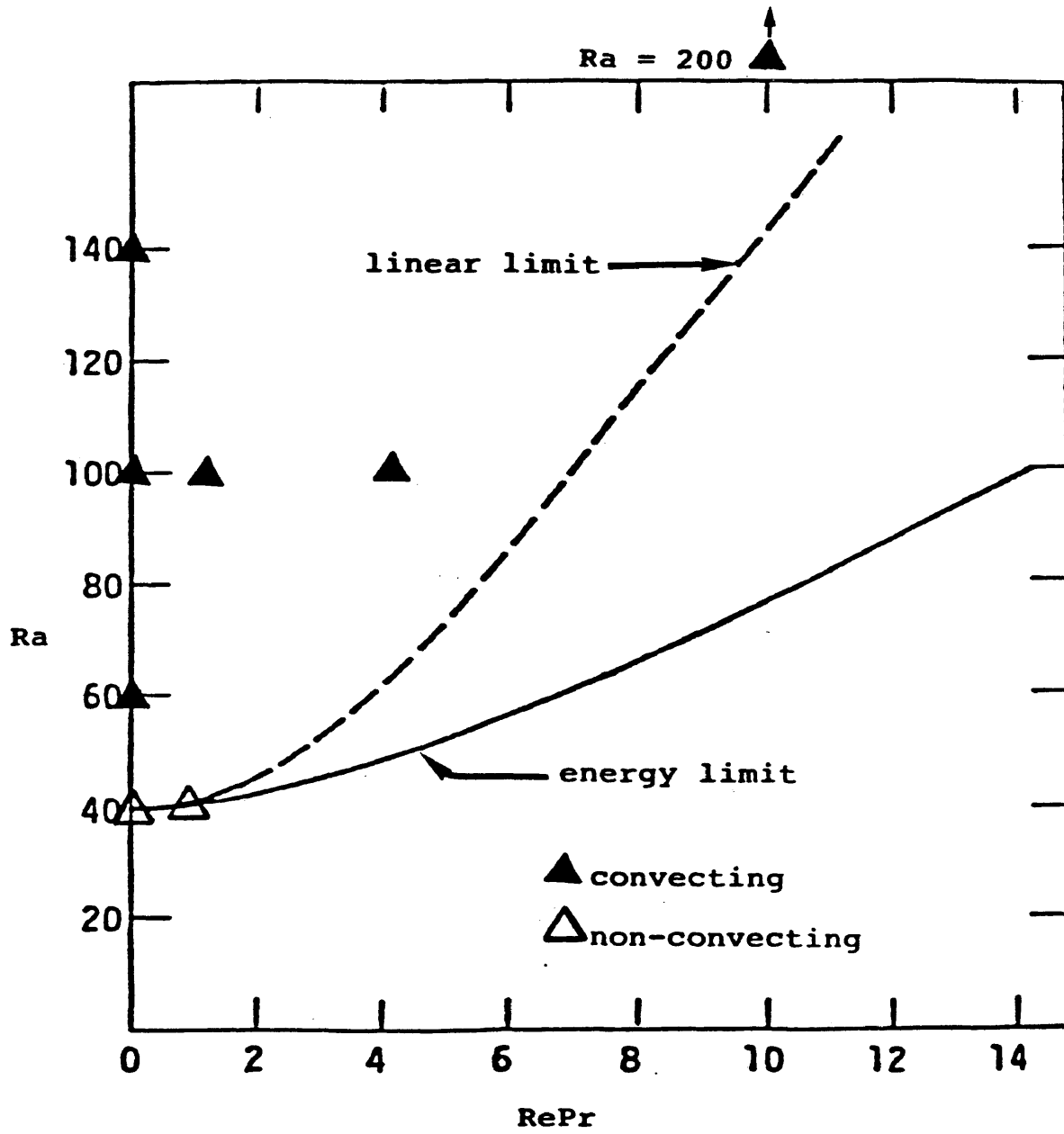


Figure 6.1
Comparison of Cases Studied with Linear Theory

The numerical calculations were neither designed nor expected to yield definitive determinations of the critical Rayleigh numbers. Nevertheless, an attempt was made to identify the critical Rayleigh number for the no-flow case, $RePr = 0$, where the well-known result for porous media, presented first by Lapwood [12] and refined by Katto and Masuoko [13] is $Ra_{cr} = 4\pi^2$. The critical Rayleigh number was estimated by plotting the slopes obtained for various Ra numbers from the Increase in Vorticity graph, $RePr = 0$, $M/N = 20/20$ (Figure 5.1), against time and extrapolating to the point of zero slope. The graph, presented in Figure 6.2 gives a critical Rayleigh number of about 52. However, careful examination of data for small rates of growth suggests that a fit over these points might well extrapolate to a value closer to $4\pi^2$.

6.3 Stream Function and Temperature Contours

The presence of free convection was confirmed by the observation of convecting cells in the stream function profiles. Both symmetrical and asymmetrical flows were observed. The number of cells increases with both Ra and $RePr$. Flow contours for varied aspect ratios show an increase in the number of cells for an increased width. For an increase in height, $RePr = 4$, $Ra = 200$, the cells became

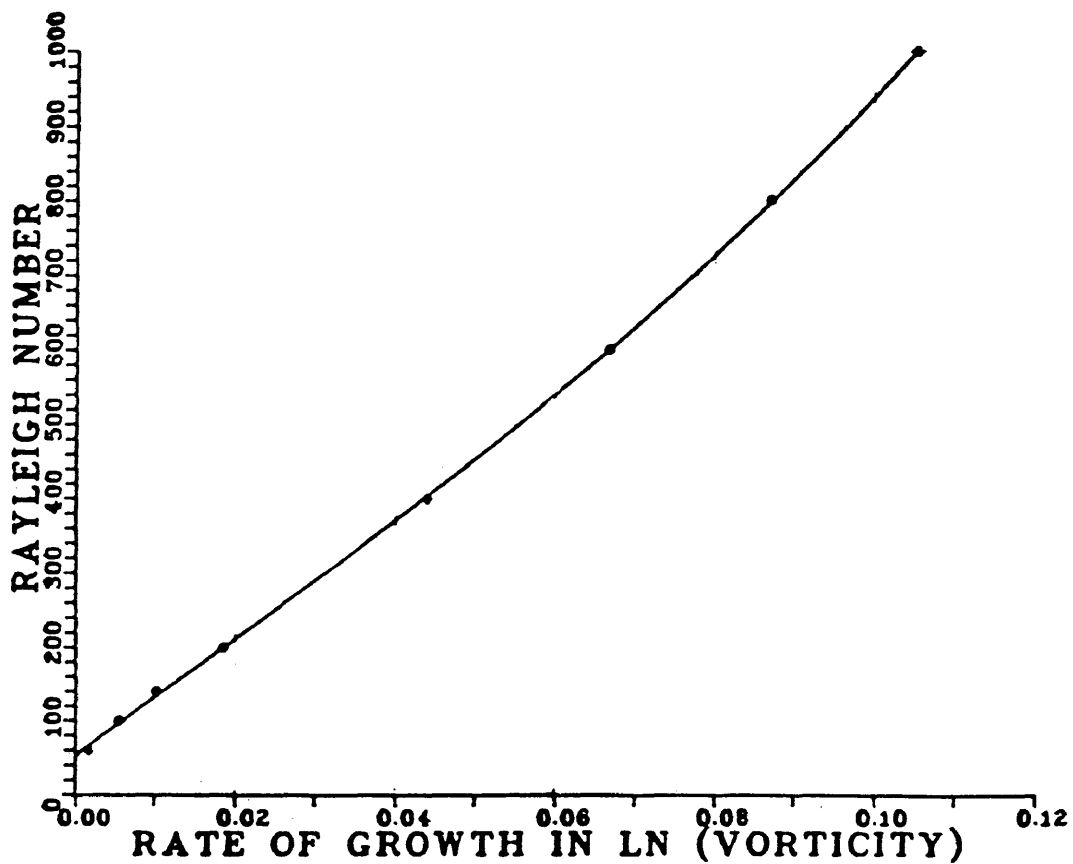


Figure 6.2
Critical Rayleigh Number Determination for No-Flow

narrower ($M/N = 20/60$) and subsequently merged ($M/N = 20/20$). For the case $RePr = 4$, $Ra = 600$, asymmetrical flow with partially stacked cells was produced.

Inspection of the paired stream function and temperature contours readily shows that the thermal gradient is the driving force for free convection. In all cases, the thermal gradient increases where upward flow is observed and decreases with downward flow.

The direction of flow rotation consistently reversed in going from no-flow to net through-flow. (Reversal also occurred for one of the aspect ratio cases.) There is no credible physical reason, within the context of this numerical study, for preferring clockwise to counter-clockwise rotation, particularly for the single cell cases. This phenomenon is not understood.

The ADI calculations are believed to be reasonably accurate and representative of steady state flow. The time step, and spatial increment chosen are satisfactory. The wisdom of the choice of the full grid rather than a half-grid with symmetry at the centerline was borne out in the results as asymmetrical flows were observed.

6.4 Analysis of the RTDs and Tracer Contours

The RTDs presented are in qualitative agreement with

the experimental work of Feuerherm [16]. Plug flow RTDs show the characteristic single peak. Flows with convection have RTDs with multiple peaks.

Contour plots of the tracer concentration, Figures 5.36 through 5.47, show movement through the flow field in agreement with the calculated RTD, Figure 5.29. The successive peaks are seen to result from recirculation of the tracer in the convection cells. Visual inspection of the RTDs indicates a dependance on $RePr$ and Ra , and none on the number of cells.

The RTDs were characterized in terms of a mixing time given by the reciprocal of the decay rate constant, where the decay rate constant is the absolute value of the slope of the log of the amplitude as a function of time. This parameter is widely used in mixing studies [2]. The amplitude was determined by taking half the value of the peak to valley distance. The first peak, first valley, and last peak were dicounted. Results for an aspect ratio of one are presented in Table 6.1. Graphs of the mixing time vs. Ra number and $RePr$ are presented in Figures 6.3 and 6.4. They show a decrease in mixing time with increasing Ra number and an increase with increasing $RePr$.

The RTD results are intermediate to the plug flow and perfectly mixed models. In general, the RTDs with high

Table 6.1

Mixing Times for Various RePr and Ra, M/N=20/20

<u>RePr</u>	<u>Ra</u>	<u>Mixing time τ^*</u>
1	200	0.2122
	600	0.0873
4	100	1.1783
	200	0.7180
	600	0.3099
	1000	0.1655
10	400	1.0524
	600	0.5172
	1000	0.4490

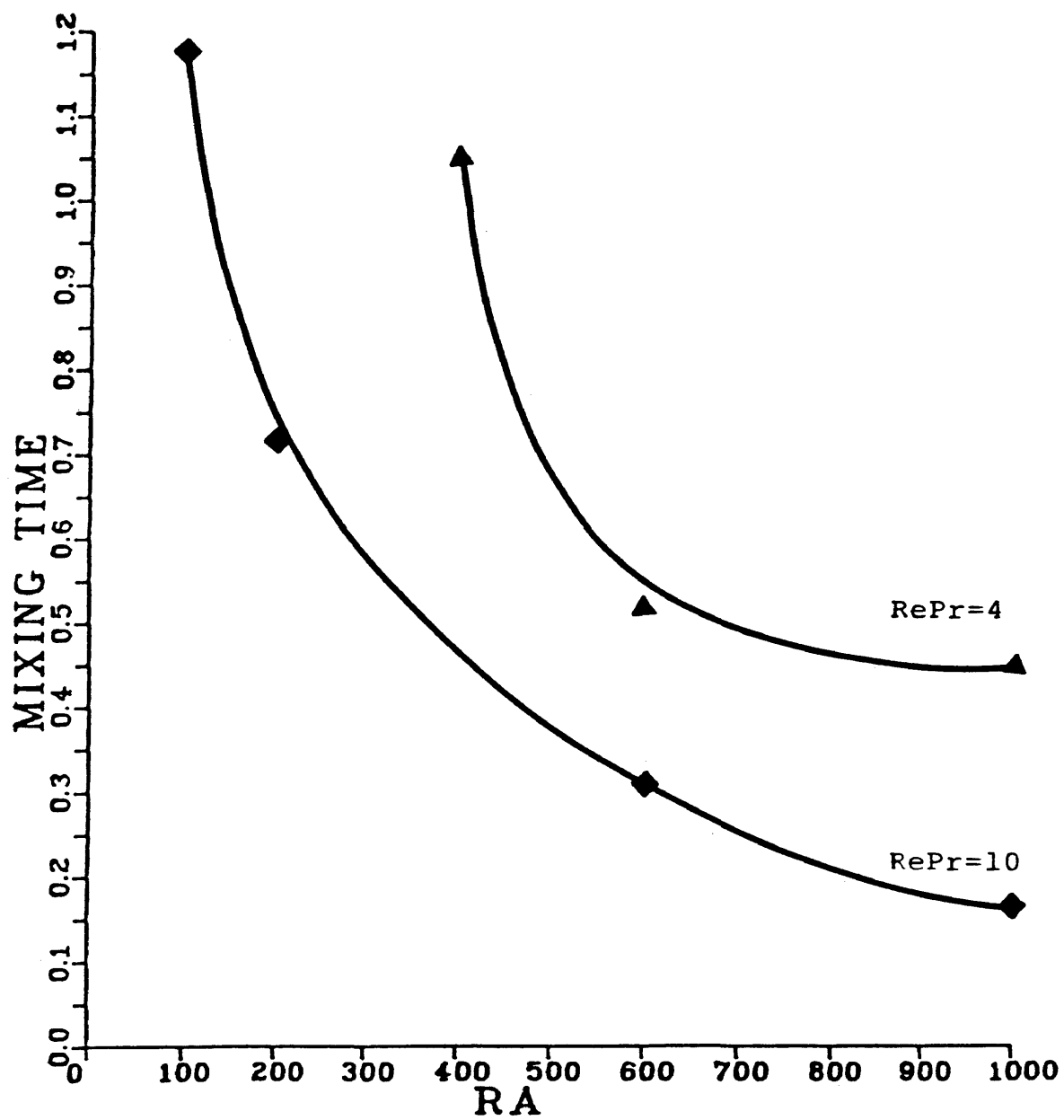


Figure 6.3
Mixing Time vs. Rayleigh Number

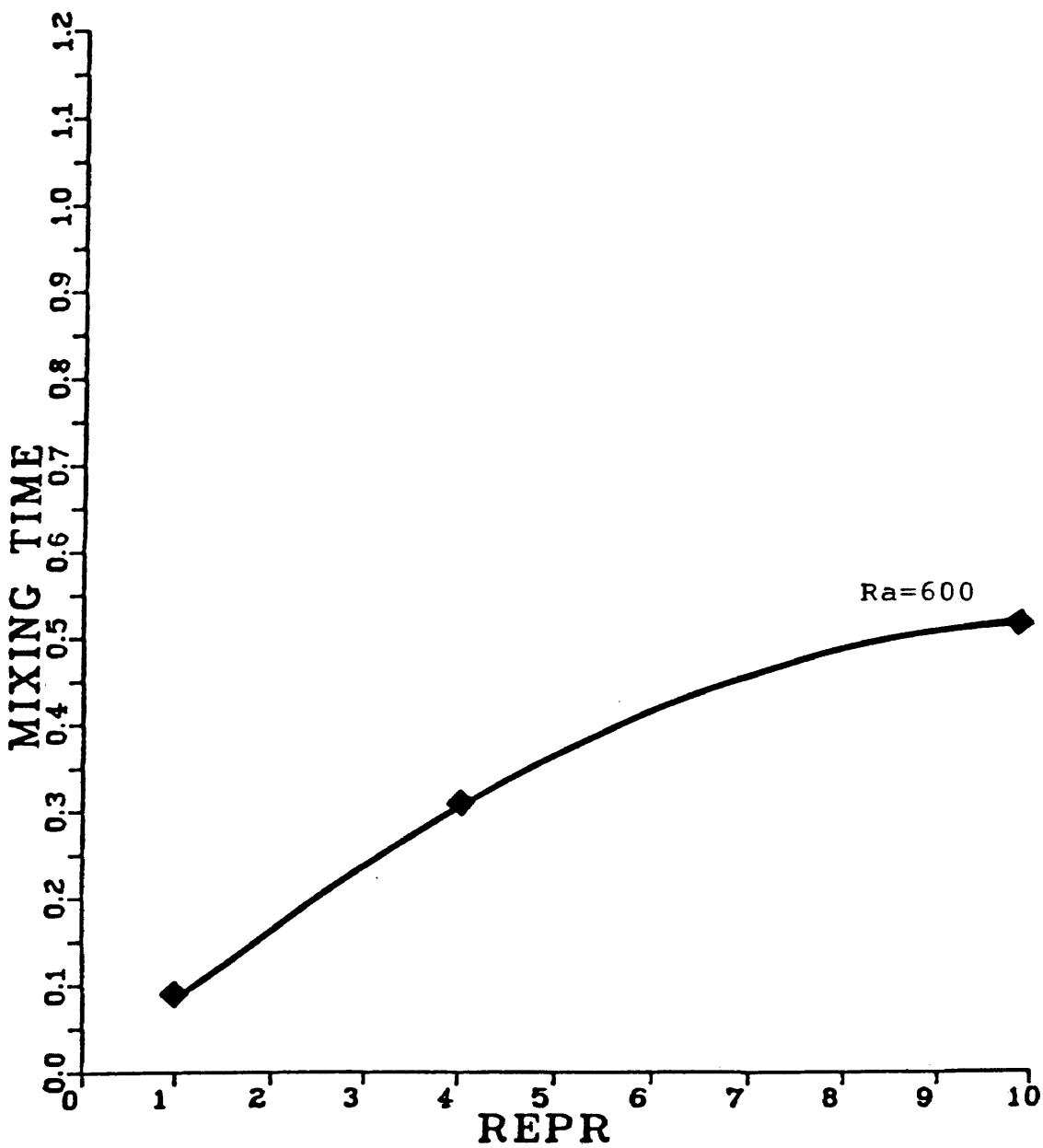


Figure 6.4
Mixing Time vs. RePr

mixing times approximate plug flow results. Those with low mixing times approach the perfectly mixed vessel model.

RTDs for the various aspect ratios showed little change in tracer response for an increase in width. (Using ADI techniques the RTDs could be superimposed; the change visible on the upwind differencing graphs is attributed to numerical dispersion.) This result is in agreement with the equations and the physical problem. An increase in height reduces the mixing time. Mixing times for the different aspect ratios are presented in Table 6.2 and in Figure 6.5.

6.5 Validity of the Tracer Response Calculations

6.5.1 Conservation of the Tracer Species

As a check on the conservation of the tracer species, and hence the precision of the numerical method, the area under each RTD curve was measured and compared to one, the value expected at infinite time. Results for plug flow were exact, those for convecting flow, aspect ratio equal to one, are summarized in Table 6.3. Agreement was good in all cases.

6.5.2 Plug Flow

The basic shape of the calculated upwind differencing

Table 6.2
Mixing Times for Various Aspect Ratios

<u>RePr = 4, Ra = 200</u>	<u>M/N</u>	<u>Aspect Ratio</u>	<u>Mixing Time τ^*</u>
	20/60	0.333	0.4646
	20/30	0.667	0.5439
	20/20	1.000	0.7180
	30/20	1.500	0.7137
	60/20	3.000	0.7428
<u>RePr = 4, Ra = 600</u>			
	20/60	0.333	0.0718
	20/20	1.000	0.3099

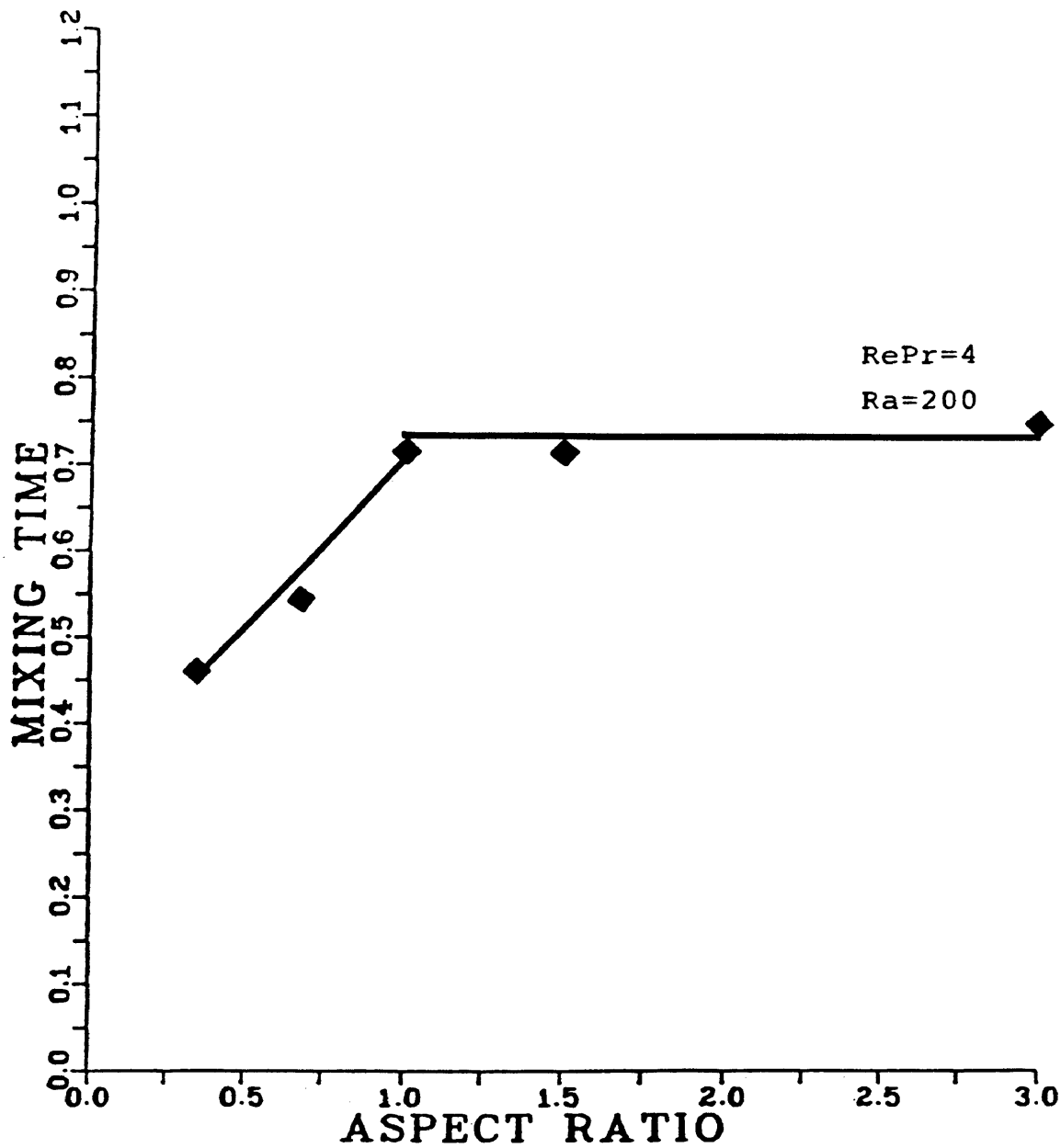


Figure 6.5
Mixing Time vs. Aspect Ratio (Width/Height)

Table 6.3
Area Under the RTD Curve

<u>RePr</u>	<u>Ra</u>	<u>Area</u>	<u>E final</u>
1	200	0.791	0.357
	600	0.844	0.486
4	100	0.854	0.088
	200	0.820	0.134
	600	0.955	0.069
	1000	0.995	0.014
10	200	0.848	0.079
	400	0.831	0.101
	600	0.853	0.123
	1000	0.900	0.109

plug flow RTDs is correct. Agreement with the theoretical calculations is best at low Re_{Pr} and increasingly worse at high Re_{Pr} . Two causes were investigated: size of the spatial increment and the dispersive effects of artificial viscosity inherent in the upwind differencing technique. A smaller spatial increment was tested with $Re_{Pr} = 10$ by increasing the grid size from 20x20 to 40x40. Some improvement in peak height is noted. Comparison of the upwind differencing plug flow RTDs with the ADI results, both generated on a 20x20 grid, suggests the dispersive effects of the upwind differencing technique are the primary cause of the low peak heights for plug flow.

6.5.3 Convecting Flows

The effects of spatial increment, time step, and numerical technique were tested on convecting cases. Variations in spatial increment and time step (as presented in Figures 5.31, 5.57 and 5.58) did not produce significant differences. Comparison of the upwind differencing and ADI methods - a check on the effects of numerical dispersion associated with upwind differencing - shows general agreement in the prediction of high/low mixing times (Figures 5.29 and 5.59; 5.31 and 5.60). Also noted for the ADI results is a substantial amount of noise, and for lower

mixing times, considerable oscillations about zero. (The effect of changing the pulse duration was also tested; no difference was noted for values of $N_{\text{trace}} = 1$ and 10.)

6.5.4 Summary

Based on the above comparison the results for convecting flows were determined to be less affected by numerical dispersion resulting from upwind differencing than were the plug flow results. Explicit upwind differencing was judged suitable for general predictions of the effect of the Re_{Pr} and Ra on the mixing time. ADI methods are unsuitable, particularly at high mixing times, because of excessive overshoot and oscillation.

6.6 Examples: Application to Oil Shale Retorts

Because work in dimensionless variables is difficult to visualize in terms of physical problems, two examples - representative of pilot scale oil shale retorts - are presented here. References and calculations for typical values of the parameters may be found in Appendix A.

Example 1

Reference figures 5.2, 5.27 and Table 6.1.

$$Le = 40$$

$$\text{RePr} = 1$$

$$\text{Ra} = 600$$

$$\text{M/N} = 20/20$$

Take the case where

$$\gamma = 2 \times 10^{-4}$$

$$\varepsilon = 0.35$$

$$\text{height} = 1.0 \text{ m}$$

$$\alpha' = 0.0033 \text{ m}^2/\text{sec}$$

The superficial velocity, v_o , may be obtained from the relationship

$$v_o = \frac{\text{RePr} \alpha'}{\text{height}} \quad (3.6-2)$$

$$v_o = 0.0033 \text{ m/sec}$$

The time for the flow pattern to reach steady state is obtained from Figure 5.2 in units of dimensionless time

$$\tau_{SS} = 1390$$

Since,

$$\tau = t \frac{\alpha'}{H} \quad (2.1-22)$$

and

$$\text{height} = \left(\frac{N-1}{20-1} \right) H \quad (3.6-4)$$

the actual time is

$$t_{SS} = 4.212 \times 10^5 \text{ sec} = 117.0 \text{ hr} = 4.875 \text{ days}$$

The residence time for the vessel, t_{res} , is obtained from the

relationship

$$\tau_{\text{res}} = \frac{\epsilon}{\text{RePr}} \left(\frac{N-1}{20-1} \right)^2 \quad (3.6-5)$$

and equation (2.1-22) as

$$t_{\text{res}} = 106.1 \text{ sec}$$

The mixing time in terms of dimensionless residence time is obtained from Table 6.1

$$\tau_{\text{mix}}^* = 0.0873$$

Applying equation (2.1-22) and

$$\tau^* = \frac{\tau \text{ RePr}}{\epsilon} \left(\frac{20-1}{N-1} \right)^2 \quad (3.6-3)$$

the mixing time is

$$t_{\text{mix}} = 9.259 \text{ sec}$$

The time to the arrival of the first peak can be read from Figure 5.27 as

$$\tau_{\text{peak}}^* = 0.0191$$

and similarly be converted to

$$t_{\text{peak}} = 2.026 \text{ sec}$$

Example 2

Reference Figures 5.3, 5.29 and Table 6.1

$$Le = 40$$

$$\text{RePr} = 4$$

$$Ra = 200$$

$$M/N = 20/20$$

Take the case where

$$\gamma = 2 \times 10^{-4}$$

$$\epsilon = 0.25$$

$$\text{height} = 3.0 \text{ m}$$

$$\alpha' = 0.0050 \text{ m}^2/\text{sec}$$

Proceeding as before, the superficial velocity is

$$v_o = 0.006667 \text{ m/sec}$$

The time to reach steady state, using Figure 5.3, is

$$t_{ss} = 2.448 \times 10^6 \text{ sec} = 680.0 \text{ hr} = 28.33 \text{ days}$$

The residence time for the vessel is

$$t_{res} = 112.5 \text{ sec}$$

Using Table 6.1, the mixing time is

$$t_{mix} = 80.77 \text{ sec}$$

and the time to the first peak, using Figure 5.29, is

$$t_{peak} = 17.88 \text{ sec}$$

7. CONCLUSIONS

From the results obtained the following conclusions are drawn:

- a) The achievement of steady state can be verified from plots of the natural log of the rms average vorticity.
- b) Points where convection was found are in agreement with linear theory.
- c) The number of cells increases with both increasing $RePr$ and Ra .
- d) Both symmetrical and asymmetrical flow patterns are possible.
- e) ADI calculations are reasonably accurate and capable of representing steady-state flows.
- f) Tracer RTDs are in qualitative agreement with the experimental results of Feuerherm
- g) Successive peaks in the RTDs result from recirculation of tracer in the rotating convection cells.
- h) Tracer concentration contours are in agreement with the RTDs based on the average exit age.
- i) RTD results for free convection are intermediate to the perfectly mixed vessel and plug flow cases.

j) RTD results for free convection are characterized by Ra , $RePr$ and the height of the vessel. They are independent of the number of cells and the vessel width.

k) Mixing times increase with increasing $RePr$ and decrease with increasing Ra and increasing height.

l) The effects of numerical dispersion, inherent in upwind differencing, are most noticeable on plug flows and of less importance with convecting flows.

m) Explicit upwind differencing is suitable for producing a qualitative representation of tracer response.

n) ADI methods alone are unsuitable for tracer response calculations because of excessive overshoot and oscillation.

In summation, RTD methods are decisive in detecting free convection and capable of qualitatively characterizing the flow in terms of mixing times.

NOMENCLATURE

A	area under the concentration-time curve
ADI	Alternating Direction Implicit; a numerical method
b	subscript for bed properties
C_A	concentration of tracer
C_{Ao}	reference concentration of tracer
$C_{initial}$	concentration of tracer in the impulse
C_p	specific heat
D	mass dispersion coefficient
$E_{initial}$	dimensionless tracer concentration
E	dimensionless tracer concentration in the impulse
f	subscript for fluid properties
g	gravity
G	transfer function
h	spatial increment
H	reference length
i	subscript for the horizontal direction
j	subscript for the vertical direction
\hat{j}	unit vector in the vertical direction
k	thermal conductivity
K	bed permeability
Le	Lewis number
M	number of grid points in the horizontal direction

n	superscript for time
N	number of grid points in the vertical direction
N _{trace}	number of time steps for pulse duration
OPTOM	relaxation factor for SOR
P	pressure
P ₁	parameter for Upwind Differencing
P ₂	parameter for Upwind Differencing
Pe	Peclet number
Ra	Rayleigh number
Ra	critical Rayleigh number
RePr	Reynolds-Prandtl
rms	root mean square
SOR	Successive Overrelaxation; a numerical method
t	time
t _{res}	residence time for the vessel
T	temperature
T ₀	temperature at the top
T ₁	temperature at the bottom
(T ₁ -T ₀)	reference temperature difference
U	dimensionless horizontal component of superficial velocity
UB	backward difference in velocity U; used in upwind differencing
UF	forward difference in velocity U;

	used in upwind differencing
\vec{v}	superficial velocity
v_0	initial superficial velocity
v_x	horizontal component of superficial velocity
v_y	vertical component of superficial velocity
V	dimensionless vertical component of superficial velocity
V_0	dimensionless initial superficial velocity
VB	backward difference in velocity V ; used in upwind differencing
VF	forward difference in velocity V ; used in upwind differencing
x	distance in the horizontal direction
X	dimensionless distance in the horizontal direction
y	distance in the vertical direction
Y	dimensionless distance in the vertical direction
α'	effective thermal diffusivity
β	coefficient of volume expansion
δ	impulse function
δ^*	impulse function in dimensionless time
ϵ	bed porosity
γ	ratio of specific heats
ρ	density
ρ_0	density at temperature T_0

ψ	stream function
Ψ	dimensionless stream function
τ	dimensionless time
τ_{res}	residence time for the vessel in dimensionless terms
τ^*	dimensionless residence time
$\Delta\tau$	dimensionless time step
θ	dimensionless temperature difference
ν	kinematic viscosity
$\vec{\xi}$	vorticity
$\vec{\omega}$	dimensionless vorticity
*	superscript for the intermediate time step, $n+1/2$

REFERENCES

1. D. B. Holmes, R. M. Voncken and J. A. Dekker, "Fluid Flow in Turbine-Stirred, Baffled Tanks-I," Chem. Eng. Sci., vol. 19, pp. 201 (1964).
2. S. J. Khang and O. Levespiel, "New Scale-up and Design Method for Stirrer Agitated Batch Mixing Vessels", Chem. Eng. Sci, vol. 31, pp. 569 (1976).
3. T. Sasakura, et al., "Mixing Process in a Stirred Vessel, "Int. Chem. Eng., vol. 20, no. 2, pp.251 (1980)..
4. S. Chandrasekhar, Hydrodynamic and Hydromagnetic Stability, London, Oxford University Press (1961).
5. B. Carnahan, H. A. Luther, and J. O. Wilkes, Applied Numerical Methods, N.Y., John Wiley and Sons, Inc. (1969).
6. G. D. Smith, Numerical Solution of Partial Differential Equations: Finite Difference Methods - 2nd Edition, Oxford University Press (1978).
7. P. J. Roache, Computational Fluid Dynamics, Albuquerque,

N.M., Hermosa Publishers (1972).

8. C.-Y. Chow, An Introducton to Computational Fluid Mechanics, N.Y., John Wiley and Sons, Inc. (1979).

9. J. O. Wilkes and S. W. Churchill "The Finite-Difference Computation of Natural Convection in a Rectangular Enclosure," AICHE J., vol 12, no. 1, pp. 161 (1966).

10. M. R. Samuels and S. W. Churchill, "Stability of a Fluid in a Rectangular Region Heated from Below," AICHE J., vol. 13, no. 1, pp. 77 (1967).

11. A. Pellew and R. V. Southwell, F.R.S. "On Maintained Convective Motion in a Fluid Heated from Below," Proc. Royal Soc. A, vol. 176, pp. 312 (1940).

12. E. R. Lapwood, "Convection of a Fluid in a Porous Medium," Proceedings of the Cambridge Philosophical Society, vol. 44, pp. 508 (1948).

13. Y. Katto and T. Masuoka, "Criterion for the Onset of Convective Flow in a Fluid in a Porous Medium," Int. J. Heat and Mass Transfer, vol. 10, pp. 297 (1967).

14. G. M. Homsy and A. E. Sherwood, "Convective Instabilities in Porous Media with Through Flow," *AICHE J.*, vol. 22, no. 1, pp. 168 (1967).
15. J. C. Friedly, Dynamic Behavior of Processes, Englewood Cliffs, N.J., Prentice-Hall Inc. (1972).
16. H. R. Feuerherm, "Onset of Convective Currents in a Heated Porous Medium with Net Through-Flow," M.S. Thesis T-2794, Colorado School of Mines (1984).
17. P. V. Danckwerts, "Continuous Flow Systems - Distribution of Residence Times," *Chem. Eng. Sci.*, vol. 2, no. 1., pp. 1 (1953).
18. J. H. Raley, W. A. Sandholtz and F. J. Ackerman, "Results from Simulated, Modified in situ Retorting in Pilot Retorts," *Eleventh Oil Shale Symposium Proceedings*, Golden, Colorado, Colorado School of Mines Press, pp. 33 (1978).
19. J. Dubow et al., "The Effects of Moisture and Organic Content on the Thermophysical Properties of Green River Oil Shale," *Eleventh Oil Shale Symposium Proceedings*, Golden,

Colorado, Colorado School of Mines Press, pp. 33 (1978).

20. S. Yagi and D. Kunii, "Studies on Effective Thermal Conductivities in Packed Beds," *AIChE J.*, vol. 3, no. 3, pp. 373 (1957).

21. D. M. Himmelblau and K. B. Bischoff, Process Analysis and Simulation - Deterministic Systems, N.Y., John Wiley and Sons, Inc. (1968).

22. R.J. Sampson, Surface II Graphics System, Lawrence, Kansas, Kansas Geological Survey (1978).

APPENDIX A
TYPICAL PARAMETERS

A.1 Laboratory Scale Oil Shale Retort Parameters

Typical values for laboratory scale oil shale retorts were obtained from Raley, Sandholtz and Ackerman [18] for 1.5 x 0.3m and 6 x 0.9m retorts using Anvil Points shale. They are presented in Table A.1 and A.2.

Bed permeabilities for the 1.5 x 0.3m shale oil retort may be calculated from Darcy's law by neglecting the effects of gravity

$$K = \frac{v_{\rho} v}{(\Delta P / \Delta Y)}$$

For a nominal fluid viscosity of

$$v_{\rho} = 0.041 \text{ g/m-sec}$$

the permeability can vary from initial values of 7.34×10^{-6} to $1.83 \times 10^{-4} \text{ m}^2$ to values at maximum pressure drop of 5.03×10^{-8} to $1.60 \times 10^{-5} \text{ m}^2$.

Values of thermal conductivity and thermal diffusivity for Anvil Points oil shale are found in DuBow et al. [19]. Typical thermal conductivities range from 0.43 to 1.51 kcal/m-hr^oC at 380^oC. Thermal diffusivities at 380^oC vary from 0.002 to 0.005 m²/sec

A.2 Experimental Velocities

Additional values for laboratory scale packed bed reactor velocities were obtained from Feuerherm [16]. They ranged

Table A.1
Oil Shale Parameters, 1.5 x 0.3m Retort

Shale									
Size Range, cm	-2.5+1.3	-2.5+.13	-7.6+0	-2.5+1.3	-7.6+0	-2.5+1.3	-7.6+0	-2.5+0	
<1.3 cm, wt%	-	0	26	0	26	0	26	73	
<0.34 cm, wt%	-	0	9	0	9	0	9	33	
Bed Porosity	0.47	0.47	0.38	0.49	0.38	0.49	0.34	0.37	
Gas Feed									
m/sec	0.0105	0.0102	0.0190	0.117	0.0117	0.117	0.117	0.117	
Pressure Drop, nt/m ²									
initial	-	4.903	9.806	-	-	-	39.226	980.64	
maximum	-	39.226	205.93	-	-	-	1098.32	14327.3	
Avg. max Temp °C	886	1003	-	887	-	-	-	-	

Table A.2

Oil Shale Parameters 6 x 0.9m Retort

Shale Size, cm	-7.6,+0 ≈20	(61 wt%) (39 wt%)
Porosity	0.25	
Gas Feed m/sec	0.02	

from 0.000715 to 0.001001 m/sec.

A.3 Calculation of Effective Thermal Conductivity and Diffusivity

The effective thermal conductivity in a packed bed may be estimated from the procedure outlined by Yagi and Kunii [20]. The effective thermal diffusivity may be obtained from this value. A typical value is calculated. Using the parameters

$$\epsilon = 0.35$$

$$P(\text{emissivity}) = 0.9$$

$$T = 700^{\circ}\text{C}$$

the heat transfer coefficients for thermal radiation are obtained. From solid surface to solid surface:

$$h_{rs} = 0.1952 \frac{P}{2-P} \left(\frac{T+273}{100} \right)^3$$

$$h_{rs} = 147.12$$

From void to void:

$$h_{rv} = \left\{ \frac{0.1952}{1 + \frac{\epsilon}{2(1-\epsilon)} \frac{1-P}{P}} \right\} \left(\frac{T+273}{100} \right)^3$$

$$h_{rv} = 174.59$$

The ratio of the effective thermal conductivity for a motionless gas, k_b^0 , to the fluid thermal conductivity is given by

$$\frac{k_b^0}{k_f} = \left\{ \frac{1 - \epsilon}{\frac{k_f}{k_s} + \frac{1}{1/\phi + d_p h_{rs}/k_f}} \right\} + \epsilon \frac{d_p h_{rv}}{k_f}$$

Using the values

$$\phi = 0.025$$

$$k_f = 0.0524$$

$$k_s = 0.9$$

$$d_p = 0.03$$

The calculated ratio is

$$\frac{k_b^0}{k_f} = 44.7927$$

$$k_b^0 = 2.347 \text{ kcal/m-hr } ^\circ\text{C}$$

For low flow rates the effective thermal conductivity of the bed, k_b , is equal to that for motionless gas

$$k_b = 2.347 \text{ kcal/m-hr } ^\circ\text{C}$$

The effective thermal diffusivity may now be calculated from

$$\alpha' = \frac{k_b}{(\rho C_p)_f}$$

for

$$\rho_f = 0.000409 \text{ g/cm}^3$$

$$C_{p_f} = 0.26 \text{ cal/g } ^\circ\text{C}$$

the value is

$$\alpha' = 0.00613 \text{ m}^2/\text{sec}$$

A.4 Calculation of Rayleigh Number and RePr

The Rayleigh number is given by

$$Ra = \frac{\beta g H (T_1 - T_0) K}{\alpha' \nu}$$

Typical parameters are

$$g = 9.8 \text{ m/sec}^2$$

$$(T_1 - T_0) = 70^\circ\text{C}$$

$$K = 1 \times 10^{-4} \text{ m}^2/\text{sec}$$

$$\alpha' = 0.005 \text{ m}^2/\text{sec}$$

$$\nu = 1.002 \times 10^{-4} \text{ m}^2/\text{sec}$$

H is the height; a value of 1.5 m is used. The coefficient of volume expansion, β , is on the order of 10^{-3} to 10^{-4} .

For ideal gases it is given by

$$\beta = 1/T$$

For a temperature of 700°C ($= 973^\circ\text{K}$), $\beta = 0.001/^\circ\text{C}$. The resulting Ra is

$$Ra = 205.4$$

A corresponding RePr can be determined from the relationship

$$RePr = \frac{v_o \text{ height}}{\alpha}$$

for a velocity of 0.02 m/sec the RePr is

$$RePr = 6.0$$

This case would exhibit free convection.

A.5 Calculation of Lewis Number

A nominal value for the Lewis number was derived based

on the relationship between the particle Reynolds number, Re_p , and the particle Peclet number, Pe_p , presented in Himmelblau and Bishoff's Figure A.10 [21]. The Re_p is obtained from

$$Re_p = \frac{RePr}{Pr} \left(\frac{d_p}{\text{height}} \right)$$

where the $RePr$ is related to the superficial velocity by

$$RePr = \frac{v_o \text{height}}{\alpha'}$$

and the effective Prandtl number is obtained from the fluid Prandtl number by

$$Pr = Pr_f \frac{k_f}{k_b}$$

The effective Peclet number, Pe , and Lewis number for mass dispersion, Le , are calculated from

$$Pe = Pe_p \frac{H}{d_p}$$

$$Le = \frac{Pe}{RePr}$$

Using the values,

$$\text{height} = 3\text{m}$$

$$d_p/\text{height} = 1/100$$

$$\alpha' = 0.005 \text{ m}^2/\text{sec}$$

$$Pr_f = 0.733$$

$$k_b/k_f = 44.7927$$

Lewis numbers were calculated for $RePr$'s of 1, 4, and 10.

Reference Table A.3. A nominal value of $Le = 40$ was selected and used in all calculations.

Table A.3
Calculation of Lewis Number

RePr	v_o	Rep	1/Pep	Pep	Pe	Le
1	.00167	0.611	1.08	0.926	92.6	92.6
4	.00667	2.445	0.63	1.587	158.7	39.7
10	.01670	6.112	0.58	1.724	172.4	17.2

APPENDIX B
COMPUTER PROGRAM

B.1 Computer Executions

All executions were performed on a DECsystem-1091. The CPU time for flow and tracer executions follows in Tables. The maximum number of iterations in the successive overrelaxation subroutine during an execution was typically 24.

All contour plots were generated using Surface II Graphics System, Sampson [22].

Table B.1
CPU Times for Flow Executions

RePr	Ra	M/N	CPU time (min:sec)
0	100	20/20	16:58
	140	20/20	9:43
	200	20/20	7:29
	400	20/20	4:17
	600	20/20	3:41
	800	20/20	3:02
1	100	20/20	7:14
	200	20/20	3:12
	600	20/20	2:44
	1000	20/20	1:15
4	100	20/20	12:26
	200	20/20	3:09
		20/30	4:59
		20/60	10:59
		30/20	5:12
		60/20	9:16
	600	20/20	1:28
	1000	20/20	1:20
		30/30	5:08
10	200	20/20	8:16
	400	20/20	2:12
	600	20/20	1:23
	800	20/20	1:25
	1000	20/20	2:27

Tabel B.2
CPU Times for Tracer Executions

RePr	Ra	M/N		CPU time (min:sec)	
1	200	20/20	.0001	2:36	
	600	20/20	.0001	1:44	
4	100	20/20	.0001	1:34	
	200	20/20	.0001	1:31	
		20/20	.0001	4:51	(ADI)
		20/30	.0001	4:55	
		20/60	.0002	5:27	
		30/20	.0001	2:40	
		60/20	.0001	5:26	
	600	20/20	.0001	1:32	
	1000	20/20	.0001	1:31	
		20/20	.0001	8:58	(ADI)
20/20		.00005	1:51		
40/40		.0002	8:27		
10	200	20/20	.0001	0:36	
	400	20/20	.0001	0:40	
	600	20/20	.0001	0:44	
	1000	20/20	.0001	0:38	

B.2 Flow Program: ADI

```

C-----
C  MAIN PROGRAM FLOW.FOR
C  INSTABILITY OF FLUID FLOW THROUGH POROUS MEDIA HEATED FROM BELOW
C  SUCCESSIVE OVERRELAXATION SOLUTION FOR THE
C  STREAM FUNCTION
C  ALTERNATING-DIRECTION IMPLICIT SOLUTION FOR TEMPERATURE
C  TWO-DIMENSIONAL RECTANGULAR COORDINATES
C  'U(I,J)' VELOCITY IN THE X-DIRECTION
C  'V(I,J)' VELOCITY IN THE Y-DIRECTION
C  'THETA(I,J)' TEMPERATURE
C  'PSI(I,J)' STREAM FUNCTION
C  'OMEGA(I,J)' VORTICITY
C  FLOW EXECUTION REQUIRES THE FOLLOWING SUBROUTINES:
C  TEMP.FOR
C  SORLX.FOR
C  IMPX.FOR
C  TRIDX.FOR
C  IMPY.FOR
C  TRIDY.FOR
C-----

C  'M' IS THE X-DIRECTION INDEX
C  'N' IS THE Y-DIRECTION INDEX

      PARAMETER M=20
      PARAMETER N=60

C  'K' IS THE GREATER OF 'M' AND 'N'

      PARAMETER K=60

C  'L' SPECIFIES WHERE TO WRITE

      PARAMETER L=4

      DIMENSION U(M,N),V(M,N),THETA(M,N),TDELTA(M,N),
      1OMEGA(M,N),OM(M,N),PSI(M,N),A(K),C(K),D(K),
      1Q(K),QS(K),BETA(K),GAMMA(K),TH(N),POLD(M,N),PS(M,N),P(M,N)
      DOUBLE PRECISION THETA,Q,QS,TH,POLD,PS,P,A,C,D,BETA,GAMMA
      DOUBLE PRECISION U,V,TDELTA,OMEGA,OM,PSI
      COMMON /BLK/ B,MM1,NM1,C1,C2,C3

      WRITE(4,100)
100  FORMAT(5X,'ENTER TODAYS DATE',/)
      READ(4,110)NDATE
110  FORMAT(I)

C  'RA' IS THE RAYLEIGH NUMBER
C  'REPR' IS THE REYNOLDS-PRANDTL NUMBER
C  'DT' IS THE TIME INCREMENT
C  'MAXSTP' IS THE MAXIMUM NUMBER OF TIME STEPS

      WRITE(4,120)
120  FORMAT(5X,'ENTER RA, REPR, DT, MAXSTP',/)
      READ(4,130)RA,REPR,DT,MAXSTP
130  FORMAT(3E,I)

```

C 'GAM' IS THE FLUID TO MEDIUM HEAT CAPACITY-DENSITY RATIO
 C 'V0' IS THE INITIAL SUPERFICIAL VELOCITY

GAM = 2.E-4
 V0 = -REPR*(19.0/(N-1.0))

C 'H' IS THE SPACE INCREMENT

MM = M
 NN = N
 MM1 = M-1
 MM2 = M-2
 NM1 = N-1
 NM2 = N-2
 H = 1./((20.-1.)
 RATIO = MM1/NM1

140 WRITE(4,140)RA,REPR,DT,MM,NN,RATIO
 FORMAT(1H1,/,/,5X,'FLOW EXECUTION',/9X,'RA=',E/9X,
 1'REPR=',E/9X,'DT=',E/9X,'X-DIRECTION INDEX M=',
 2I3/9X,'Y-DIRECTION INDEX N=',I3/9X,'ASPECT RATIO=',E)

C 'C1', 'C2', 'C3' AND 'B' ARE CONSTANTS IN THE ENERGY
 C EQUATION

C1 = 1./(H*H)
 C2 = 2.*H
 C3 = 2./(GAM*DT)
 B = C3+2.*C1

C SPECIFY INITIAL CONDITIONS FOR VORTICITY AND VELOCITY

T = 0.
 NTUNIT = 1
 DO 10 J=1,N
 DO 10 I=1,M
 OMEGA(I,J) = 0.
 10 CONTINUE
 DO 12 I=1,M
 U(I,1) = V0
 U(I,N) = V0
 12 CONTINUE

C SUBROUTINE TEMP SPECIFIES THE INITIAL TEMPERATURE
 C PROFILE

CALL TEMP(REPR,M,N,TH,THETA,ITEMP)
 IF (ITEMP .EQ. 0) GO TO 14
 WRITE(4,150)
 150 FORMAT(9X,'UNIT STEP INITIAL TEMPERATURE DISTRIBUTION',/)
 GO TO 16
 14 WRITE(4,160)
 160 FORMAT(9X,'STEADY STATE INITIAL TEMPERATURE DISTRIBUTION',/)

C CALCULATE INITIAL AND BOUNDARY CONDITIONS FOR STREAM FUNCTION

```

16   AM = MM1
      DO 18 I=1,M
          ZETA = V0*(AM/19.)*(0.5-(I-1)/AM)
          FTOT = FTOT+ABS(ZETA)
          DO 18 J=1,N
              PSI(I,J) = ZETA
18   CONTINUE
      FRMS = FTOT/M
      FTOT = 0.

```

C BEGIN ITERATIVE PROCEDURE

C SUBROUTINE SORLX CALCULATES THE STREAM FUNCTION
C FROM THE VORTICITY FIELD

```

1     DO 20 I=1,M
          DO 20 J=1,N
              OM(I,J) = -OMEGA(I,J)
20   CONTINUE

      CALL SORLX(PSI,OM,M,N,H,.0010,ITER,RE,FRMS,ITMAX)

```

C CALCULATE VELOCITY FIELD

```

      DO 24 J=2,NM1
          DO 22 I=2,MM1
              U(I,J) = (PSI(I,J+1)-PSI(I,J-1))/C2
              V(I,J) = (-PSI(I+1,J)+PSI(I-1,J))/C2
22   CONTINUE
          V(1,J) = V(2,J)
          V(M,J) = V(MM1,J)
24   CONTINUE

```

C 'NSTEP' IS THE STEP NUMBER

C TERMINATE COMPUTATION IF NSTEP EXCEEDS MAXSTP

C INCREMENT TIME STEP BY ONE

```

      NSTEP = NSTEP+1
      IF (NSTEP .GT. MAXSTP) GO TO 2
      T = T+DT

```

C DETERMINE TEMPERATURE FIELD AT THE NEW TIME STEP WITH
C SUBROUTINES IMPX, IMPY, TRIDX, AND TRIDY

```

      DO 30 I=1,M
          DO 30 J=1,N
              POLD(I,J) = THETA(I,J)
30   CONTINUE

      CALL IMPX(POLD,PS,U,V,M,N,A,C,D,GS,BETA,GAMMA)

      CALL IMPY(PS,THETA,U,V,M,N,A,C,D,G,NM2,BETA,GAMMA)

```

C CALCULATE VORTICITY FIELD

```

      DO 32 J=2,NM1
          DO 32 I=2,MM1
              OMEGA(I,J) = RA*(THETA(I+1,J)-THETA(I-1,J))/C2
32   CONTINUE

```

C CALCULATE RMS AVERAGE VORTICITY

```

      OMTOT = 0.
      DO 34 J=2,NM1
        DO 34 I=2,MM1
          OMTOT = OMTOT+ABS(OMEGA(I,J))
34      CONTINUE

      OMRMS = OMTOT/(NM2*MM2)
      OMLN = ALOG(OMRMS)
      WRITE(10,300)T,OMLN
300     FORMAT(2X,2E19.12)
      NOMEGA = NOMEGA+1
      IF (NOMEGA .NE. 10) GO TO 36
      NOMEGA = 0
      WRITE(4,310)NSTEP,T,OMLN
310     FORMAT(1X,'NSTEP=',I5,2X,'TIME=',E13.6,2X,'OMLN=',E12.5)

```

C OPTIONAL PLOTS OF STREAM FUNCTION AND TEMPERATURE
C CONTOURS

```

36     NPLOT = NPLOT+1
      IF (NPLOT .EQ. 50) GO TO 38
      GO TO 1

38     NPLOT = 0
      WRITE(4,320)
320     FORMAT(//2X,'TYPE 1 FOR CONTOURS',/)
      READ(4,330)NP
330     FORMAT(I)
      IF (NP .NE. 1) GO TO 1

```

C OPTIONAL EXIT

```

      WRITE(4,400)
400     FORMAT(10X,'TYPE 1 TO ESCAPE PROGRAM EXECUTION',/)
      READ(4,410)NEXIT
410     FORMAT(I)
      IF (NEXIT .EQ. 1) GO TO 2

```

C OPTIONAL GENERATION OF DATA FILES BEFORE STEADY STATE
C IS REACHED

```

      IF (NTUNIT .GT. 2) GO TO 1
      IF (NTUNIT .EQ. 2) GO TO 40
      WRITE(4,420)
420     FORMAT(10X,'TYPE 1 FOR OPTIONAL TRACER DATA NO.1',/)
      READ(4,410)NOPT1
      IF (NOPT1 .EQ. 1) GO TO 3
      GO TO 1

40     WRITE(4,430)
430     FORMAT(10X,'TYPE 1 FOR OPTIONAL TRACER DATA NO.2',/)
      READ(4,410)NOPT2
      IF (NOPT2 .EQ. 1) GO TO 4
      GO TO 1

```

```

C   EXIT AT THE STEADY STATE

2       WRITE(4,500)NSTEP,T,ITMAX
500     FORMAT(1H1,/,/5X,'END OF EXECUTION',/9X,
1       'NUMBER OF TIME STEPS=',I/9X,'TIME=',
2E/9X,'MAXIMUM ITERATIONS IN SORLX=',I)

C   CREATE FOR15.DAT FOR STREAM FUNCTION CONTOUR
C   AT STEADY STATE

      DO 50 J=1,N
        JJ = N+1-J
        WRITE(39,510)(PSI(I,JJ),I=1,M)
50     CONTINUE
510     FORMAT(1X,F22.16)
        WRITE(39,140)RA,REPR,DT,MM,NN,RATIO
        WRITE(39,520)T,NDATE
520     FORMAT(5X,'STREAM FUNCTION DATA',/9X,'FLOW TIME=',
1         E/9X,'TODAYS DATE ',I)

C   CREATE FOR17.DAT FOR TEMPERATURE CONTOUR
C   AT STEADY STATE

      DO 52 J=1,N
        JJ=N+1-J
        WRITE(49,530)(THETA(I,JJ),I=1,M)
52     CONTINUE

530     FORMAT(1X,5F10.4)
        WRITE(49,140)RA,REPR,DT,MM,NN,RATIO
        WRITE(49,540)T,NDATE
540     FORMAT(5X,'TEMPERATURE DATA',/9X,'FLOW TIME=',E/9X,
1         'TODAYS DATE ',I)

C   CREATE FOR03.DAT FOR VELOCITY COMPONENTS AT
C   STEADY STATE
C   USED FOR TRACER RESPONSE EXECUTION

      DO 54 J=1,N
        WRITE(9,550)(U(I,J),I=1,M)
54     CONTINUE

      DO 56 J=1,N
        WRITE(9,550)(V(I,J),I=1,M)
56     CONTINUE

550     FORMAT(2X,5E19.12)
        WRITE(9,560)RA,REPR,MM,NN,T,NDATE
560     FORMAT(2X,2E19.12,2I3,E19.12,I6)
        WRITE(9,140)RA,REPR,DT,MM,NN,RATIO
        WRITE(9,570)T,NDATE
570     FORMAT(5X,'VELOCITY DATA FOR U AND V COMPONENTS',/9X,
1         'FLOW TIME=',E/9X,'TODAYS DATE ',I)
        GO TO 5

C   OPTIONAL DATA NO.1

3       DO 60 J=1,N
        WRITE(7,550)(U(I,J),I=1,M)
60     CONTINUE

```



```

DO 62 J=1,N
  WRITE(7,550)(V(I,J),I=1,M)
62 CONTINUE
  NTUNIT = 2
  WRITE(7,560)RA,REPR,MM,NN,T,NDATE
  WRITE(7,140)RA,REPR,DT,MM,NN,RATIO
  WRITE(7,570)T,NDATE

DO 64 J=1,N
  JJ = N+1-J
  WRITE(37,510)(PSI(I,JJ),I=1,M)
64 CONTINUE
  WRITE(37,140)RA,REPR,DT,MM,NN,RATIO
  WRITE(37,520)T,NDATE

DO 66 J=1,N
  JJ = N+1-J
  WRITE(47,530)(THETA(I,JJ),I=1,M)
66 CONTINUE
  WRITE(47,140)RA,REPR,DT,MM,NN,RATIO
  WRITE(47,540)T,NDATE

GO TO 1

C  OPTIONAL DATA NO.2

4  DO 70 J=1,N
  WRITE(8,550)(U(I,J),I=1,M)
70 CONTINUE
  DO 72 J=1,N
  WRITE(8,550)(V(I,J),I=1,M)
72 CONTINUE
  NTUNIT = 3
  WRITE(8,560)RA,REPR,MM,NN,T,NDATE
  WRITE(8,140)RA,REPR,DT,MM,NN,RATIO
  WRITE(8,570)T,NDATE

DO 74 J=1,N
  JJ = N+1-J
  WRITE(38,510)(PSI(I,JJ),I=1,M)
74 CONTINUE
  WRITE(38,140)RA,REPR,DT,MM,NN,RATIO
  WRITE(38,520)T,NDATE

DO 76 J=1,N
  JJ = N+1-J
  WRITE(48,530)(THETA(I,JJ),I=1,M)
76 CONTINUE
  WRITE(48,140)RA,REPR,DT,MM,NN,RATIO
  WRITE(48,540)T,NDATE

GO TO 1

C  EXIT

5  WRITE(10,140)RA,REPR,DT,MM,NN,RATIO
  WRITE(10,800)NDATE
800 FORMAT(5X,'NSTEP,T,OMLN DATA',/8X,'TODAYS DATE ',I)
END

```

```

      SUBROUTINE TEMP(REPR,M,N,TH,THETA,ITEMP)
C-----
C  PROGRAM TEMP.FOR
C  CALCULATES THE INITIAL TEMPERATURE PROFILE
C-----
      DIMENSION TH(N),THETA(M,N)
      DOUBLE PRECISION TH,THETA
      COMMON /BLK/  B,MM1,NM1,C1,C2,C3

C  NEXT STATEMENT ACTIVE FOR UNIT STEP INITIAL
C  TEMPERATURE DISTRIBUTION
C  INACTIVE FOR STEADY STATE PROFILE IN THE ABSENCE
C  OF FREE CONVECTION

C      ITEMP = 1
C      GO TO 49

      ITEMP = 0
      H = 1./(N-1.)
      ABSRE = ABS(REPR)
      IF (ABSRE .LT. 10.E-5) GO TO 29
      IF (REPR .GT. 50.) GO TO 49
      IF (REPR .LT. -50.) GO TO 69

      DO 19 J=1,N
          Y = 1.-(J-1.)*H
          TH(J) = (EXP(REPR*Y)-1.)/(EXP(REPR)-1.)
19      CONTINUE
          GO TO 89

      DO 29 J=1,N
          TH(J) = 1.-(J-1.)*H
39      CONTINUE
          GO TO 89

      TH(1) = 1.
      DO 59 J=2,N
          TH(J) = 0.
59      CONTINUE
          GO TO 89

      DO 79 J=1,NM1
          TH(J) = 1.
79      CONTINUE
          TH(N) = 0.

      DO 89 J=1,N
          DO 99 I=1,M
              THETA(I,J) = TH(J)
99      CONTINUE

      RETURN
      END

```

```

      SUBROUTINE SORLX(F,G,M,N,H,ERRMAX,ITER,RE,FRMS,ITMAX)
C-----
C   PROGRAM SORLX.FOR
C   SUCCESSIVE OVERRELAXATION SOLUTION OF POISSON'S
C   EQUATION FOR THE STREAM FUNCTION
C-----

      DIMENSION F(M,N),G(M,N)
      COMMON /BLK/ B,MM1,NM1,C1,C2,C3
      DOUBLE PRECISION F,G

C   CALCULATE THE RELAXATION FACTOR, OPTOM

      PI = 4.*ATAN(1.)
      ALPHA = COS(PI/M)+COS(PI/N)
      OPTOM = (8.-4.*SQRT(4.-ALPHA**2))/ALPHA**2
      ITER = 0

      FBC = 0.
      DO 10 I=1,M
         FBC = FBC+ABS(F(I,1))+ABS(F(I,N))
10      CONTINUE

      DO 12 J=2,NM1
         FBC = FBC+ABS(F(1,J))+ABS(F(M,J))
12      CONTINUE

C   BEFORE EACH ITERATION ADD ONE TO ITER

      ITER = ITER+1
      ERROR = 0.
      FTOT = FBC

C   CALCULATE F(I,J) AT INTERIOR POINTS

      DO 3 J=2,NM1
         DO 3 I=2,MM1
            FOLD = F(I,J)
            F(I,J) = F(I,J)+.25*OPTOM*(F(I-1,J)+F(I+1,J)
1          +F(I,J-1)+F(I,J+1)-4.*F(I,J)-H*H*G(I,J))
            ERROR = ERROR+ABS(F(I,J)-FOLD)
            FTOT = FTOT+ABS(F(I,J))
3          CONTINUE

C   CONVERGENCE TEST

      IF (ITER .LT. 5) GO TO 2
      IF (ITER .EQ. 30) GO TO 7
      ERTEST = FTOT*ERRMAX
      IF (ERROR .GT. ERTEST) GO TO 2
7      FRMS = FTOT/(N*M)
      IF (ITER .GT. ITMAX) ITMAX = ITER

      RETURN
      END

```

```

      SUBROUTINE IMPX(POLD,PS,U,V,M,N,A,C,D,GS,BETA,GAMMA)
C-----
C   PROGRAM IMPX.FOR
C   X-IMPLICIT HALF OF ADI SOLUTION, DETERMINES TEMPERATURES
C   'PS(I,J)' AT TIME 'T+(1/2)DT' BY SOLVING FOR THE 'ATTI',
C   'B', 'C(I)', AND 'D(I)' COEFFICIENTS OF A TRIDIAGONAL MATRIX
C-----

      DIMENSION POLD(M,N),PS(M,N),GS(M),U(M,N),V(M,N),A(M),
        IC(M),D(M)
      DIMENSION BETA(M),GAMMA(M)
      DOUBLE PRECISION POLD,PS,GS,A,C,D,BETA,GAMMA
      DOUBLE PRECISION U,V
      COMMON /BLK/  B,MM1,NM1,C1,C2,C3

C   SET TEMPERATURE AT THE ENTRANCE AND EXIT,
C   'PS(I,1)' AND 'PS(I,N)'

      DO 01 I=1,M
        PS(I,1) = POLD(I,1)
        PS(I,N) = POLD(I,N)
01      CONTINUE

C   FOR EACH 'J', DETERMINE THE NEW TEMPERATURES 'PS(I,J)'
C   FOR I=1 THROUGH I=M

      DO 11 J=2,NM1

C   DETERMINE COEFFICIENTS OF NEIGHBORING POINTS

        DO 21 I=2,MM1
          A(I) = -U(I-1,J)/C2-C1
          C(I) = U(I+1,J)/C2-C1
21      CONTINUE

C   DETERMINE VALUE OF KNOWN QUANTITY 'D(I)'

        DO 31 I=1,M
          D(I) = C3*POLD(I,J)+(-V(I,J+1)*POLD(I,J+1)+U(I,J-1)*
1          POLD(I,J-1))/C2+C1*(POLD(I,J+1)-2.*POLD(I,J)+
1          POLD(I,J-1))
31      CONTINUE

C   CALL SUBROUTINE TRIDX TO SOLVE TRIDIAGONAL MATRIX

        CALL TRIDX(GS,A,C,D,M,BETA,GAMMA)

C   ASSIGN VALUES OF SINGLE-INDEX ARRAY TO TWO-DIMENSIONAL
C   ARRAY

        DO 41 I=2,MM1
          PS(I,J) = GS(I)
41      CONTINUE

```

```

C   SET NEW TEMPERATURES AT THE WALLS, 'PS(1,J)'
C   AND 'PS(M,J)'

```

```

      PS(1,J) = PS(2,J)
      PS(M,J) = PS(MM1,J)
11  CONTINUE

```

```

      RETURN
      END

```

SUBROUTINE TRIDX(G,A,C,D,M,BETA,GAMMA)

```

-----
C   PROGRAM TRIDX.FOR
C   SOLUTION OF A TRIDIAGONAL MATRIX IN 'Q(M)', GIVEN 'A(M)',
C   'B', 'C(M)', AND 'D(M)'
-----

```

```

      DIMENSION G(M),A(M),C(M),D(M),BETA(M),GAMMA(M)
      DOUBLE PRECISION G,A,C,D,BETA,GAMMA
      COMMON /BLK/ B,MM1,NM1,C1,C2,C3

```

```

C   DETERMINE RECURSION CONSTANTS 'BETA' AND 'GAMMA'

```

```

      BETA(2) = B+A(2)
      GAMMA(2) = D(2)/BETA(2)

      DO 10 K=3,M-2
        BETA(K) = B-(A(K)*C(K-1)/BETA(K-1))
        GAMMA(K) = (D(K)-A(K)*GAMMA(K-1))/BETA(K)
10  CONTINUE
      BETA(MM1) = B+C(MM1)-(A(MM1)*C(M-2)/BETA(M-2))
      GAMMA(MM1) = (D(MM1)-A(MM1)*GAMMA(M-2))/BETA(MM1)

```

```

C   DETERMINE 'Q(K)'

```

```

      Q(MM1) = GAMMA(MM1)
      DO 20 KK=2,M-2
        K = M-KK
        Q(K) = GAMMA(K)-C(K)*Q(K+1)/BETA(K)
20  CONTINUE

      RETURN
      END

```

```

SUBROUTINE IMPY(PS,P,U,V,M,N,A,C,D,G,NM2,BETA,GAMMA)
C-----
C PROGRAM IMPY.FOR
C Y-IMPPLICIT HALF OF ADI SOLUTION, DETERMINES TEMPERATURES
C 'P(I,J)' AT NEW TIME STEP BY SOLVING FOR THE 'A(I)', 'B',
C 'C(I)', AND 'D(I)' COEFFICIENTS OF A TRIDIAGONAL MATRIX
C-----

      DIMENSION PS(M,N),P(M,N),G(N),U(M,N),V(M,N),A(N),C(N),D(N)
      DIMENSION BETA(N),GAMMA(N)
      DOUBLE PRECISION PS,P,G,A,C,D,BETA,GAMMA
      DOUBLE PRECISION U,V
      COMMON /BLK/ B,MM1,NM1,C1,C2,C3

C SET TEMPERATURE AT THE ENTRANCE AND EXIT

      DO 02 I=1,M
          P(I,1) = PS(I,1)
          P(I,N) = PS(I,N)
02      CONTINUE

C FOR EACH 'I', DETERMINE THE NEW TEMPERATURES 'P(I,J)'
C FOR I=1 THROUGH I=M

      DO 12 I=2,MM1

C DETERMINE COEFFICIENTS OF NEIGHBORING POINTS

          DO 22 J=2,NM1
              A(J) = -V(I,J-1)/C2-C1
              C(J) = V(I,J+1)/C2-C1

C DETERMINE VALUE OF KNOWN QUANTITY 'D(J)'

              D(J) = C3*PS(I,J)+(-U(I+1,J)*PS(I+1,J)+U(I-1,J)*PS(I-1,J)
1          )/C2+C1*(PS(I+1,J)-2.*PS(I,J)+PS(I-1,J))
22      CONTINUE

              D(2) = D(2)-A(2)*PS(I,1)
              D(NM1) = D(NM1)-C(NM1)*PS(I,N)
              A(2) = 0.
              C(NM1) = 0.

C CALL SUBROUTINE TRIDY TO SOLVE TRIDIAGONAL MATRIX

          CALL TRIDY(G,A,C,D,N,BETA,GAMMA)

C ASSIGN VALUES OF SINGLE-INDEX ARRAY TO TWO-DIMENSIONAL
C ARRAY

          DO 32 J=2,NM1
              P(I,J) = G(J)
32      CONTINUE
12      CONTINUE

```

```

C   SET NEW TEMPERATURES AT THE WALLS, 'P(1,J)'
C   AND 'P(M,J)'

```

```

      DO 42 J=2,NM1
        P(1,J) = P(2,J)
42     P(M,J) = P(MM1,J)

```

```

      RETURN
      END

```

```

      SUBROUTINE TRIDY(G,A,C,D,N,BETA,GAMMA)

```

```

C-----
C   PROGRAM TRIDY.FOR
C   SOLUTION OF A TRIDIAGONAL MATRIX IN 'G(N)', GIVEN 'A(N)',
C   'B', AND 'C(N)', 'D(N)'
C-----

```

```

      DIMENSION G(N),A(N),C(N),D(N),BETA(N),GAMMA(N)
      DOUBLE PRECISION G,A,C,D,BETA,GAMMA
      COMMON /BLK/ B,MM1,NM1,C1,C2,C3

```

```

C   DETERMINE RECURSION CONSTANTS 'BETA' AND 'GAMMA'

```

```

      BETA(2) = B
      GAMMA(2) = D(2)/BETA(2)

```

```

      DO 10 K=3,NM1
        BETA(K) = B-(A(K)*C(K-1)/BETA(K-1))
        GAMMA(K) = (D(K)-A(K)*GAMMA(K-1))/BETA(K)
10     CONTINUE

```

```

C   DETERMINE 'G(K)'

```

```

      G(NM1) = GAMMA(NM1)
      DO 20 KK=2,N-2
        K = N-KK
        G(K) = GAMMA(K)-C(K)*G(K+1)/BETA(K)
20     CONTINUE

```

```

      RETURN
      END

```

B.3 Tracer Program: Explicit Upwind Differencing

```

C-----
C  MAIN PROGRAM T2UP.FOR
C  TRACER RESPONSE SOLUTION AT STEADY STATE
C  EXPLICIT UPWIND DIFFERENCING SOLUTION
C  TWO-DIMENSIONAL RECTANGULAR COORDINATES
C  'U(I,J)' VELOCITY IN THE X-DIRECTION
C  'V(I,J)' VELOCITY IN THE Y-DIRECTION
C  'ECONC(I,J)' DIMENSIONLESS CONCENTRATION
C  VELOCITY COMPONENTS U, V FROM FLOW EXECUTION
C  DATA FILE FOR03.DAT
C  T2UP EXECUTION REQUIRES THE FOLLOWING SUBROUTINES:
C  SET2.FOR
C  UP2.FOR
C-----

C  'M' IS THE X-DIRECTION INDEX
C  'N' IS THE Y-DIRECTION INDEX

      PARAMETER M=20
      PARAMETER N=60

C  'K' IS THE GREATER OF 'M' AND 'N'

      PARAMETER K=60
      PARAMETER LC=15

C  'LC' IS THE NUMBER OF CONTOURS SPECIFIED

      DIMENSION NCONT(LC)
      DIMENSION U(M,N),V(M,N),ECONC(M,N),POLD(M,N),PS(M,N),
      1P(M,N),A(K),C(K),D(K),G(K),QS(K),BETA(K),GAMMA(K)
      DIMENSION V1(M,N),V2(M,N),V3(M,N),U1(M,N),U2(M,N),U3(M,N)
      DOUBLE PRECISION U,V,ECONC,POLD,PS,P,A,C,D,G,QS,BETA,GAMMA
      DOUBLE PRECISION V1,V2,V3,U1,U2,U3
      DOUBLE PRECISION UF,UFA,UB,UBA,VF,VFA,VB,VBA
      COMMON /BLK/  B,MM1,NM1,C1,C2,C3
      DATA NCONT/30,40,50,70,90,120,140,180,180,200,210,
      1230,250,270,300/
      LL = 21

C  'XLE IS THE LEWIS NUMBER
C  'EPS' IS THE POROSITY
C  'DT' IS THE TIME INCREMENT
C  'NTRACE' SPECIFIES THE DURATION OF THE INPUT
C  PULSE IN TIME INCREMENTS

      XLE = 40.0
      EPS = 0.35
      DT = 0.0002
      NTRACE = 10
      NT = NTRACE+1

C  'MAXSTP' IS THE MAXIMUM NUMBER OF TIME INCREMENTS

      WRITE(4,100)
100  FORMAT(5X,'ENTER MAXSTP',/)
      READ(4,110)MAXSTP
110  FORMAT(I)

```



```

C   'H' IS THE SPACE INCREMENT

      MM=M
      NN=N
      WRITE(4,120)MM,NN
120   FORMAT(5X,'M, THE X-DIRECTION INDEX =',I3,5X,
1     'N, THE Y-DIRECTION INDEX =',I3/)
      WRITE(4,130)DT
130   FORMAT(5X,'DT=',E13.8/)
      MM1=M-1
      MM2=M-2
      NN1=N-1
      NN2=N-2
      H=1./(20.-1.)
      RATIO=MM1/NN1

C   'C1', 'C2', 'C3', AND 'B' ARE CONSTANTS

      C1 = DT/(2.*EPS*H)
      C2 = DT/(EPS*XLE*H*H)
      C3 = 2.*EPS/DT
      B = C3+2.*C1

C   READ VELOCITY COMPONENTS U, V FROM DATA FILE
C   GENERATED BY FLOW EXECUTION

      DO 10 J=1,N
        READ(3,140)(U(I,J),I=1,M)
10     CONTINUE

      DO 12 J=1,N
        READ(3,140)(V(I,J),I=1,M)
12     CONTINUE
140    FORMAT(2X,5E19.12)

C   SUBROUTINE SET2 CALCULATES THE UPWIND
C   DIFFERENCING VELOCITIES

      CALL SET2(U,V,M,N,U1,U2,U3,V1,V2,V3,
1UF,UFA,UB,UBA,VF,VFA,VB,UBA)

      READ(3,150)RA,REPR,MM,NN,FT,NDATE
150    FORMAT(2X,2E19.12,2I3,E19.12,I6)
      WRITE(4,160)RA,REPR,MM,NN,FT,NDATE
160    FORMAT(5X,'FROM FLOW EXECUTION :',/9X,'RA=',E/9X,'REPR=',E/9X,
1      'M=',I/9X,'N=',I/9X,'TIME=',E/9X,'DATE ',I/)

C   'DTAU' THE INCREMENT FOR DIMENSIONLESS RESIDENCE TIME

      T = 0.0
      DTAU = (DT*REPR/EPS)*(((19.0/(N-1.0))**2.0)

C   'EINIT' THE INITIAL DIMENSIONLESS CONCENTRATION

      EINIT = (EPS/(REPR*DT*NTRACE))*(((N-1.0)/19.0)**2.0)
      WRITE(4,900)EINIT
900    FORMAT(5X,' EINIT=',E/)

      DO 14 I=1,M
        EONC(I,N) = EINIT
14     CONTINUE

```

```

C 'NSTEP' IS THE STEP NUMBER
C TERMINATE COMPUTATION IF NSTEP EXCEEDS MAXSTP
C INCREMENT TIME STEP BY ONE

1     NSTEP = NSTEP+1
      IF(NSTEP.GT.MAXSTP) GO TO 3
      T = T+DTAU
      IF(NSTEP .NE. NT) GO TO 22

      DO 20 I=1,M
        ECONC(I,N) = 0.0
20    CONTINUE

C DETERMINE CONCENTRATION FIELD AT THE NEW TIME STEP WITH
C SUBROUTINE UP2

22    DO 24 I=1,M
      DO 24 J=1,N
        POLD(I,J) = ECONC(I,J)
24    CONTINUE

      CALL UP2(POLD,ECONC,U1,U2,U3,V1,V2,V3,M,N)

C DETERMINE AREA UNDER THE RTD CURVE

      NETOT = NETOT+1
      IF(NETOT .EQ. 1) GO TO 30
      GO TO 1

30    NETOT = 0
      ETOT = 0.
      DO 32 I=1,M
        ETOT = ETOT+ECONC(I,1)
32    CONTINUE
      EAVG = ETOT/M
      AREA = AREA+(DTAU*EAVG)

C CREATE FOR12.DAT FOR AVERAGE EXIT CONCENTRATION, TIME

      WRITE(12,300)T,EAVG,AREA
300   FORMAT(2X,3E19.12)

      NPLOT = NPLOT + 1
      IF(NPLOT .NE. 10) GO TO 1
      NPLOT = 0
      WRITE(4,310)NSTEP,T,EAVG
310   FORMAT(2X,'NSTEP=',I5,2X,'TIME=',E13.6,2X,'EAVG=',E13.6)

C CREATE DATA FILES FOR TRACER CONCENTRATION CONTOUR
C PLOTS

C DO 44 L=1,LC
C IF (NSTEP .EQ. NCONT(L)) GO TO 46
C44  CONTINUE
      GO TO 2
46   WRITE(4,420)
420  FORMAT(10X,'CONTOUR',/)

```

```
      LI = LL+1
      DO 42 J=1,N
        JJ = N+1-J
        WRITE(LL,430)(ECONC(I,JJ),I=1,M)
42     CONTINUE
430    FORMAT(1X,5F12.6)
      WRITE(LL,160)RA,REPR,MM,NN,FT,NDATE
      WRITE(LL,440)T
440    FORMAT(5X,'FLOW TIME FOR TRACER EXECUTION=',E)
      GO TO 2

C   OPTIONAL EXIT

2     WRITE(4,700)
700   FORMAT(10X,'TYPE 2 TO ESCAPE PROGRAM EXECUTION'.//)
      READ(4,710)NEXIT
710   FORMAT(I)
      IF(NEXIT .EQ. 2) GO TO 3
      GO TO 1

3     WRITE(12,800)
800   FORMAT(5X,'T,EAUG DATA')
      WRITE(12,160)RA,REPR,MM,NN,FT,NDATE
      AREA = AREA-(DTAU*EAUG/2.0)
      WRITE(4,810)AREA
810   FORMAT(2X,'AREA UNDER CURVE= ',E)

      END
```

```

SUBROUTINE SET2(U,V,M,N,U1,U2,U3,V1,V2,V3,
1UF,UFA,UB,UBA,VF,VFA,VB,VBA)

```

```

C-----
C PROGRAM SET2.FOR
C CALCULATES THE UPWIND DIFFERENCING VELOCITIES
C EXPLICIT SOLUTION
C-----

```

```

DIMENSION U(M,N),V(M,N),U1(M,N),U2(M,N),U3(M,N),V1(M,N),V2(M,N),
1V3(M,N)
DOUBLE PRECISION U,V,U1,U2,U3,V1,V2,V3
DOUBLE PRECISION UF,UFA,UB,UBA,VF,VFA,VB,VBA
COMMON /BLK/ B,MM1,NM1,C1,C2,C3

```

```

DO 10 J=2,NM1
DO 20 I=2,MM1

```

```

UF = (U(I+1,J)+U(I,J))/2.0
UFA = ABS(UF)
UB = (U(I-1,J)+U(I,J))/2.0
UBA = ABS(UB)
VF = --(V(I,J+1)+V(I,J))/2.0
VFA = ABS(VF)
VB = (V(I,J-1)+V(I,J))/2.0
VBA = ABS(VB)

```

```

U1(I,J) = (UF-UFA)*C1
U2(I,J) = (UF+UFA-UB+UBA)*C1
U3(I,J) = (UB+UBA)*C1
V1(I,J) = (VF-VFA)*C1
V2(I,J) = (VF+VFA-VB+VBA)*C1
V3(I,J) = (VB+VBA)*C1

```

```

20 CONTINUE
10 CONTINUE

```

```

RETURN
END

```

```

      SUBROUTINE UP2(POLD,ECONC,U1,U2,U3,V1,V2,V3,M,N)
C-----
C  PROGRAM UP2.FOR
C  EXPLICIT UPWIND DIFFERENCING SOLUTION FOR TRACER
C  CONCENTRATION AT THE NEW TIME STEP
C-----

      DIMENSION POLD(M,N),ECONC(M,N),U1(M,N),U2(M,N),U3(M,N)
      DIMENSION V1(M,N),V2(M,N),V3(M,N)
      DOUBLE PRECISION POLD,ECONC
      DOUBLE PRECISION U1,U2,U3,V1,V2,V3,P1,P2,P4
      COMMON /BLK/ B,MM1,NM1,C1,C2,C3

      DO 10 I=1,M
        ECONC(I,N) = POLD(I,N)
10     CONTINUE

      DO 20 I=2,MM1
        DO 20 J=2,NM1

          P1 = U1(I,J)*POLD(I+1,J)+U2(I,J)*POLD(I,J)-U3(I,J)*POLD(I-1,J)
          P2 = V1(I,J)*POLD(I,J+1)+V2(I,J)*POLD(I,J)-V3(I,J)*POLD(I,J-1)
          P4 = POLD(I+1,J)+POLD(I-1,J)+POLD(I,J+1)+POLD(I,J-1)-
1         4.0*POLD(I,J)

          ECONC(I,J) = POLD(I,J)-P1-P2+(C2*P4)

20     CONTINUE
        DO 30 J=2,NM1
          ECONC(1,J) = ECONC(2,J)
          ECONC(M,J) = ECONC(MM1,J)
30     CONTINUE

      DO 40 I=1,M
        ECONC(I,1) = ECONC(I,2)
40     CONTINUE

      RETURN
      END

```

B.4 Tracer Problem: ADI

```

C-----
C  MAIN PROGRAM T2.FOR
C  TRACER RESPONSE SOLUTION AT STEADY STATE
C  ALTERNATING-DIRECTION IMPLICIT SOLUTION
C  TWO-DIMENSIONAL RECTANGULAR COORDINATES
C  'U(I,J)' VELOCITY IN THE X-DIRECTION
C  'V(I,J)' VELOCITY IN THE Y-DIRECTION
C  'ECONC(I,J)' DIMENSIONLESS CONCENTRATION
C  VELOCITY COMPONENTS U, V FROM FLOW EXECUTION
C  DATA FILE FOR03.DAT
C  T2 EXECUTION REQUIRES THE FOLLOWING SUBROUTINES:
C  IMPXT.FOR
C  TRIDX.FOR
C  IMPYT.FOR
C  TRIDYT.FOR
C-----

C  'M' IS THE X-DIRECTION INDEX
C  'N' IS THE Y-DIRECTION INDEX

      PARAMETER M=20
      PARAMETER N=20

C  'K' IS THE GREATER OF 'M' AND 'N'

      PARAMETER K=20
      PARAMETER LC=15

C  'LC' IS THE NUMBER OF CONTOURS SPECIFIED

      DIMENSION NCONT(LC)
      DIMENSION U(M,N),V(M,N),ECONC(M,N),POLD(M,N),PS(M,N),
      1P(M,N),A(K),C(K),D(K),Q(K),QS(K),BETA(K),GAMMA(K)
      DOUBLE PRECISION U,V,ECONC,POLD,PS,P,A,C,D,Q,QS,BETA,GAMMA
      COMMON /BLK/  B,MM1,NM1,C1,C2,C3
      DATA NCONT/30,40,50,70,90,120,140,160,180,200,210,
      1230,250,270,300/
      LL = 21

C  'XLE' IS THE LEWIS NUMBER
C  'EPS' IS THE POROSITY
C  'DT' IS THE TIME INCREMENT
C  'NTRACE' SPECIFIES THE DURATION OF THE INPUT
C  PULSE IN TIME INCREMENTS

      XLE=-.40-0-
      EPS = 0.35
      DT = 0.0001
      NTRACE = 1
      NT = NTRACE+1

C  'MAXSTP' IS THE MAXIMUM NUMBER OF TIME STEPS

      WRITE(4,100)
      FORMAT(5X,'ENTER MAXSTP',/)
.100  READ(4,110)MAXSTP
      FORMAT(I)
.110

```

C 'H' IS THE SPACE INCREMENT

```

MM=M
NN=N
WRITE(4,120)MM,NN
120  FORMAT(5X,'M, THE X-DIRECTION INDEX =',I3,5X,
      1'N, THE Y-DIRECTION INDEX =',I3/)
WRITE(4,130)DT
130  FORMAT(5X,'DT=',E13,6/)
MM1=M-1
MM2=M-2
NM1=N-1
NM2=N-2
H=1./(20.-1.)
RATIO=MM1/NM1

```

C 'C1', 'C2', 'C3', AND 'B' ARE CONSTANTS

```

C1 = 1./(XLE*H*H)
C2 = 2.*H
C3 = 2.*EPS/DT
B = C3+2.*C1

```

C READ VELOCITY COMPONENTS U, V FROM DATA FILE
 C GENERATED BY FLOW EXECUTION

```

DO 10 J=1,N
  READ(3,140)(U(I,J),I=1,M)
10  CONTINUE

DO 12 J=1,N
  READ(3,140)(V(I,J),I=1,M)
12  CONTINUE
140  FORMAT(2X,5E19,12)

READ(3,150)RA,REPR,MM,NN,FT,NDATE
150  FORMAT(2X,2E18,12,2I3,E19,12,I6)
WRITE(4,160)RA,REPR,MM,NN,FT,NDATE
160  FORMAT(5X,'FROM FLOW EXECUTION :',/9X,'RA=',E/9X,'REPR=',E/9X,
      1 'M=',I/9X,'N=',I/9X,'TIME=',E/9X,'DATE ',I/)

```

C 'DTAU' THE INCREMENT FOR DIMENSIONLESS RESIDENCE TIME

```

T = 0.0
DTAU = (DT*REPR/EPS)*(((19.0/(N-1.0))**2.0)

```

C 'EINIT' THE INITIAL DIMENSIONLESS CONCENTRATION

```

EINIT = (EPS/(REPR*DT*NTRACE))*(((N-1.0)/19.0)**2.0)
WRITE(4,900)EINIT
900  FORMAT(5X,' EINIT=',E/)

DO 14 I=1,M
  ECONC(I,N) = EINIT
14  CONTINUE

```

C 'NSTEP' IS THE STEP NUMBER

```

C TERMINATE COMPUTATION IF NSTEP EXCEEDS MAXSTP
C INCREMENT TIME STEP BY ONE

```

```

1      NSTEP = NSTEP+1
      IF(NSTEP.GT.MAXSTP) GO TO 3
      T = T+DTAU
      IF(NSTEP .NE. NT) GO TO 22

      DO 20 I=1,M
        ECONC(I,N) = 0.0
20     CONTINUE

C      DETERMINE CONCENTRATION FIELD AT THE NEW TIME STEP WITH
C      SUBROUTINES IMPX, IMPY, TRIDX, AND TRIDY

22     DO 24 I=1,M
        DO 24 J=1,N
          POLD(I,J) = ECONC(I,J)
24     CONTINUE

      CALL IMPX(POLD,PS,U,V,M,N,A,C,D,GS,BETA,GAMMA)

      CALL IMPY(PS,ECONC,U,V,M,N,A,C,D,G,NM2,BETA,GAMMA)

C      DETERMINE AREA UNDER THE RTD CURVE

      NETOT = NETOT+1
      IF(NETOT .EQ. 1) GO TO 30
      GO TO 1

30     NETOT = 0
      ETOT = 0.
      DO 32 I=1,M
        ETOT = ETOT+ECONC(I,1)
32     CONTINUE
      EAVG = ETOT/M
      AREA = AREA+(DTAU*EAVG)

C      CREATE FOR12.DAT FOR AVERAGE EXIT CONCENTRATION, TIME

      WRITE(12,300)T,EAVG
300    FORMAT(2X,2E19.12)

      * NPLOT = NPLOT + 1
      IF(NPLOT .NE. 10) GO TO 1
      NPLOT = 0
      WRITE(4,310)NSTEP,T,EAVG
310    FORMAT(2X,'NSTEP=',I5,2X,'TIME=',E13.6,2X,'EAVG=',E13.6)

C      CREATE DATA FILES FOR TRACER CONCENTRATION CONTOUR
C      PLOTS

      DO 44 L=1,LC
        IF (NSTEP .EQ. NCONT(L)) GO TO 46
44     CONTINUE
        GO TO 2

46     WRITE(4,420)
420    FORMAT(10X,'CONTOUR',/)

      LL = LL+1
      DO 42 J=1,N
        JJ = N+1-J
        WRITE(LL,430)(ECONC(I,JJ),I=1,M)
42     CONTINUE

```



```
430     FORMAT(1X,5F12.6)
        WRITE(LL,160)RA,REPR,MM,NN,FT,NDATE
        WRITE(LL,440)T
440     FORMAT(5X,'FLOW TIME FOR TRACER EXECUTION=',E)
        GO TO 2

C     OPTIONAL EXIT

2       WRITE(4,700)
700     FORMAT(10X,'TYPE 2 TO ESCAPE PROGRAM EXECUTION',/)
        READ(4,710)NEXIT
710     FORMAT(I)
        IF(NEXIT .EQ. 2) GO TO 3
        GO TO 1
3       WRITE(12,800)
800     FORMAT(5X,'T,EAVG DATA')

        WRITE(12,160)RA,REPR,MM,NN,FT,NDATE

        AREA = AREA-(DTAU*EAVG/2.0)
        WRITE(4,810)AREA
810     FORMAT(2X,'AREA UNDER CURVE= ',E)

        END
```

```

SUBROUTINE IMPX(POLD,PS,U,V,M,N,A,C,D,GS,BETA,GAMMA)
C-----
C PROGRAM IMPXT.FOR
C X-IMPLICIT HALF OF ADI SOLUTION, DETERMINES CONCENTRATIONS
C 'PS(I,J)' AT TIME 'T+(1/2)DT' BY SOLVING FOR THE 'A(I)',
C 'B', 'C(I)', AND 'D(I)' COEFFICIENTS OF A TRIDIAGONAL MATRIX
C-----

      DIMENSION POLD(M,N),PS(M,N),GS(M),U(M,N),V(M,N),A(M),
      IC(M),D(M)
      DIMENSION BETA(M),GAMMA(M)
      DOUBLE PRECISION POLD,PS,GS,A,C,D,BETA,GAMMA
      DOUBLE PRECISION U,V
      COMMON /BLK/ B,MM1,NM1,C1,C2,C3

C SET NEW CONCENTRATIONS AT THE ENTRANCE, 'PS(I,N)'

      DO 01 I=1,M
        PS(I,N)=POLD(I,N)
01      CONTINUE

C FOR EACH 'J', DETERMINE THE NEW CONCENTRATIONS 'PS(I,J)'
C FOR I=1 THROUGH I=M

      DO 11 J=2,NM1

C DETERMINE COEFFICIENTS OF NEIGHBORING POINTS

      DO 21 I=2,MM1
        A(I)=-U(I-1,J)/C2-C1
21      C(I)=U(I+1,J)/C2-C1

C DETERMINE VALUE OF KNOWN QUANTITY 'D(I)'

      DO 31 I=1,M
        D(I)=C3*POLD(I,J)+(-V(I,J+1)*POLD(I,J+1)+V(I,J-1)*
1      POLD(I,J-1))/C2+C1*(POLD(I,J+1)-2.*POLD(I,J)+
1      POLD(I,J-1))
31      CONTINUE

C CALL SUBROUTINE TRIDX TO SOLVE TRIDIAGONAL MATRIX

      CALL TRIDX(GS,A,C,D,M,BETA,GAMMA)

C ASSIGN VALUES OF SINGLE-INDEX ARRAY TO TWO-DIMENSIONAL
C ARRAY

      DO 41 I=2,MM1
        PS(I,J)=GS(I)
41      CONTINUE

C SET NEW CONCENTRATIONS AT THE WALLS, 'PS(1,J)'
C AND 'PS(M,J)'

      PS(1,J)=PS(2,J)
      PS(M,J)=PS(MM1,J)
11      CONTINUE

```

```

C   SET NEW CONCENTRATIONS AT THE EXIT, 'PS(1,J)'
      DO 51 I=1,M
        PS(I,1) = PS(I,2)
51    CONTINUE

      RETURN
      END

```

```

      SUBROUTINE TRIDX(Q,A,C,D,M,BETA,GAMMA)
C-----
C   PROGRAM TRIDX.FOR
C   SOLUTION OF A TRIDIAGONAL MATRIX IN 'Q(M)', GIVEN 'A(M)',
C   'B', 'C(M)', AND 'D(M)'
C-----

      DIMENSION Q(M),A(M),C(M),D(M),BETA(M),GAMMA(M)
      DOUBLE PRECISION Q,A,C,D,BETA,GAMMA
      COMMON /BLK/ B,MM1,NM1,C1,C2,C3

C   DETERMINE RECURSION CONSTANTS 'BETA' AND 'GAMMA'

      BETA(2) = B+A(2)
      GAMMA(2) = D(2)/BETA(2)

      DO 10 K=3,M-2
        BETA(K) = B-(A(K)*C(K-1)/BETA(K-1))
        GAMMA(K) = (D(K)-A(K)*GAMMA(K-1))/BETA(K)
10    CONTINUE
      BETA(MM1) = B+C(MM1)-(A(MM1)*C(M-2)/BETA(M-2))
      GAMMA(MM1) = (D(MM1)-A(MM1)*GAMMA(M-2))/BETA(MM1)

C   DETERMINE 'Q(K)'

      Q(MM1) = GAMMA(MM1)
      DO 20 KK=2,M-2
        K = M-KK
        Q(K) = GAMMA(K)-C(K)*Q(K+1)/BETA(K)
20    CONTINUE

      RETURN
      END

```

```

SUBROUTINE IMPY(PS,P,U,V,M,N,A,C,D,G,NM2,BETA,GAMMA)
C-----
C PROGRAM IMPYT.FOR
C Y-IMPLICIT HALF OF ADI SOLUTION, DETERMINES CONCENTRATIONS
C 'P(I,J)' AT NEW TIME STEP BY SOLVING FOR THE 'A(I)', 'B',
C 'C(I)', AND 'D(I)' COEFFICIENTS OF A TRIDIAGONAL MATRIX
C-----

      DIMENSION PS(M,N),P(M,N),G(N),U(M,N),V(M,N),A(N),C(N),D(N)
      DIMENSION BETA(N),GAMMA(N)
      DOUBLE PRECISION PS,P,G,A,C,D,BETA,GAMMA
      DOUBLE PRECISION U,V
      COMMON /BLK/ B,MM1,NM1,C1,C2,C3

C SET NEW CONCENTRATIONS AT THE ENTRANCE, 'P(I,N)'
      DO 02 I=1,M
        P(I,N)=PS(I,N)
02      CONTINUE

C FOR EACH 'I', DETERMINE THE NEW CONCENTRATIONS 'P(I,J)'
C FOR I=1 THROUGH I=M
      DO 12 I=2,MM1

C DETERMINE COEFFICIENTS OF NEIGHBORING POINTS
      DO 22 J=2,NM1
        A(J)=-V(I,J-1)/C2-C1
        C(J)=U(I,J+1)/C2-C1

C DETERMINE VALUE OF KNOWN QUANTITY 'D(J)'
      D(J)=C3*PS(I,J)+(-U(I+1,J)*PS(I+1,J)+U(I-1,J)*PS(I-1,J)
1      )/C2+C1*(PS(I+1,J)-2.*PS(I,J)+PS(I-1,J))
22      CONTINUE

      D(NM1)=D(NM1)-C(NM1)*PS(I,N)

C CALL SUBROUTINE TRIDY TO SOLVE TRIDIAGONAL MATRIX
      CALL TRIDY(G,A,C,D,N,BETA,GAMMA)

C ASSIGN VALUES OF SINGLE-INDEX ARRAY TO TWO-DIMENSIONAL
C ARRAY
      DO 32 J=2,NM1
        P(I,J)=G(J)
32      CONTINUE
12      CONTINUE

C SET NEW CONCENTRATIONS AT THE WALLS, 'P(1,J)'
C AND 'P(M,J)'
      DO 42 J=2,NM1
        P(1,J)=P(2,J)
        P(M,J)=P(MM1,J)
42      CONTINUE

```

```

C   SET NEW CONCENTRATIONS AT THE EXIT. 'P(I,1)'
      DO 52 I=1,M
        P(I,1) = P(I,2)
52   CONTINUE

      RETURN
      END

      SUBROUTINE TRIDY(G,A,C,D,N,BETA,GAMMA)
C-----
C   PROGRAM TRIDYT.FOR
C   SOLUTION OF A TRIDIAGONAL MATRIX IN 'G(N)', GIVEN 'A(N)',
C   'B', 'C(N)', AND 'D(N)'
C-----

      DIMENSION G(N),A(N),C(N),D(N),BETA(N),GAMMA(N)
      DOUBLE PRECISION G,A,C,D,BETA,GAMMA
      COMMON /BLK/ B,MM1,NM1,C1,C2,C3

C   DETERMINE RECURSION CONSTANTS 'BETA' AND 'GAMMA'

      BETA(2) = B+A(2)
      GAMMA(2) = D(2)/BETA(2)

      DO 10 K=3,NM1
        BETA(K) = B-(A(K)*C(K-1)/BETA(K-1))
        GAMMA(K) = (D(K)-A(K)*GAMMA(K-1))/BETA(K)
10   CONTINUE

C   DETERMINE 'G(K)'

      G(NM1) = GAMMA(NM1)
      DO 20 KK=2,N-2
        K = N-KK
        G(K) = GAMMA(K)-C(K)*G(K+1)/BETA(K)
20   CONTINUE

      RETURN
      END

```